Contract No. 950228

Report No. TE-48-64

FINAL REPORT FOR SERIES VII SOLAR ENERGY THERMIONIC CONVERTER DEVELOPMENT PROGRAM

February 1964

by

S. Merra

Prepared for:

Jet Propulsion Laboratory
Pasadena, California

Approved by: Peter G. Pantazelos

P. G. Pantazelos
Director, SET Program

TABLE OF CONTENTS (Continued)

CHAPTER		PAGE
5	Fabrication and Acceptance Testing of Series VII SET Converters	5-1
	5.1 Construction	5-1
	5.2 Acceptance Testing	5-1
6	Life and Reliability Test	6-1
	6.1 Life Test Equipment	6-1
	6.1.1 Introduction	6-1
	6.1.2 Vacuum Chamber	6-1
	6.1.3 Electron Gun and Converter Support Structure	6-3
	6.1.4 Power Supplies and Regulator	6-3
	6.1.5 Instrumentation	6-4
	6.1.6 Protection Features	6-5
	6.2 Life Test of Five Converters	6-11

TABLE OF CONTENTS

CHAPTER		PAGE
1	Design and Component Testing of a Series VII SET Converter	1-1
	1.1 Preliminary Design	1-1
	1.2 Component Development and Testing	1-2
	1.2.1 Machining of Thin Tantalum Sleeves	1-2
	1.2.2 Metallurgical Analysis of Thin-Walled Sleeves	1-3
	1.2.3 Electron Bombardment Pinch Off	1-6
	1.2.4 Photomicrographs of Brazed Joints	1-7
	1.2.5 Cesium Purity	1-8
2	Fabrication and Mapping Converters EX-7, EX-8, EX-9	2-1
	2.1 Introduction	2-1
	2.2 Fabrication of EX-7	2-2
	2.3 Testing of EX-7	2-3
	2.4 Construction of EX-8 and EX-9	2-5
	2.5 Testing of EX-8 and EX-9	2-5
3	Mapping of EX-2 and EX-6	3-1
	3.1 Introduction	3-1
	3.2 Testing of EX-2	3-1
	3.3 Testing of EX-6	3-2
4	Prototype Converter Development	4-1

LIST OF FIGURES (Continued)

FIGURE		PAGE
2-14	IV Envelopes for EX-1 and EX-7 at 1891° K (TES)	2-19
2-15	EX-7 at T_E = 1993° K	2-20
2-16	EX-7 at T_E = 1933° K	2-20
2-17	EX-7 at T_E = 1891° K (corrected)	2-21
2-18	EX-7 Spacing versus Emitter Temperature	2-22
2-19	Current Density Vs. Spacing for a Rhenium Diode with an Emitter Temperature of 1850° K	2-23
2-20	Current Density Vs. Spacing for a Rhenium Diode with an Emitter Temperature of 1950° K	2-24
2-21	Current Density Vs. Spacing for a Rhenium Diode with an Emitter Temperature of 2050° K	2-25
2-22	Performance of EX-7 Compared with that of a Research Rhenium Diode	2-26
2-23	Cross-section of EX-8 Converter (Volume II)	2-27
2-24	Cross-section of EX-9 Converter (Volume II)	2-28
2-25	EX-8 and EX-9 Spacing Vs. Emitter Temperature	2-29
2-26	Emitter and Collector Temperature Drop Vs. Output Current Density for EX-8 and EX-9	2-30
2-27(a)	EX-8 at T_E = 1850° K	2-31
2-27(b)	EX-9 at T_E = 1850° K	2-31
2-28(a)	EX-9 at T_E = 1850° K and Several Cesium Temperatures	2-32
2-28(b)	EX-8 at T_E = 1850° K and Several Cesium Temperatures	2-32
2-29(a)	EX-8 at T_E = 1900° K	2-33
2-29(b)	EX-9 at T_E = 1900° K	2-33
2-30(a)	EX-8 at T_E = 1950° K	2-34
2-30(b)	EX-9 at T_E = 1950° K	2-34
2-31(a)	EX-8 at T_E = 2000° K	2-35
2-31(b)	EX-9 at T_E = 2000° K	2-35

LIST OF FIGURES

FIGURE		PAGE
1-1	Preliminary Design of Series VII Converter	1-9
1-2	Oblique Section through Ringed Zone of Thin Wall (150X)	1-10
1-3	Precipitate Particles in Thin Wall Section (300X)	1-11
1-4	Precipitate Particles in Thin Wall Section (560X)	1-11
1-5	CT-A and CT-B Braze Locations	1-12
1-6	Photomicrograph of Ceramic (386-5) to Emitter Flange (386-6) (150X)	1-13
1-7	Key to Tukon Indentations for Seal Structure (2001)	1-14
1-8	Hardness Map of Ceramic (386-5) to Emitter Flange (386-6)	1-15
2-1	Photomicrograph of Pyrolytically Deposited Rhenium on Molybdenum (100X)	2-8
2-2	Photomicrograph of Pyrolytically Deposited Rhenium on Molybdenum (255X)	2-9
2-3	Photomicrograph of Pyrolytically Deposited Rhenium on Molybdenum (520X)	2-10
2-4	Ground Specimen for Examination of Rhenium Deposited on Molybdenum	2-11
2-5	Photomicrograph of Molybdenum Brazed to Tantalum (266X)	2-12
2-6	Cross-section of EX-7 Converter (Volume II)	2-13
2-7	EX-7 at T_E = 1850° K	2-14
2-8	EX-7 at T_E = 1900° K	2-14
2-9	EX-7 at T_E = 1950° K	2-15
2-10	EX-7 at T_E = 2000° K	2-15
2-11	EX-7 at T_E = 2050° K	2-16
2-12	IV Envelopes for EX-1 and EX-7 at 1993° K (TES)	2-17
2-13	IV Envelopes for EX-1 and EX-7 at 1933° K (TES)	2-18

LIST OF FIGURES (Continued)

FIGURE		PAGE
3-18(a)	EX-6 at T_E = 1850° K	3-21
3-18(b)	EX-6 at T_E = 1850° K	3-21
3-19(a)	EX-6 at T_E = 1900° K	3-22
3-19(b)	EX-6 at T_E = 1900° K	3-22
3-20(a)	EX-6 at T_E = 1950° K	3-23
3-20(b)	EX-6 at T_E = 1950° K	3-23
3-21(a)	EX-6 at T_E = 2000° K	3-24
3-21(b)	EX-6 at T_E = 2000° K	3-24
3-22(a)	EX-6 at T_E = 2050° K	3-25
3-22(b)	EX-6 at T_E = 2050° K	3-25
3-23	Current Density Vs. Spacing for a Rhenium Diode with an Emitter Temperature of 1950° K	3-26
3-24	Current Density Vs. Spacing for a Rhenium Diode with an Emitter Temperature of 2050° K	3-27
3-25	Performance of EX-6 Compared with that of a Research Diode	3-28
4-1	Layout Drawing of Series VII Prototype (Volume II)	4-5
4-2	Results of Ten Diagnostic Experimental Runs for Collector Work Function Determination	4-6
4-3	Free Energy Vs. Absolute Temperature	4-7
4-4	Detail Drawing of Series VII Collector (Volume II)	4-8
5-1	SET VII Diode	5-7
5-2	SET VII Spacer	5-8
5-3	Seven SET VII Diodes	5-9
5-4	Dust Free Hood, Microscope, Exploded View SET VII Parts and SET VII Diode	5-10
5-5	Exploded View of SET VII Parts and SET VII Diode	5-11

LIST OF FIGURES (Continued)

FIGURE		PAGE
3-1(a)	EX-2 at T_E = 1850° K	3-4
3-1(b)	EX-2 at T_E = 1850° K	3-4
3-2(a)	EX-2 at T_E = 1850° K	3-5
3-2(b)	EX-2 at T_E = 1850° K	3-5
3-3	EX-2 at T_E = 1850° K	3-6
3-4(a)	EX-2 at T_E = 1900° K	3-7
3-4(b)	EX-2 at T_E = 1900° K	3-7
3-5	EX-2 at T_E = 1900° K	3-8
3-6(a)	EX-2 at T_E = 1950° K	3-9
3-6(b)	EX-2 at T_E = 1950° K	3-9
3-7(a)	EX-2 at T_E = 1950° K	3-10
3-7(b)	EX-2 at T_E = 1950° K	3-10
3-8	EX-2 at T_E = 2000° K	3-11
3-9(a)	EX-2 at T_E = 2000° K	3-12
3-9(b)	EX-2 at T_E = 2000° K	3-12
3-10(a)	EX-2 at T_E = 2050° K	3-13
3-10(b)	EX-2 at T_E = 2050° K	3-13
3-11(a)	EX-2 at T_E = 2050° K	3-14
3-11(b)	EX-2 at T_E = 2050° K	3-14
3-12	Emitter and Collector Temperature Drop Vs. Output Current Density for EX-2	3-15
3-13	Comparison of EX-1 and EX-2 at T_E = 1850° K	3-16
3-14	Comparison of EX-1 and EX-2 at T_E = 1900° K	3-17
3-15	Comparison of EX-1 and EX-2 at T_E = 1950° K	3-18
3-16	Comparison of EX-1 and EX-2 at T_E = 2000° K	3-19
3-17	Comparison of EX-1 and EX-2 at T_E = 2050° K	3-20

LIST OF FIGURES (Continued)

FIGURE		PAGE
6-1	Cooling Coil in Life Test Chamber	6-15
6-2	Five Life Test Units	6-16
6-3	Life Test Base Plate	6-17
6-4	Base Plate Gask-O-Seal	6-17
6-5	Bell Jar with Protective Pyrometer Window	6-18
6-6	Pierce Type Electron Gun	6-18
6-7	Vacuum Chamber with Connections to Elements	6-19
6-8	Instrument Panel and Chamber of a Complete Life Test Unit	6-20
6-9	Instrument Panel of a Complete Life Test Unit	6-21
6-10	Converter VI-S-18, Power Input, Power Output, and Observed Emitter Temperature Vs. Time	6-22
6-11	Converter VII-S-4, Power Input, Power Output and Observed Emitter Temperature Vs. Time	6-23
6-12	Converter VII-S-5, Power Input, Power Output and Observed Emitter Temperature Vs. Time	6-24
6-13	Converter VI-S-14, Power Input, Power Output and Observed Emitter Temperature Vs. Time	6-25
6-14	Converter VI-TEP-1, Power Input, Power Output and Observed Emitter Temperature Vs. Time	6-26
6-15	SET VII-S-5 Mounted in Electron Gun	6-27
6-16	SET VII-S-5 Removed after 3000 Hours of Operation	6-28
6-17	Exploded View of Electron Gun after Testing	6-29
6-18	Five Life Test Diodes after 3000 Hours of Operation	6-30
6-19	VI-S-18, View of Converter before and after Life Testing	6-31
6-20	VII-S-4, View of Converter before and after Life Testing	6-32
6-21	VII-S-5, View of Converter before and after Life Testing	6-33
6-22	VI-S-14, View of Converter before and after Life Testing	6-34
6-23	VI-TEP-1, View of Converter before and after Life Testing	6-34a

PRECEDING PAGE BLANK NOT FILMED.

PRECEDING PAGE BLANK NOT FILMED.

LIST OF TABLES

TABLE		PAGE
1-1	Tabulation of Knoop Hardness Numbers	1-16
4-1	Series VII Converter Prototype Program History	4-9
5-1	Material Survey SET VII	5-4
5-2	Tube Record VII-S-6, 7, 8, 9, 10, 11, 12	5-5
5-3	Summary of Diode Acceptance Test Results (VII-S-6, 7, 8, 9, 10, 11, 12)	5-6
6-1	Summary of Diode Acceptance Test Results (VII-S-4, VII-S-5, VI-S-18, VI-TEP-1)	6-35
6-2	Report of Initial Life Test Results (VI-S-18, VII-S-4, VII-S-5, VI-S-14, VI-TEP-1)	6-36
6-3 to 6-22	Life Test Data Sheets (Volume II) (SET VI-S-18, VII-S-4, VII-S-5, VI-S-14, VI-TEP-1)	6-37
6-23 to 6-42	Weekly Summaries of Life Test Results (SET VI-S-18, VII-S-4, VII-S-5, VI-S-14, VI-TEP-1)	6-38 to 6-57
6-43	Output Power Density, Power Input, Cesium Temperature Seal Temperature, and Observed Emitter Temperature at Starting Conditions, 1000 Hour Level, 2000 Hour Level and 3000 Hour Level (VI-S-18, VII-S-4, VII-S-5, VI-S-14, VI-TEP-1)	6-58

During the course of the program the Series VII Converter was developed. Two of these converters were placed on life test and exceeded 3000 hours of operation. Both of these were still operating satisfactorily at the end of this time and were delivered for testing at JPL. Seven more Series VII Converters were constructed, acceptance tested and also delivered to JPL.

Three Series VI Converters were also placed on life test and operated for more than 3000 hours without failure. These were also delivered to JPL for further testing.

In addition to the development of the Series VII Converter, three experimental converters were also constructed and tested. One incorporated a rhenium emitter and a molybdenum collector, the second incorporated a tantalum emitter and a molybdenum collector, and the third incorporated a tantalum emitter and tantalum collector. Two experimental converters, one with a rhenium emitter and one with a tungsten emitter, constructed prior to this program, were also extensively tested during this time.

PRECEDING PAGE BLANK NOT FILMED.

INTRODUCTION

This document constitutes the final report of the work performed on the Series VII Solar Energy Thermionic Converter Development Program. The program was the part of the work of Thermo Electron's contract No. 950228 with Jet Propulsion Laboratories covered by Work Statement No. 2739 and is a portion of JPL's contract NAS7-100 with the National Aeronautics and Space Administration.

The objectives of the program called for the development of an improved thermionic converter designated as the Series VII Converter. The converter was to be of an improved mechanical design which would simplify the method of manufacture to the extent that the end product would be a less complex mechanical unit and more amenable to complete quality control. By such improvements it was expected that the life of the device would be lengthened so that, by the end of the program, the object of 2000 hours of continuous operation would have been achieved.

In order to enhance the probability of successful life testing, and to remove to as great a degree as possible any external effects, five carefully designed and specially manufactured life test stands, with completely integrated auxiliary equipment, were to be constructed and used for life test.

In prior tests, tantalum carburization from oil vapors and excessive emitter crystallization because of overly concentrated heating had been observed. The new test stands proved to be a significant improvement over earlier test equipment in that the diodes showed no damage that could be traced to the vacuum environment or the method of heating.

1.2 COMPONENT DEVELOPMENT AND TESTING

1.2.1 Machining of Thin Tantalum Sleeves

In an effort to improve the quality and yield of the thin tantalum sleeves, several machining techniques not previously used were evaluated, and rigorous quality-assurance inspections were adopted. The use of honing, grinding, or burnishing did not result in substantial improvement in the quality of the sleeves. Component tests revealed that the major defects developed,not while achieving the high-quality finishes but rather in the handling, inspection, and processing of the sleeve. Therefore, more detailed specifications of each operation were prepared and issued in order to reduce to a minimum the human errors which adversely affect the spacer quality. Furthermore, with several quality-control inspections during the fabrication, spacers which have suffered damage at some point prior to the final operations are quickly rejected. Thus cost is kept to a minimum by not processing imperfect pieces.

In addition to incorporating more frequent quality-assurance steps, methods of measuring bore diameters and wall thicknesses were evolved which also minimized damage to the completed part. This was primarily accomplished by using an air gauge designed specifically for the SET VII thin-wall spacers. This device uses the flow of air between the measuring piece and the inside bore to determine the inside diameter without contacting the finished surface. Gaging techniques previously used were dependent upon plug gages which left visible score marks on the soft tantalum surface. Calibration is accomplished by registering the flow between the measuring head and a standard bore. Accuracy of measurement is 0.0001 inch. The technique has proven highly satisfactory and has been adapted as the standard inside diameter measuring technique for spacer manufacture. Reliable techniques for measuring wall

CHAPTER 1

DESIGN AND COMPONENT TESTING OF A SERIES VII SET CONVERTER

1.1 PRELIMINARY DESIGN

The general goal of the Series VII program was to develop an improved version of the SET VI converter from the standpoints of life and reliability. An initial design decision was to leave the geometry of the generator cavity defined by the emitter pieces of Series VI converters unchanged, and to redesign the converter support structure so as to permit easier assembly and disassembly procedures in generator fabrication and testing.

The original design of a Series VII converter is shown in Figure(I-1). The major design changes incorporated from previous SET converters built by TEE were a one-piece molybdenum collector, a seal structure utilizing pressed niobium flanges which eliminated the attachment of a separate emitter output lead ring, a less massive emitter (reduction of the mass by approximately 20%) to minimize the rate of creep, a cesium reservoir capable of achieving and maintaining optimum cesium vapor pressure during operation with minimum electrical power input, pinch-off formed by electron-bombardment melting rather than mechanical crimping, and a radiator capable of maintaining the optimum collector temperature during operation without an electrical heater. Component development was pursued throughout the entire program with a major effort in the first two quarters and follow-on work during the rest of the program in an effort to thoroughly investigate the usefulness of each of these design changes. Those that proved worthwhile were then to be incorporated in complete converters.

2. Material which has been cold worked during fabrication may contain inclusions which are not homogeneous within the bulk of the material.

3. The attack of the tantalum spacer, occurs over a limited temperature range in which tantalum carbide, oxide, and nitride are stable as second phases in tantalum. One or more of these compounds accumulating as a second phase can alter the appearance of the tantalum.

As a result of these observations, an in-house quality control effort was pursued to prepare tantalum samples for hardness measurements and photomicrographs. In this manner, correlations could be drawn between chemical analyses, metallurgical history, and the life and performance of the emitters in converters.

The presence of rings on thin-walled tantalum spacers has been observed in the 1200° to 1400° C temperature range on the spacer, and correlates with the presence of a second phase in the microstructure of the tantalum as shown in Figures (1-2, 1-3, and 1-4). Figure (1-4) shows an oblique section through the ringed zone of a thin-walled tantalum spacer. The inside of the spacer is to the left and the outside is to the right of the photograph. Although the specimen is somewhat over-etched, the photomicrographs reveal that the second phase precipitate is widely distributed through out the wall thickness; and the precipitate is found in the grain boundary at the outside, while near the inside of the wall it is more concentrated within the grain boundaries. Figures (1-3) and (1-4) show the precipitate particles at different magnifications exhibiting the lamellar structure of the precipitate. This second phase is not found in the lower temperature parts of the spacer. Such a distribution as found

thicknesses without contacting the thin wall in an unsupported state were also developed.

1.2.2 Metallurgical Analysis of Thin-Walled Sleeves

During the program, a major effort was applied to the reduction of chemical attack of the thin tantalum emitter spacer in order to produce a sounder and longer lived structure. In particular, an attempt was made to define those elements which enter into chemical reaction with tantalum, when the emitter is at operating temperature, utilizing such tools as color photography, photomicrographs, and x-ray diffraction. From a careful observation of the spacers after each step in their fabrication and processing, it was obvious that no perceptible changes occurred in the tantalum spacer until outgassing began. Two points stood out during outgassing. The spacer was exposed for long periods of time to an oil diffusion vacuum system with liquid nitrogen trapping; and the cesium capsule was in place and was heated by the diode tubulation. Steps were taken to minimize contamination of the sleeve by residual impurities in the vacuum environment, to prevent air leakage into the vacuum, and to maintain the cesium capsule cooler. Measurement of the leak rate into the vacuum chamber prior to each outgassing as well as periodic leak checking of base plate and vac-ion components were instituted. Also, additional cooling was added to the cesium reservoir during outgassing.

In pursuing this investigation further, consultation with experts in tantalum metallurgy revealed the following points.

1. The quantitative analysis of tantalum and cesium by different sources usually resulted in inconsistent reports.

carbide rather than tantalum-oxide or vice-versa. Also, from the photomicrographs, it is difficult to conclude whether diffusion of a second phase precipitate is occurring from the inside or from the outside of the spacer.

In a further attempt to identify the observed second phase precipitate, a second spacer with evidence of reaction was filed into a power and investigated by x-ray diffraction. In summary, the diffraction pattern, using a Norelco high-angle x-ray diffractometer, could not identify the second phase precipitate. As a result, it is concluded that there is less than 3% precipitate present in the sample.

1.2.3 ELECTRON BOMBARDMENT PINCH OFF

Another goal of the program was to investigate the use of electron bombardment to pinch off the tubulation rather than by mechanically crimping. During component testing it became obvious that a significant amount of gas is released during melting of a tubulation.

In an effort to measure the amount of gas released when the Kovar tubulation is melted, tests were made with the following apparatus:

> A 1/8" Kovar tube which had been fuse brazed to a copper tube was mounted on an 8 liter/sec vac ion pump, and the top of the Kovar tube was mechanically pinched off. With the internal pressure of the tubulation at a steady state value, the Kovar tube was melted and sealed and the pressure rise within the internal volume versus time was recorded until the tube melted completely. The results of two such tests indicated that

in the ringed zone is not compatible with the diffusion of an alloying element from some other component such as the seal. Therefore, the contaminant is probably present in the environment around the spacer, inside or outside. Four elements, carbon, hydrogen, oxygen, and nitrogen, which are known to affect deleteriously the mechanical properties of tantalum, have the following characteristics.

Tantalum loses hydrogen at temperatures of 1300° C according to usual outgassing data. Hydrogen also is very soluble in tantalum. Over a concentration of 0.4%, it precipitates a second phase. Since the ring is found at temperatures higher than 1300° C, it is unlikely that hydrogen is responsible for the reaction.

Tantalum-nitride tends to precipitate as irregular particles rather than the lamellar ones shown in Figures (1-3) and (1-4), and forms only with a considerable volume increase. Therefore, nitrogen is unlikely as a reacting substance.

Tantalum-carbide is quite stable at high temperatures, and carbon is much less soluble than either nitrogen or hydrogen in tantalum. Further, it precipitates to give a microstructure similar to those shown in Figures (1-3) and (1-4). Ths most obvious source of carbon contamination is the breakdown of hydrocarbon oil vapors. Consequently, carbon is a likely cause of the reaction.

Like tantalum-carbide, oxides are reported to precipitate preferentially as lamellar particles on the ⟨100⟩ planes in the lattice. Further, the tantalum-oxide is reported to be a somewhat volatile oxide above 1600° C. From the photomicrographs there is no means of identifying the precipitate as tantalum-

development phase. These tests, however, were conducted on assemblies which were run for relatively short periods of time.

1.2.5 CESIUM PURITY

Contamination of the cesium was studied by chemical analysis of residues taken from the reservoirs of converters which had operated for various periods of time. Within the limitations of the methods used, significantly higher concentrations of impurities were found than those reported from various suppliers. However, it was found that, in order to perform meaningful chemical analysis, it is necessary to have significantly more cesium available than is typically used in the SET converters.

the gas being released could cause a positive pressure of several mm Hg when the diode is at operating temperature. Consequently, it was deemed impractical to use this technique for sealing the diode.

1.2.4 PHOTOMICROGRAPHS OF BRAZED JOINTS

All the braze areas in typical converters VII were examined early in the program by cutting sections and taking photomicrographs and microhardness readings. With the exception of the seal area, relatively high hardness readings were found in those brazes using nickel, but throughout the program no failures were encountered in these areas of a converter in checking the five life test converters which all exceeded 3000 hours without failure Hardness readings were taken using a Tukon Hardness Tester. The hardness readings are tabulated in Table (1-1) and Figure (1-5) shows the braze locations. A photomicrograph of the seal area is shown in Figure (1-6) while (1-7) shows the location of the indents, and Figure (1-8) shows the measured Knoop hardness number. The diamond shaped black spots which are apparent in these figures, are the indentations made by the hardness tester.

From Table (1-1) it may be observed that braze 2002 has a relatively high hardness indicating a brittle interface. The braze material used is copper with nickel plating. Nickel and niobium form a brittle compound at 1180° C. A number of other brazes also indicate brittle interfaces but there was no difference between those cesiated for 10 hours and non-cesiated samples.

Dimensional stability of various key parts, including flatness of the electrodes before and after operation, revealed no deviation from measurements prior to fabrication at least for the short term tests possible in this component

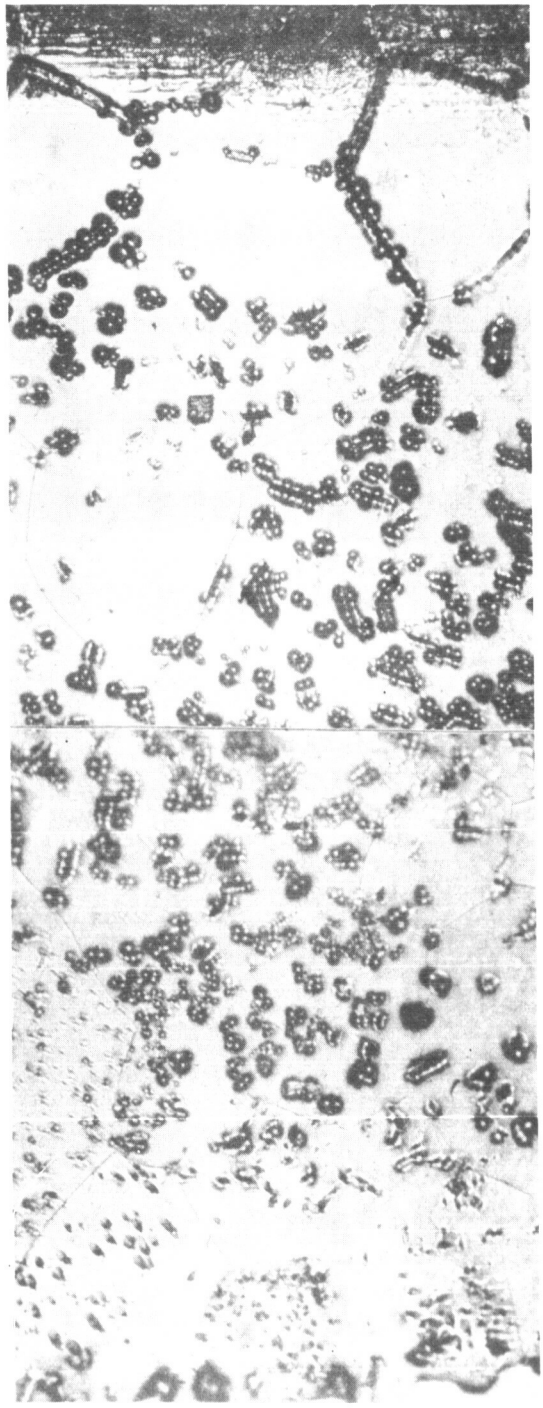


Figure 1-2. Oblique Section through Ringed Zone of Thin Wall (150X)

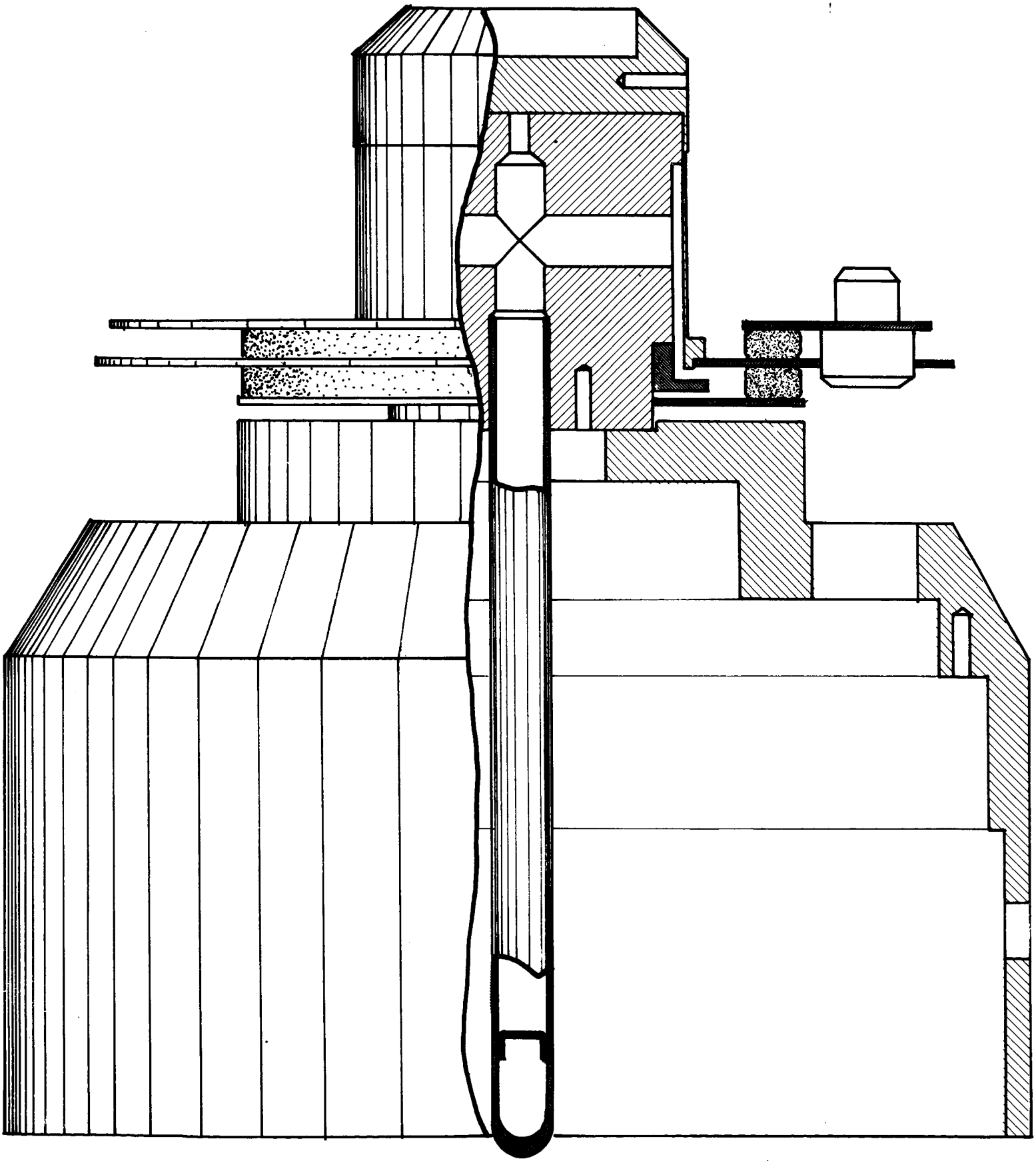


Figure 1-1. Preliminary Design of Series VII Converter.

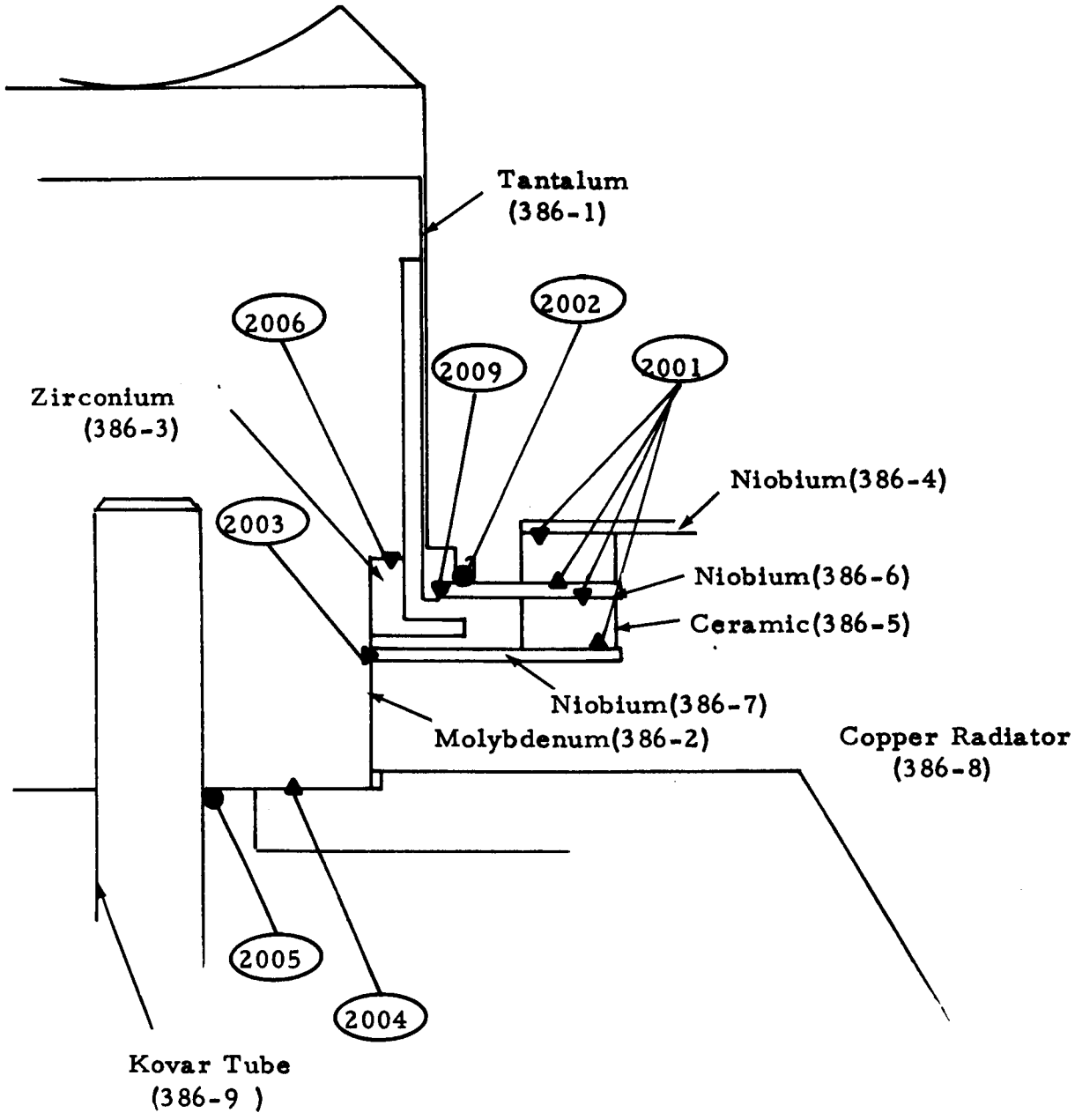


Figure 1-5. CT-A and CT-B Braze Locations

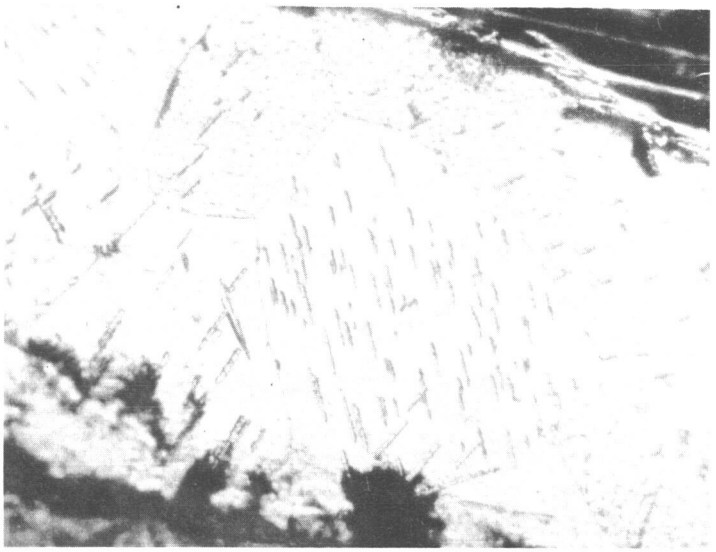


Figure 1-3. Precipitate Particles in Thin Wall Section (300X)

5095

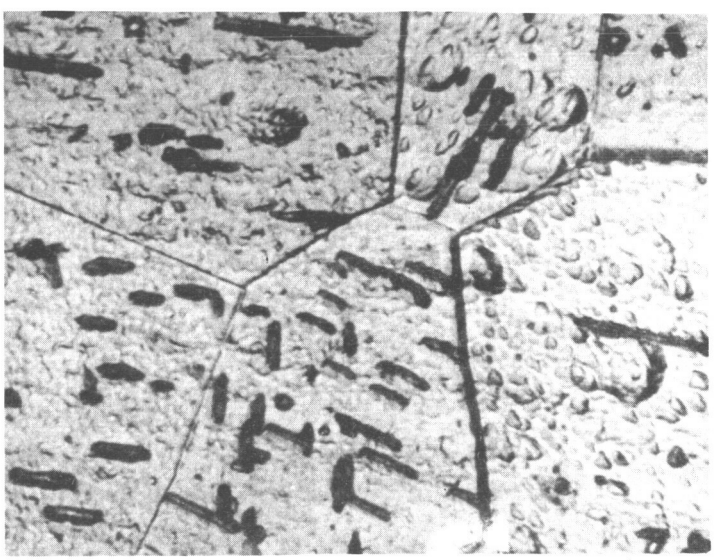


Figure 1-4. Precipitate Particles in Thin Wall Section (560X)

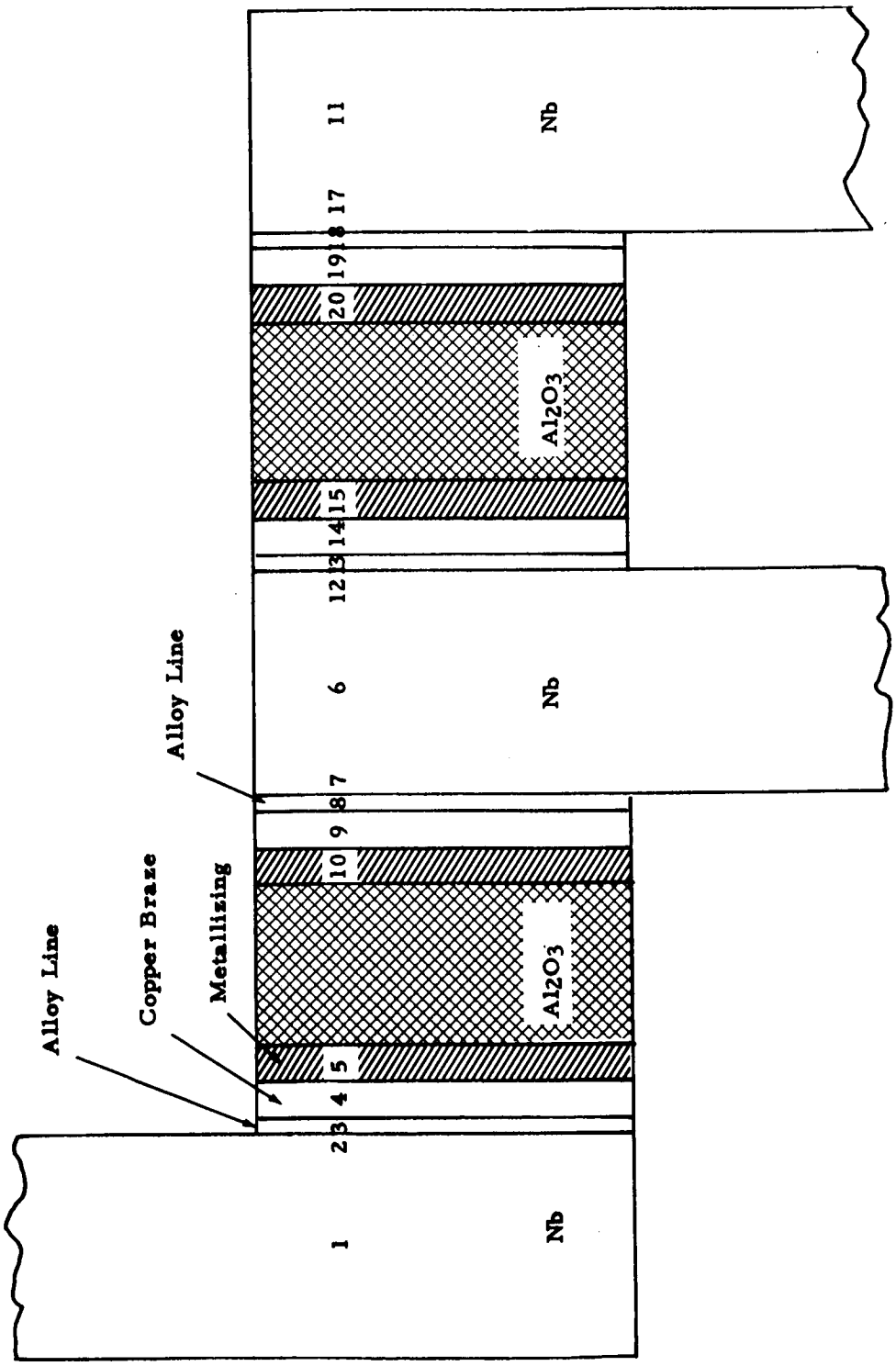


Figure 1-7. Key to Tukon Indentations for Seal Structure (2001)

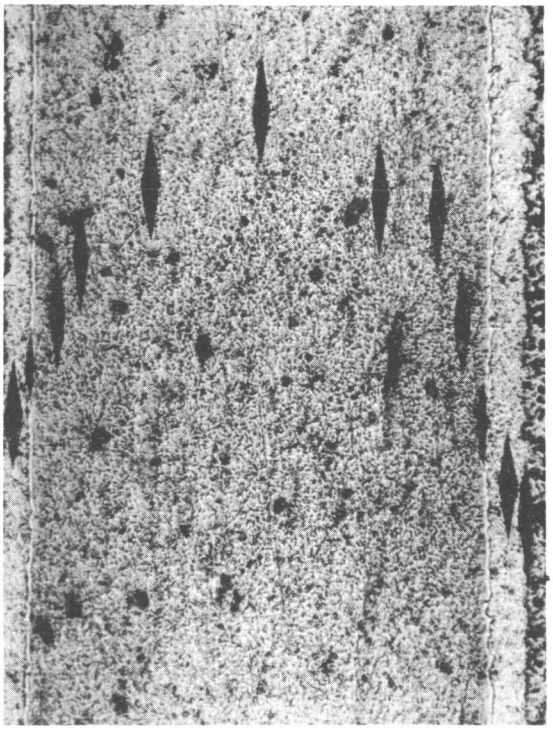


Figure 1-6. Photomicrograph of Ceramic (386-5) to Emitter Flange (386-6). (150X)

TABLE 1-1

TABULATION OF KNOOP HARDNESS NUMBERS

Location	Indent. No.	CT-A_1*	CT-B_3	CT-B_2	CT-B_2	CT-B_2
Braze 2001						
Nb flange	1			129		
adj to braze	2	147	168	144		111
alloy line	3					
copper braze	4					
metallization	5					
Nb flange	6			192	140	
	7	152	134	176	154	
	8			137	260	
	9			150	158	
	10				246	
Nb flange	11	158	141	113		
	12	148	146	143	157	
	13				253	
	14			156	151	
	15				259	
Nb flange	16					
	17	137	142	120		
	18					
	19					
	20					
Braze 2002						
Ta	21					
Ta adj	22	206	582			
Copper braze	23	451	534			
Nb adj	24	163	114			
Nb	25					
Braze 2004						
Mo	31					248
Mo adj	32	290	274			240
Ti br. interface	33	520	470			438
Copper adj	34	140	106			358
Copper	35					93

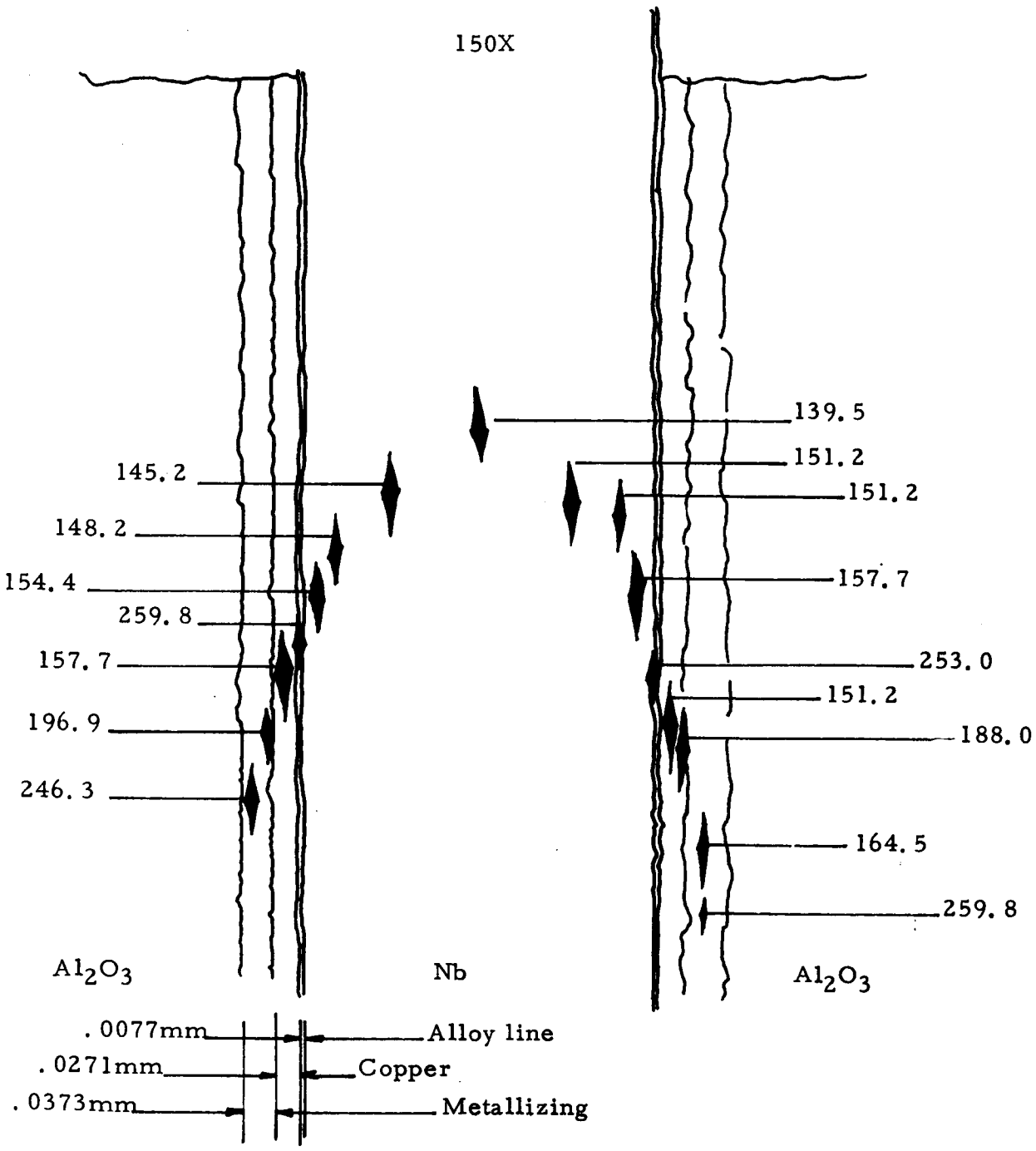


Figure 1-8. Hardness Map of Ceramic (386-5) to Emitter Flange (386-6)

TABLE 1-1 (Cont' d)

Location	Indent No.	CT-A_1*	CT-B_3	CT-B_2	CT-B_2	CT-B_2
Braze 2005						
Mo	36					290
Mo adj	37	271	271			234
Cu braze	38	157	331			145
Kovar adj	39	260	190			210
Kovar	40					168
Braze 2006						
Mo	41					
Mo adj	42	575	558			
Braze	43	632	547			
Mo adj	44	318	295			
Mo	45					
Braze 2009						
Ta	46					
Ta adj	47	630	166			
Braze	48	562	666			
Nb adj	49	156	156			
Nb	50					
Pinch off						
Fuze-out	51	176				
Fuze	52	222				
Fuze-inside	53					
Wall 1	54	172				
Wall 2	55	128				
Ta Tail-Thin Section	56					

* Subscripts refer to different quartered-sections from subassemblies CT-A or CT-B. CT-A refers to section of a converter charged with cesium while CT-B refers to a section of an uncesiated but complete converter.

Two additional experimental converters, EX-8 and 9, were also constructed this year. These were identical except for the collector surface material. EX-8 used a molybdenum collector and EX-9 a tantalum collector. The purpose of constructing these two converters was to compare the performance of tantalum versus molybdenum collectors. Standard SET converters at the time used tantalum collectors. The collector was fabricated by brazing a sheet of tantalum to a molybdenum support. Use of a solid molybdenum collector could simplify the converter' s construction and increase its reliability. As will be shown, the converter with the molybdenum collector gave the best performance.

2.2 FABRICATION OF EX-7

In view of the difficulties encountered in converters EX-1, 2, and 3 when trying to braze rhenium sheet directly to a tantalum substrate, EX-7 was constructed by pyrolitically depositing the rhenium onto a molybdenum substrate and then brazing the molybdenum to the tantalum emitter structure.

A 2-mil layer of rhenium was deposited on a molybdenum slug. Figures (2-1), (2-2), and (2-3) are photomicrographs of the rhenium surface at 100, 255, and 520 magnifications, respectively. The uniformity of the surface is readily seen. To check the adherence of the rhenium coating to the molybdenum substrate, a sample of molybdenum on which 1.5 mils of rhenium had been deposited was ground at an angle as shown in Figure (2-4), so that the molybdenum was exposed at one end, point C, and so that the layer of rhenium varied from its full thickness, point A, to practically zero, point B, where it blends into the exposed molybdenum base. At no point was there any indication of separation of the rhenium from the substrate.

Prior to construction of EX-7 detailed tests were also made of molybdenum

CHAPTER 2

FABRICATION AND MAPPING CONVERTERS EX-7, EX-8, EX-9

2.1 INTRODUCTION

In parallel with the main effort of the SET program, a smaller supplementary task was pursued endeavoring to explore certain promising converter concepts. If successful, these might at a later date be incorporated into the standard SET converter. Converters constructed in this program were designated with the prefix EX as identification of their experimental nature.

Prior to the work reported herein six such EX converters had been constructed. Of these, the first three, EX-1, 2 and 3, were built to explore the use of rhenium emitters in SET type converters. Data taken by the Thermo Electron research department on other converters showed performance considerably better than that achieved with tantalum emitters, and EX-1, 2, and 3 were constructed in an attempt to reproduce this performance in SET type converters. However, to incorporate the rhenium emitters required the development of a method of brazing the rhenium to a tantalum substrate and of the three converters only one, EX-1, reproduced the prior rhenium data. One, EX-3, encountered braze difficulties that masked its true performance. The third, EX-2, is discussed in more detail in Chapter 3. The performance of EX-1, however, was very promising and another rhenium converter, EX-7, was constructed on this year' s program to determine the reproducibility of the EX-1 data. As will be shown, to the extent to which the conductivity of the heat path through the emitter structure can be determined, converters EX-1 and EX-7 compared well. Furthermore, a careful comparison of the EX-7 data with data taken by Thermo Electron' s research department on other rhenium converters also shows excellent correspondence.

(2-16), and (2-17). In view of the very close correspondence between the corrected curves of EX-7 and those of EX-1, the assumption of a high thermal resistance in the emitter braze appeared verified. Furthermore, the conclusion can be drawn that this converter with a deposited emitter and EX-1 with a sheet rhenium emitter give comparable results. It is clear, however, that, to obtain the benefits of the use of a rhenium emitter, better means of incorporating the rhenium in the converter than those used on either EX-1 or EX-7 must be found.

A comparison of the temperature-corrected results of EX-7 with those of Thermo Electron's research department on rhenium converters* was also a goal of the program, in order to determine the extent to which SET converters could be made to reproduce the research converter results. Figure (2-18) shows the variation in interelectrode spacing of EX-7 as a function of emitter temperature. For the three emitter temperatures for which EX-7 data is available, namely 1891°, 1933° and 1993° K, the spacing is very nearly 1.9 mils. Figure (2-19) shows the research results* at 1850° K replotted to show the variation of current density versus spacing for several output voltages. In Figures (2-20) and (2-21) the same results have been plotted at 1950° and 2050° K, respectively. Figures (2-19), (2-20), and (2-21) have then been used to interpolate to the expected performance at a spacing of 1.9 mils, and this performance is plotted in Figure (2-22). Included also in Figure (2-22) is the measured performance of EX-7 at emitter temperatures of 1891°, 1933° and 1993° K. As can be seen, the EX-7 data corresponds very well with the research data.

---

* "Second Annual Technical Summary Report for the Thermionic Emitter Materials Research Program" (1 July 1962 through 30 Sept. 1963) by S.S. Kitrilakis and J.H. Weinstein, Report No. 27-64, prepared for ONR Power Branch, Dept. of the Navy, Wash. 25, D.C.

pieces brazed to the converter' s tantalum emitter structure. Figure (2-5) is a photomicrograph of the braze cross section showing the tantalum cup at the top, the braze in the center, and the molybdenum piece at the bottom. Microscopic examination and physical tests showed excellent adherence. Hardness tests indicated that satisfactory ductility had been maintained in the tantalum and molybdenum parts in the area of the braze.

The remainder of converter EX-7 was basically the same as other EX converters. A drawing of EX-7 is shown in Figure (2-6).

2.3 TESTING OF EX-7

Converter EX-7 was first tested at emitter temperatures of 1850°, 1900°, 1950°, 2000°, and 2050° K. The performance maps are shown as Figures (2-7) through (2-11). These temperatures were based on calculated values of the thermal resistance of the emitter structure which is composed of the tantalum base, the molybdenum slug, and the rhenium emitter. This data did not coincide with EX-1 results, most probably because the braze between the molybdenum and tantalum could not be made homogeneous throughout the interface, resulting in high thermal resistance. Further testing was conducted to verify this conclusion. By raising the emitter temperature to 2018° K observed, it was found that the resulting data matched the 1993° K (TES) envelopes of EX-1 reported in the diode improvement program final report, July, 1962. This suggested a thermal resistance four times greater than the predicted value computed from the thermal conductivity of tantalum and molybdenum. Using this resistance in the calculation of emitter temperatures, the EX-7 results were compared with EX-1 data at the 1938° K and 1891° K levels. The comparative results are shown in Figures (2-12), (2-13), and (2-14), and the corresponding maps in Figures (2-15),

diodes. Figure (2-27) shows performance maps of the two converters at an emitter temperature of 1850° K. Figure (2-28) shows the comparitive performance at a few discrete cesium temperatures. Maps were also made at other collector temperatures, but for comparison purposes, those with the highest performance have been chosen. There clearly exists at this emitter temperature a difference between EX-8 and EX-9. The envelope of EX-9 is shifted to the left of that of EX-8. The slopes of the unignited and ignited modes of the two converters appear very similar in the two maps. The major change in slope in the EX-8 map, Figure (2-27), occurs at an output voltage of approximately 0.85 volt.* The change of slope in the EX-9 map occurs at an output voltage of approximately 0.7 volt. The difference between these two voltages can be used as a measure of the shift in the envelopes. Alternatively, the difference can be measured by comparing output currents at the same output voltage. At 0.75 volt output, EX-8 has an output of 13 amperes compared with 6 for EX-9.

Similar observations can be made from the envelopes taken at an emitter temperature of 1900° K and are shown in Figure (2-29). As the emitter temperature is raised to 1950° K, with the resulting envelopes shown in Figure (2-30), and 2000° K, as shown in Figure (2-31), the differences between the two converters become much less. However, the required radiating area to achieve optimum collector temperature had been underestimated, and, at the higher emitter temperatures with the resulting higher heat fluxes through the

*Note: Each major division of the abscissa is equal to 0.25 volt, and each major division of the ordinate is equal to 5 amperes. The origin is marked by the scale intersection closest to the bright dot.

2.4 CONSTRUCTION OF EX-8 AND EX-9

Converters EX-8 and EX-9 were virtually identical in design and construction, with the one exception that EX-8 had a molybdenum collector while EX-9 had a tantalum collector. Figures (2-23) and (2-24) are drawings of EX-8 and EX-9, respectively. Figure (2-25) shows the variation in spacing of these converters as a function of the emitter surface temperature. This curve is obtained by calculation of the expansion of each structural member from the collector surface to the emitter surface. Figure (2-26) shows the emitter and collector temperature drop versus the converter's output current density. The corrections implied by these curves must be applied both to the emitter temperature measured in the pyrometer hole to obtain the emitter surface temperature and to the collector base temperature measured with the collector thermocouple to determine the true collector surface temperature. Both sets of curves of Figure (2-26) have been calculated by using the thermal and electrical conductivity of the appropriate materials.

2.5 TESTING OF EX-8 AND EX-9

The performance of converters EX-8 and EX-9 was mapped using a dynamic test setup. Various discrete collector temperatures were chosen at each emitter temperature of interest and the cesium temperature was then scanned through its range of interest. By observing the resulting I-V curves on an oscilloscope and recording these photographically, performance envelopes of the converters are obtained. The upper boundary of each envelope is the converter's optimum performance.

The reason for testing EX-8 and EX-9 is to compare the performance of a molybdenum collector versus a tantalum collector in two otherwise identical

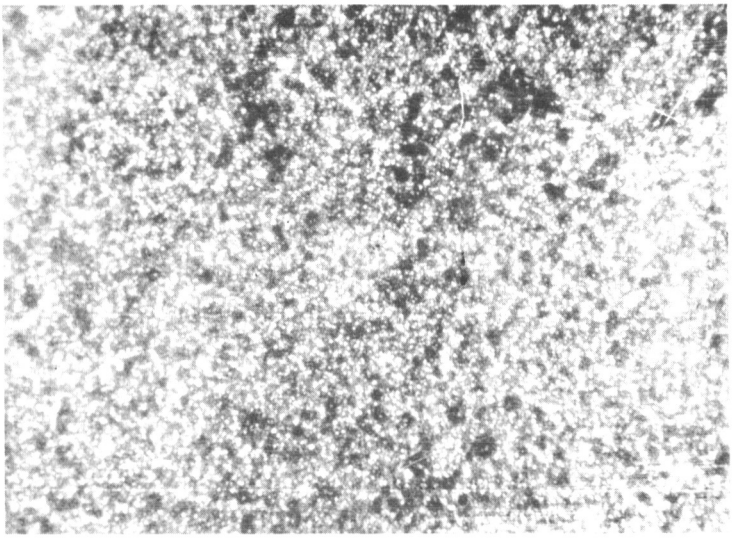


Figure 2-1. Photomicrograph of Pyrolytically Deposited Rhenium on Molybdenum. (100X)

collector, it was not possible to adequately cool and optimize the collector. The 1850° and 1900° K data, therefore, reflect much more accurately the differences between the optimum performances of the two diodes. This data suggests that the use of a molybdenum versus a tantalum collector results in a converter with higher performance. Further verification by constructing and testing diodes with more versatile collector cooling and heating provisions for high-emitter-temperature performance would be very desirable.

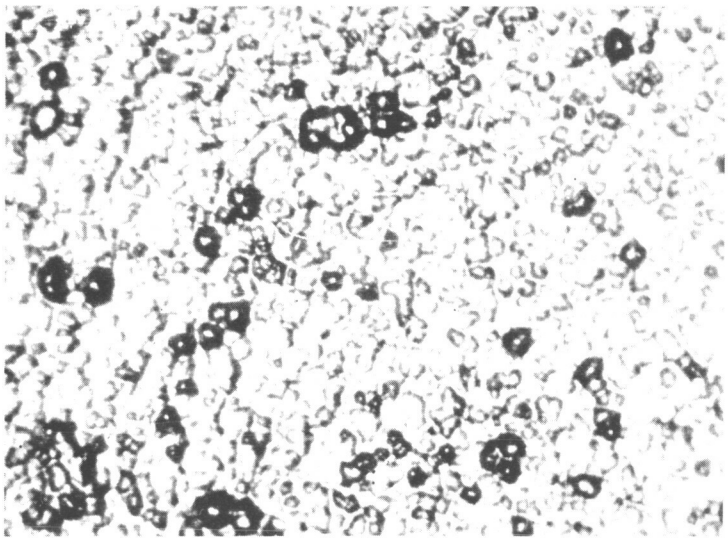


Figure 2-2. Photomicrograph of Pyrolytically Deposited Rhenium on Molybdenum (255X)

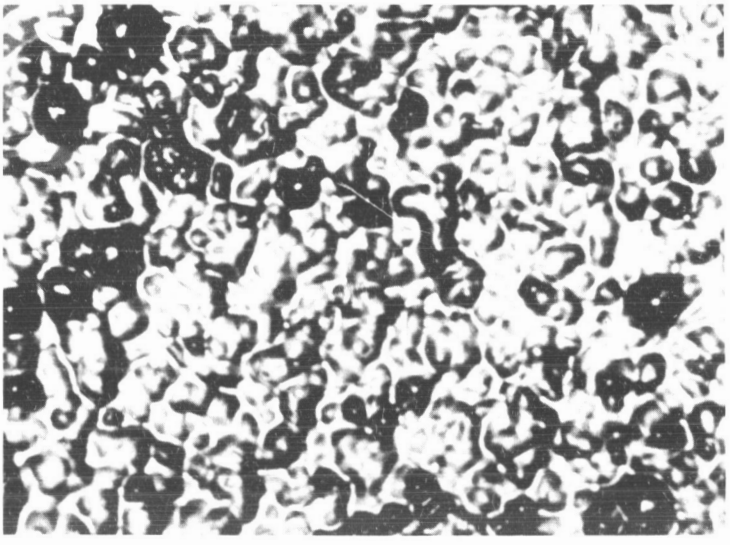


Figure 2-3. Photomicrograph of Pyrolytically Deposited Rhenium on Molybdenum. (520X)

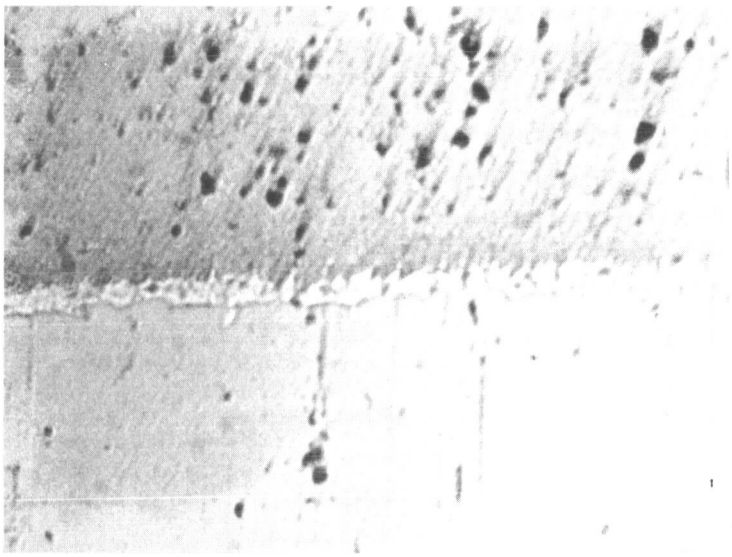


Figure 2-5. Photomicrograph of Molybdenum Brazed to Tantalum (266X)

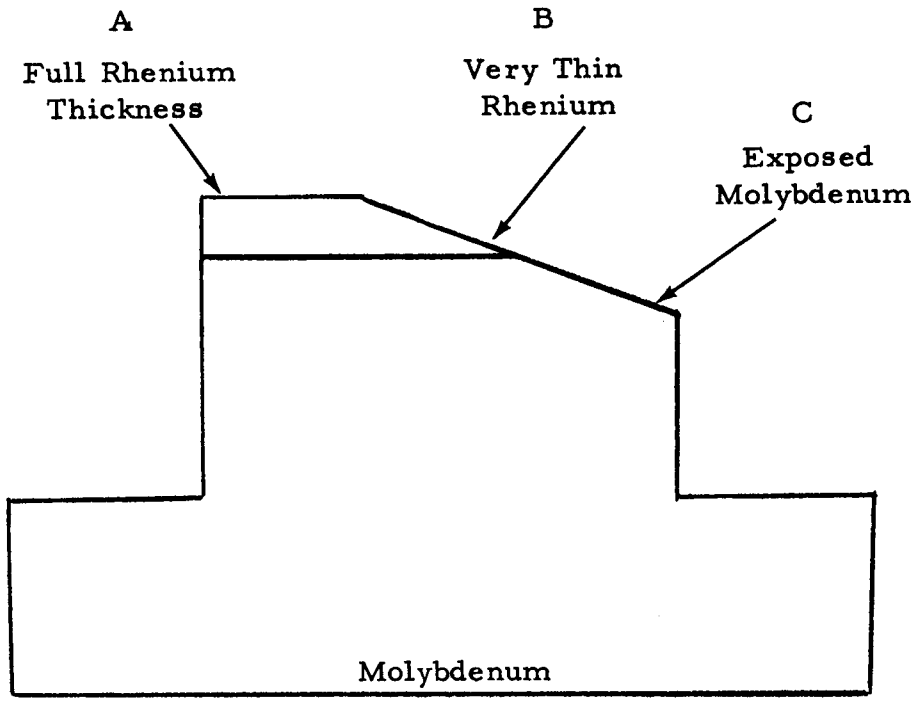


Figure 2-4. Ground Specimen for Examination of Rhenium Deposited on Molybdenum

5096

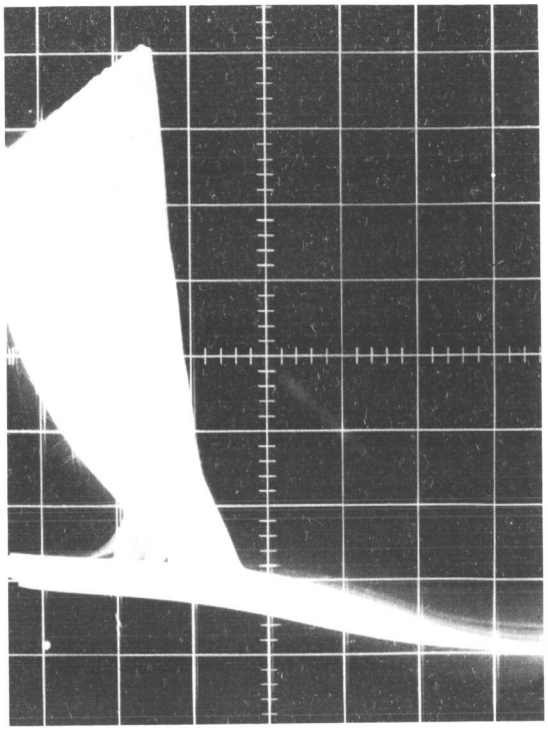


Figure 2-7, EX-7 at T_E = 1850°K

T_E = 1850°K

$T_{(Coll)}$ = 885°K

T_{Cs} = 532-618°K

5097

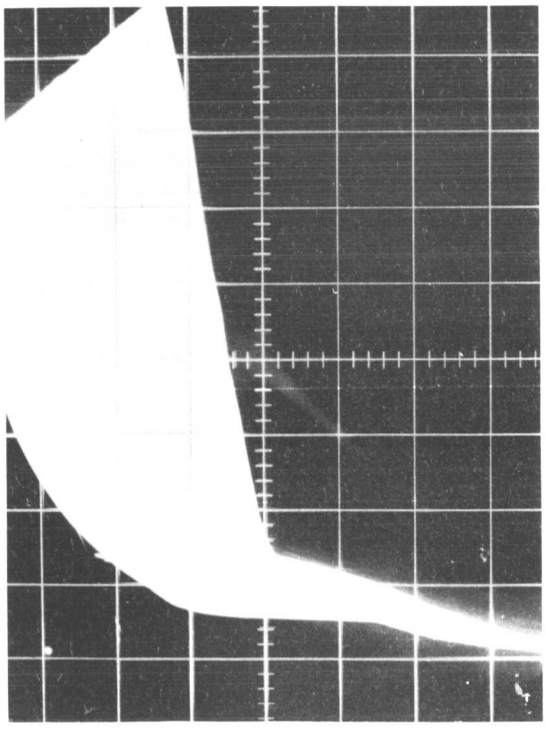


Figure 2-8, EX-7 at T_E = 1900°K

T_E = 1900°K

$T_{(Coll)}$ = 863°K

T_{Cs} = 541-622°K

Figure 2-6. Cross-section of EX-7 Converter

(See Volume II)

5100

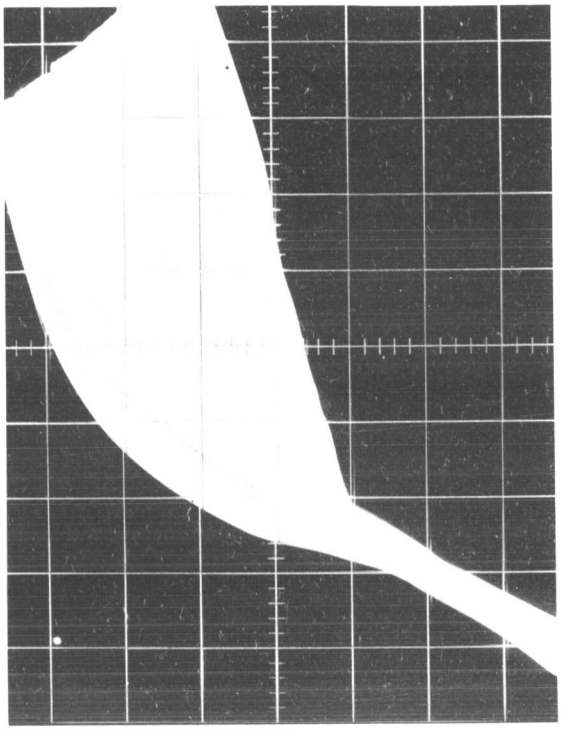


Figure 2-11, EX-7 at T_E = 2050°K

T_E	=	2050°K
$T_{(Coll)}$	=	899°K
T_{Cs}	=	575-626°K

5098

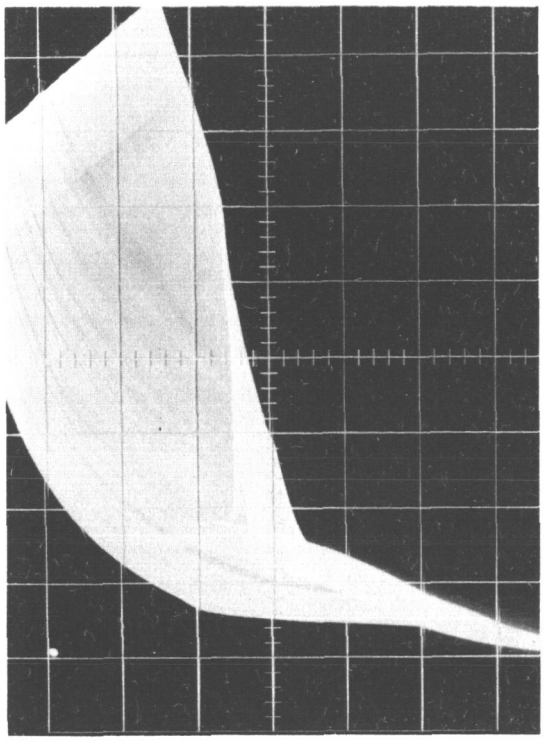


Figure 2-9, EX-7 at T_E = 1950°K

T_E = 1950°K
$T_{(Coll)}$ = 874°K
T_{Cs} = 541-616°K

5099

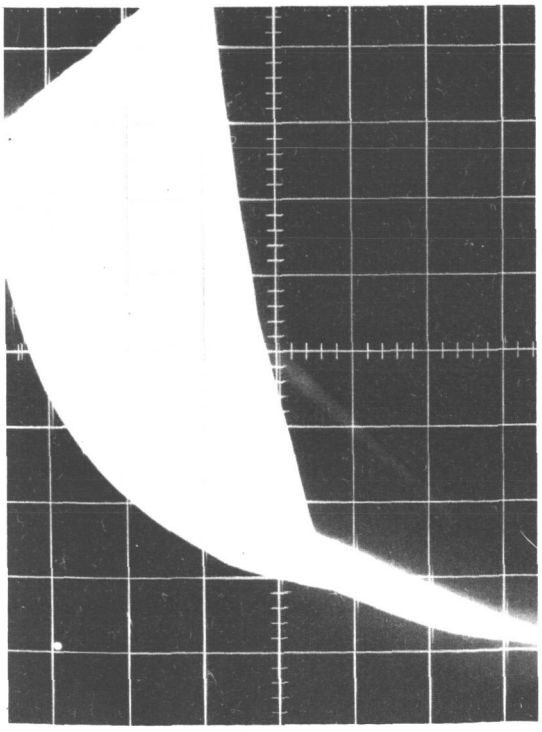


Figure 2-10, EX-7 at T_E = 2000°K

T_E = 2000°K
$T_{(Coll)}$ = 879°K
T_{Cs} = 558-641°K

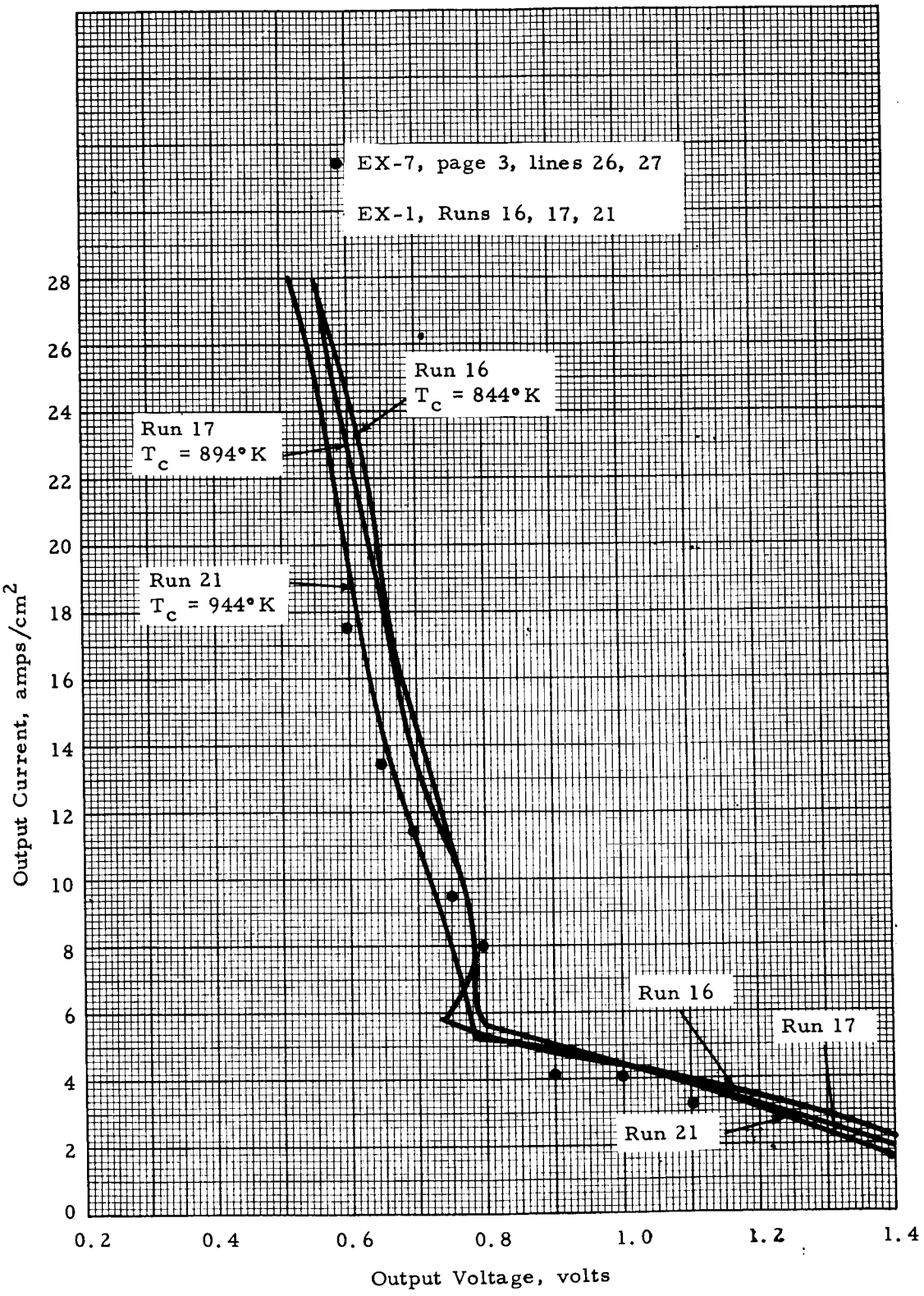


Figure 2-13. IV Envelopes for EX-1 and EX-7 at 1933°K (TES)

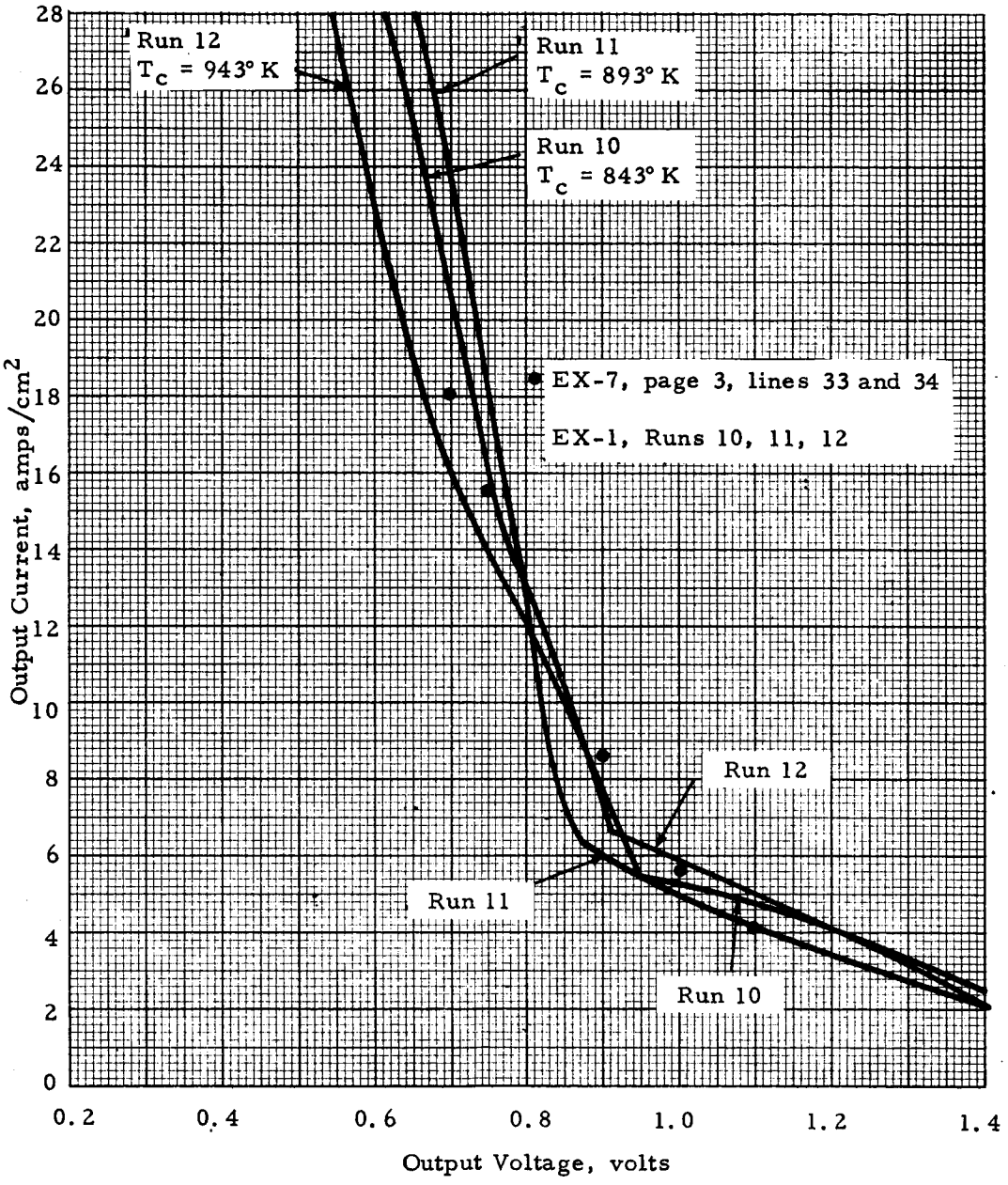


Figure 2-12. IV Envelopes for EX-1 and EX-7 at 1993°K (TES)

5101

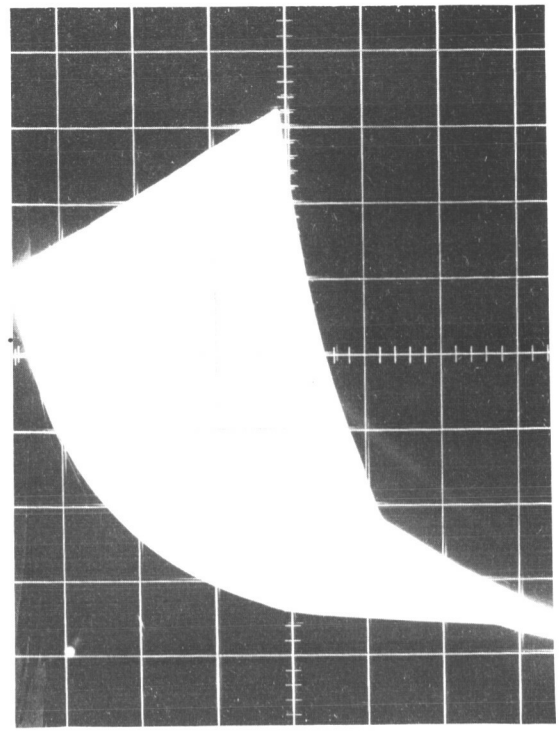


Figure 2-15, EX-7 at T_E = 1993°K (corrected)

T_E = 1993°K

$T_{(Coll)}$ = 876°K

T_{Cs} = 546-642°K

5102

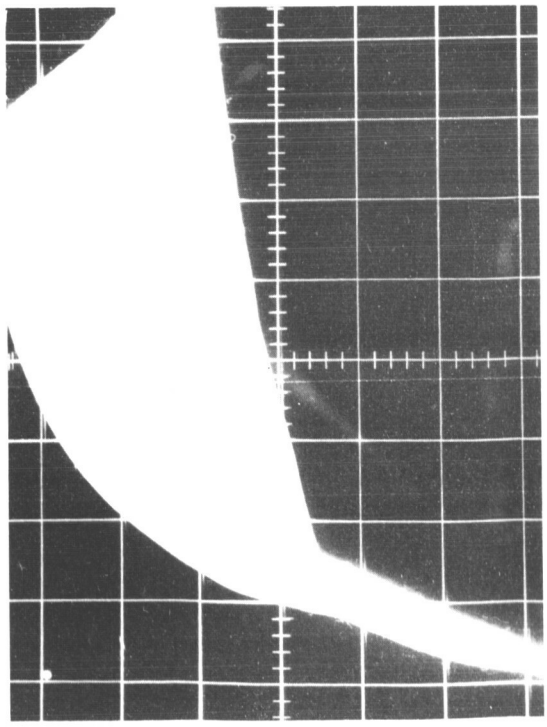


Figure 2-16, EX-7 at T_E = 1933°K (corrected)

T_E = 1933°K

$T_{(Coll)}$ = 880°K

T_{Cs} = 558-641°K

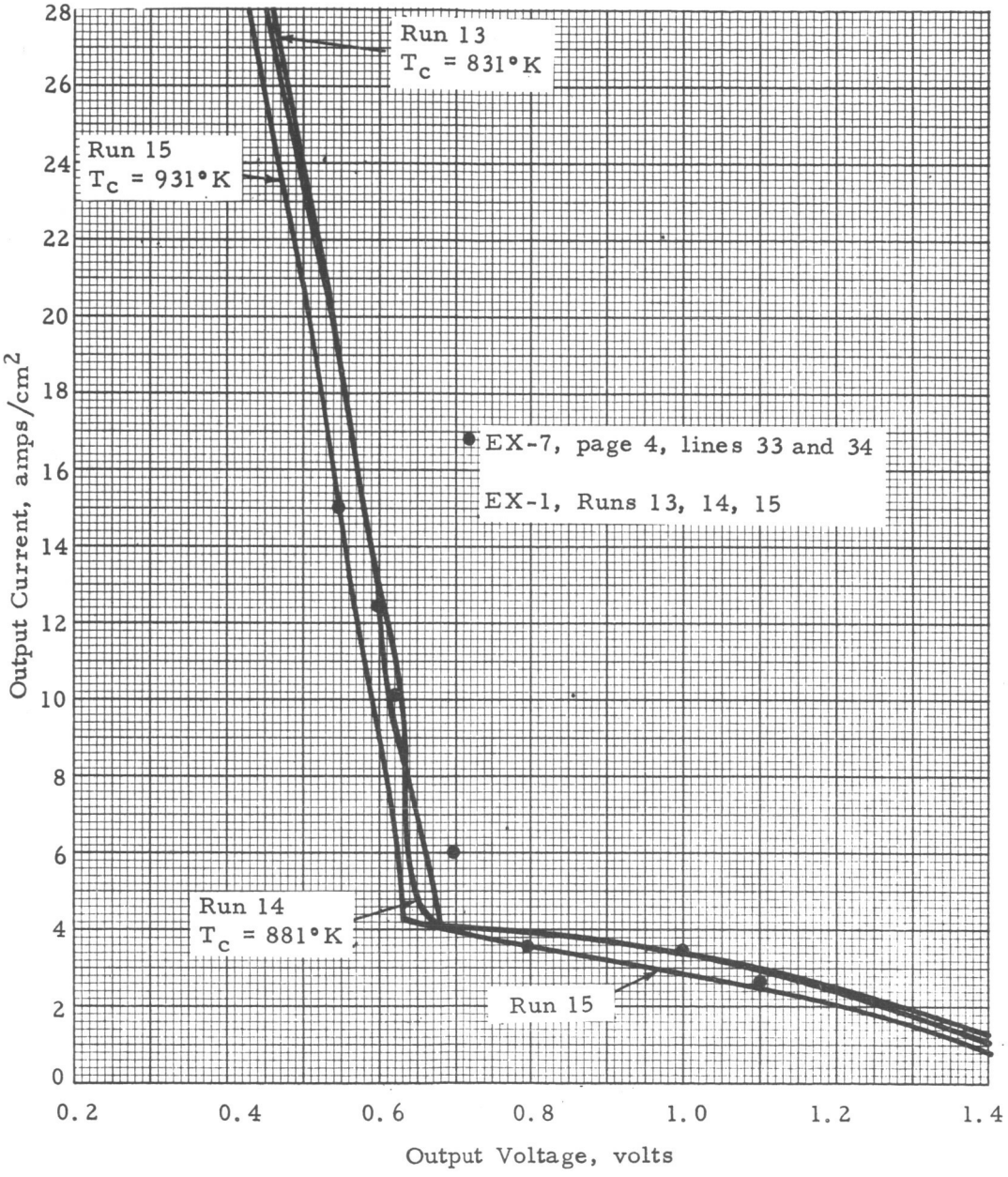


Figure 2-14. IV Envelopes for EX-1 and EX-7 at 1891°K (TES)

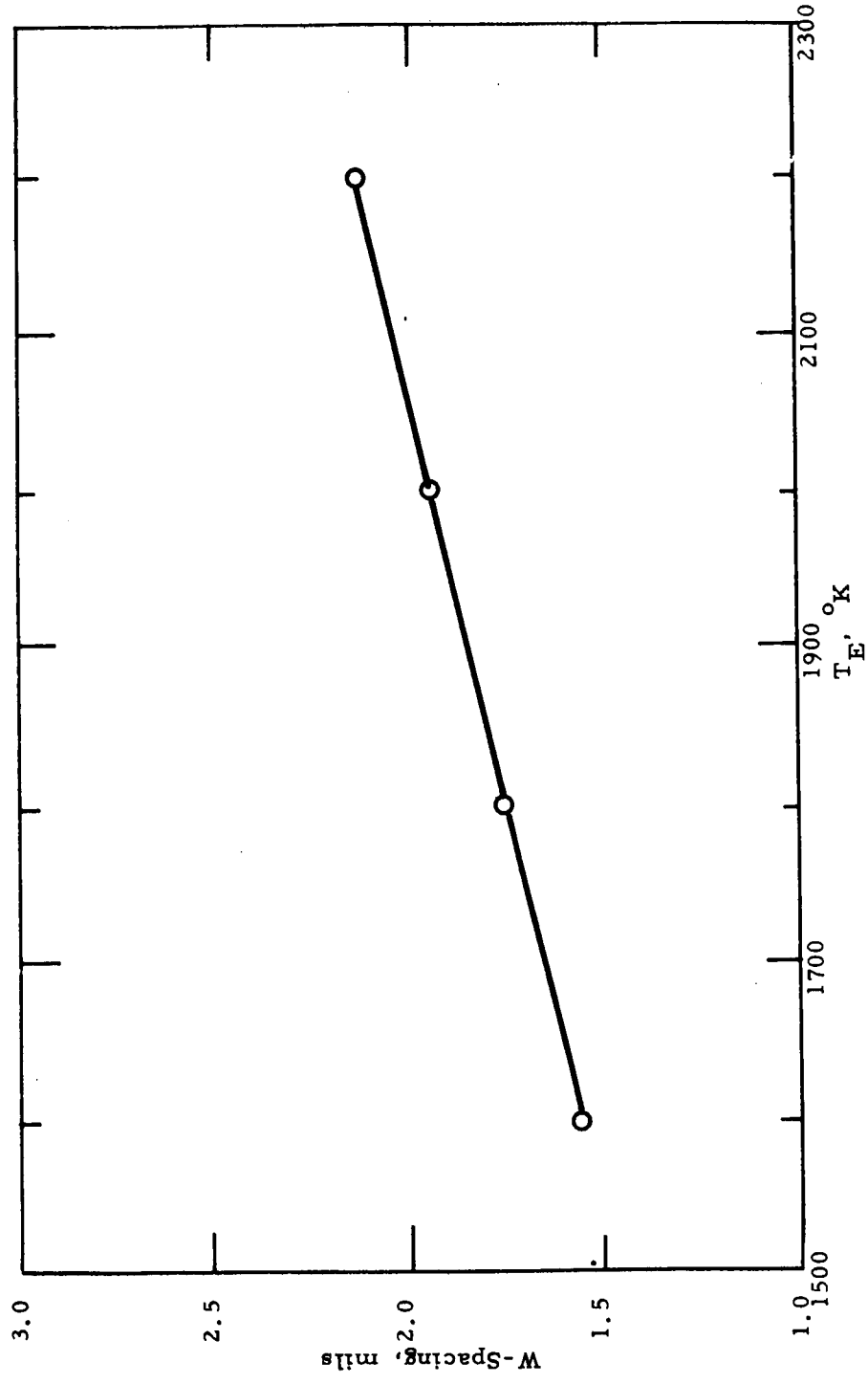


Figure 2-18

EX-7 Spacing vs. Emitter Temperature

5103

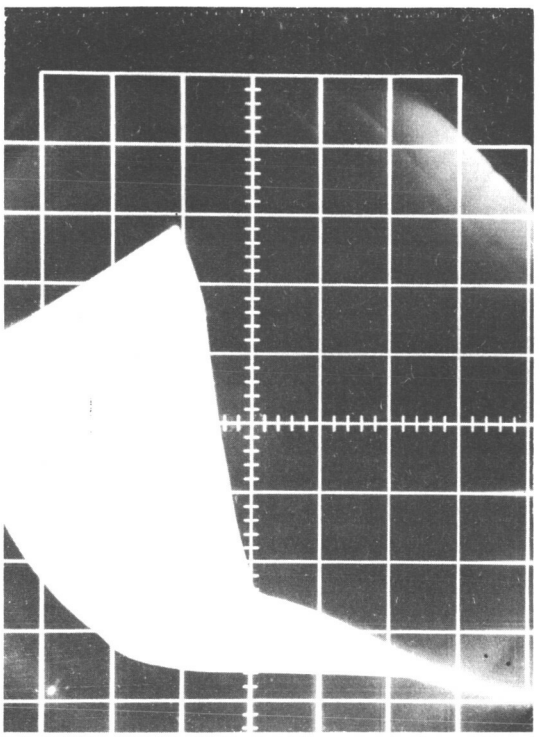


Figure 2-17, EX-7 at T_E = 1891°K(corrected)

T_E = 1891°K

$T_{(Coll)}$ = 909°K

T_{Cs} = 558-641°K

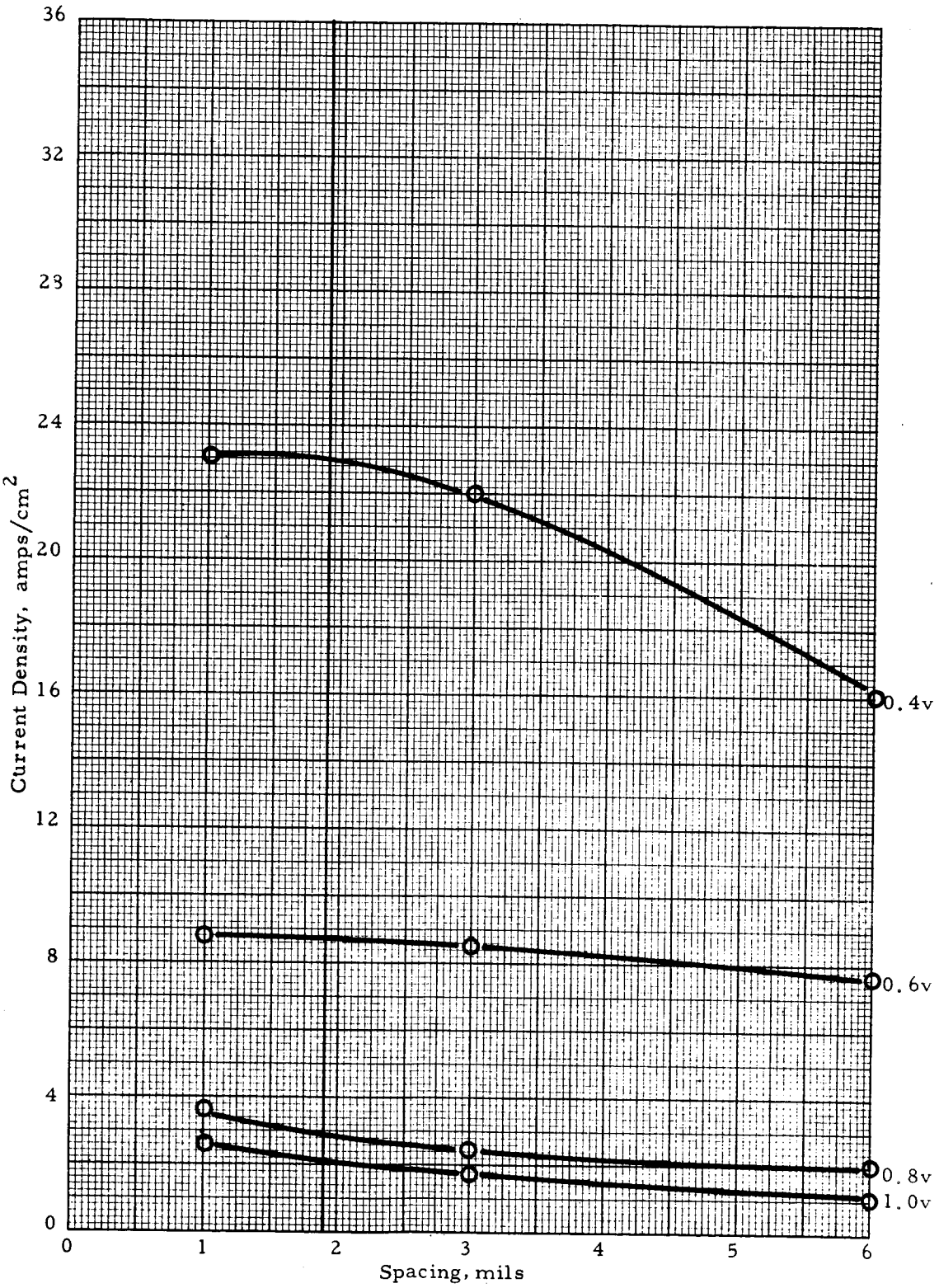


Figure 2-19. Current Density Vs. Spacing for a Rhenium Diode with an Emitter Temperature of 1850°K

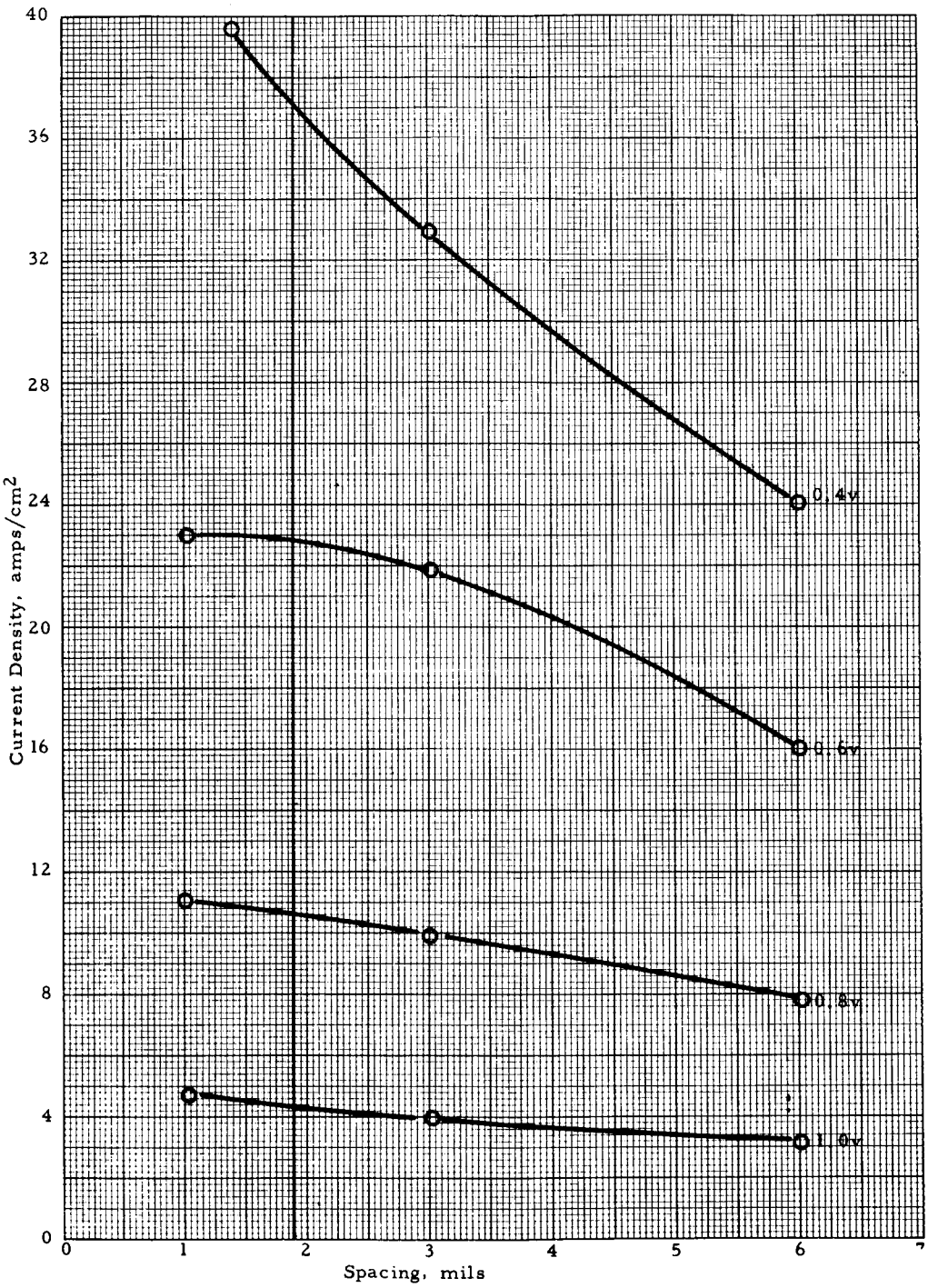


Figure 2-20. Current Density Vs. Spacing for a Rhenium Diode with an Emitter Temperature of 1950°K

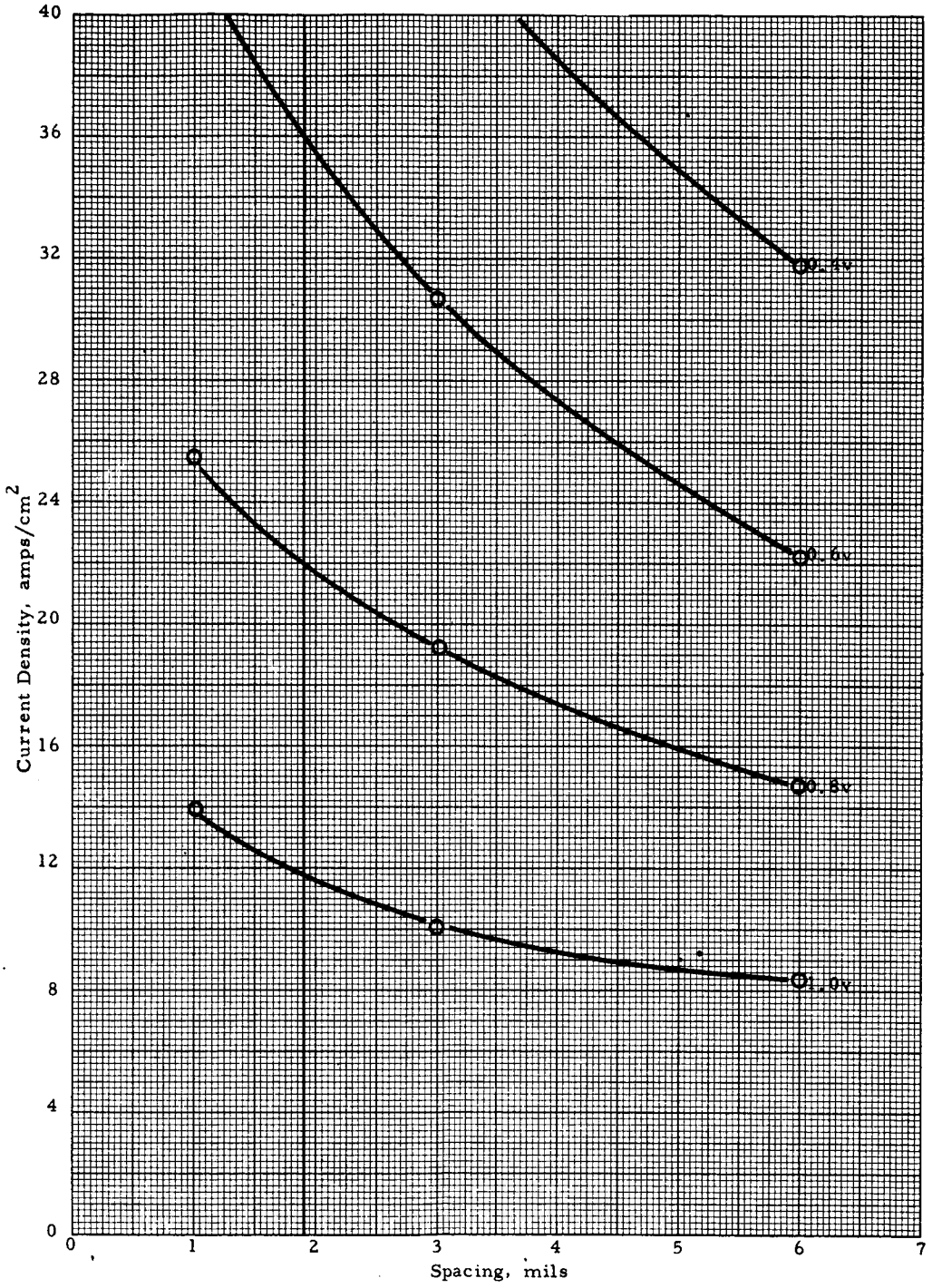


Figure 2-21. Current Density Vs. Spacing for a Rhenium Diode with an Emitter Temperature of 2050°K

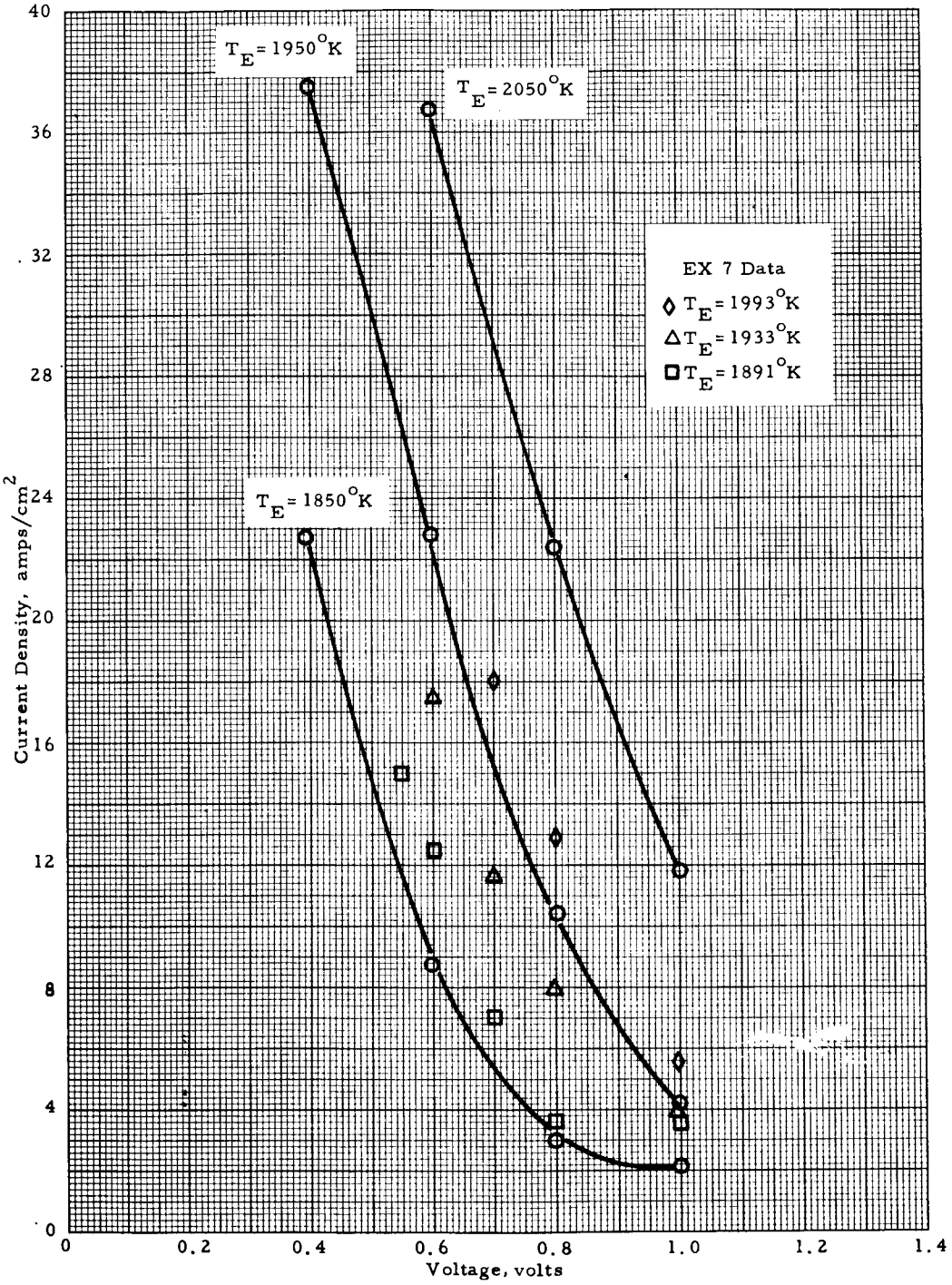


Figure 2-22. Performance of EX-7 compared with that of a Research Rhenium Diode.

Figure 2-23. Cross-section of EX-8 Converter

(See Volume II)

Figure 2-24. Cross-section of EX-9 Converter

(See Volume II)

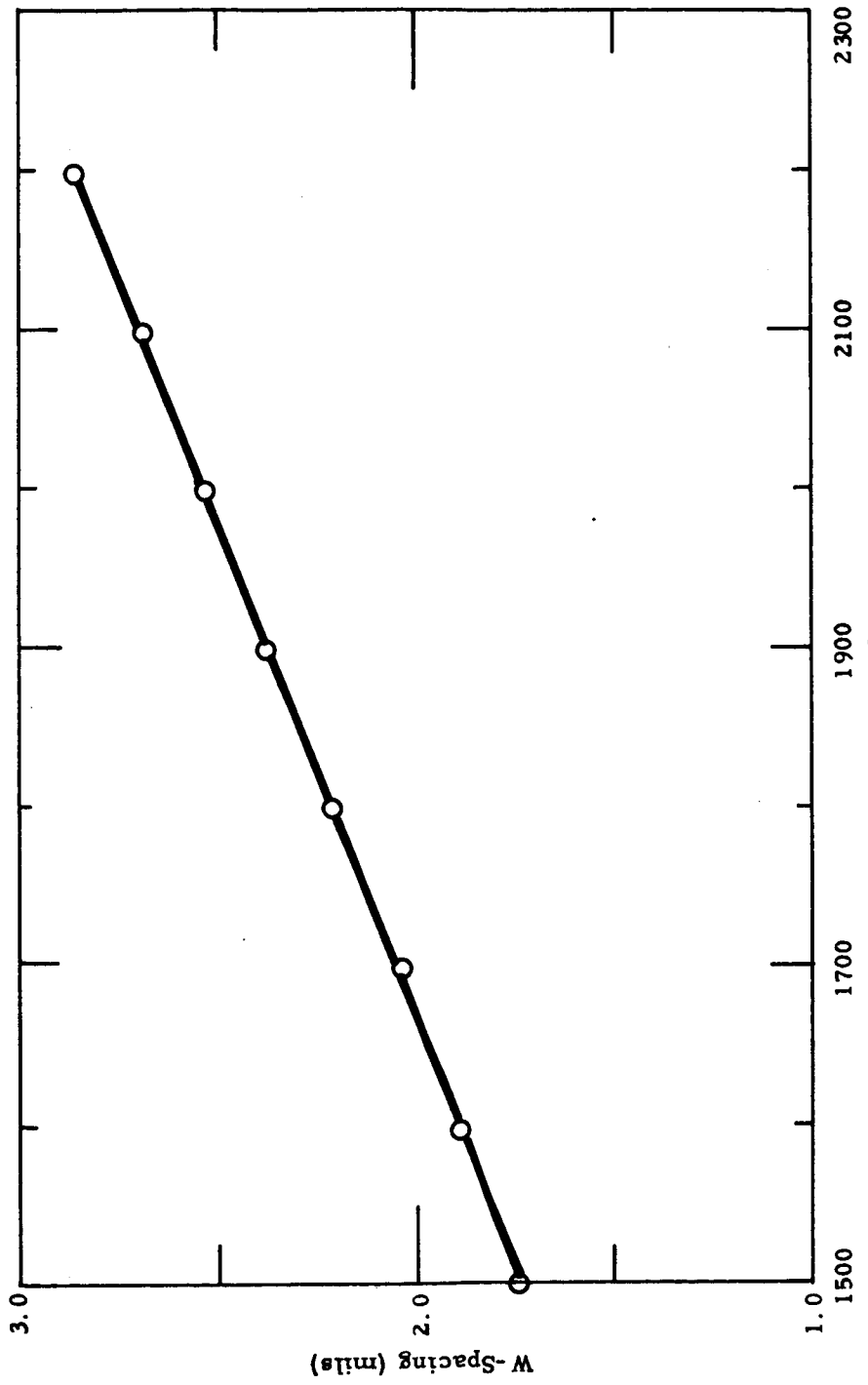


Figure 2-25. EX-8 and EX-9 Spacing Vs. Emitter Temperature

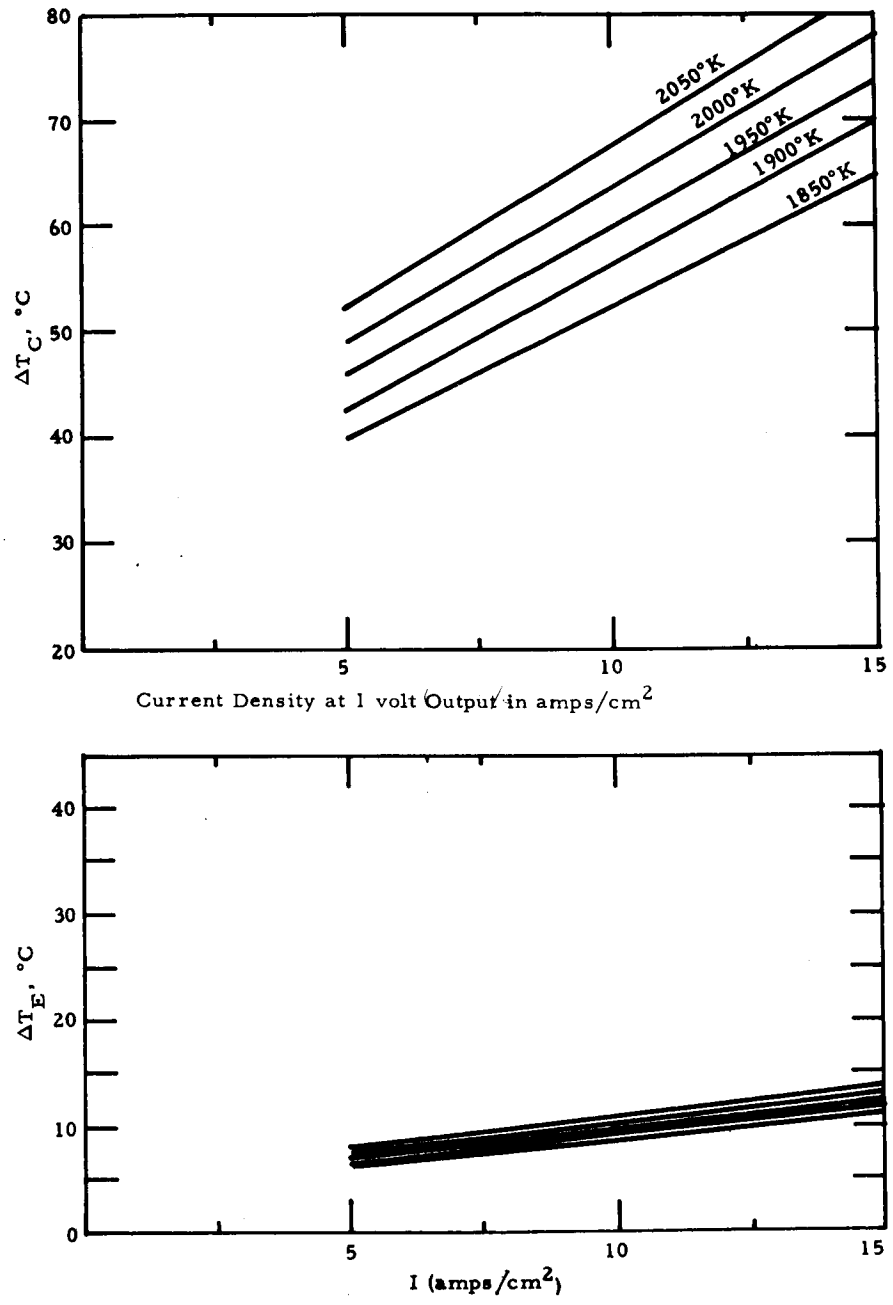


Figure 2-26. Emitter and Collector Temperature Drop Vs. Output Current Density for EX-8 and EX-9.

5104

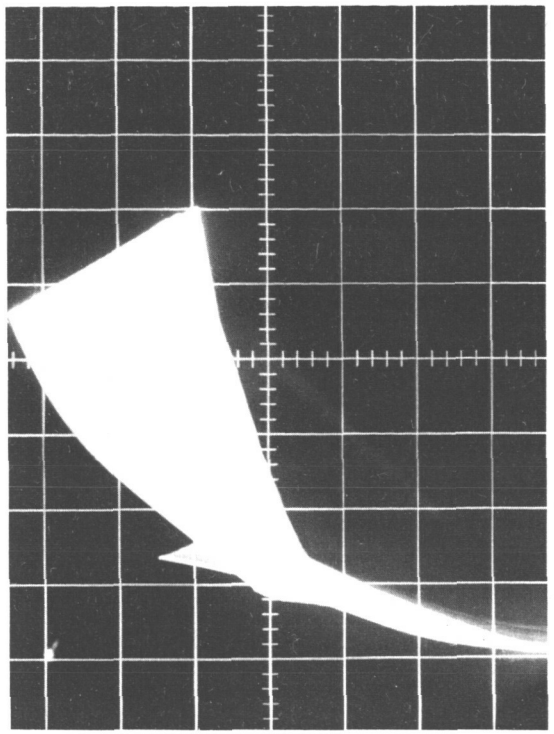


Figure 2-27(a), EX-8 at T_E 7 1850°K

T_E = 1850°K
$T_{(Coll)}$ = 845°K
T_{Cs} = 580-647°K

5105

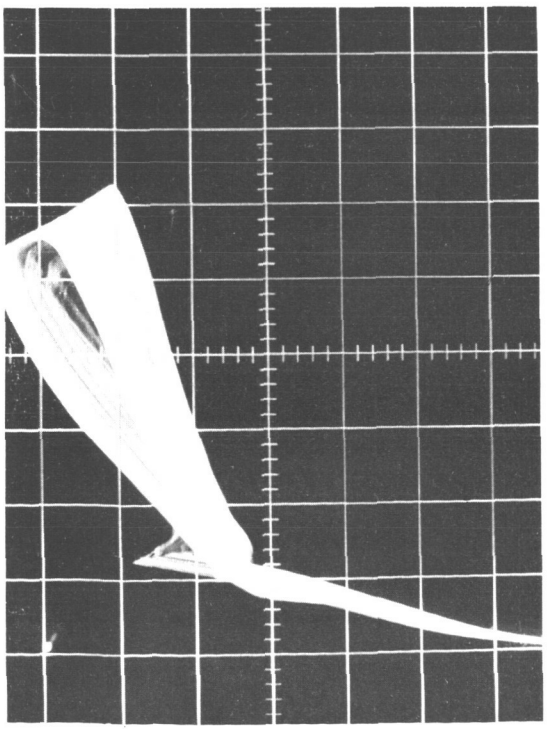


Figure 2-27(b), EX-9 at T_E = 1850°K

T_E = 1850°K
$T_{(Coll)}$ = 865°K
T_{Cs} = 592-652°K

5106

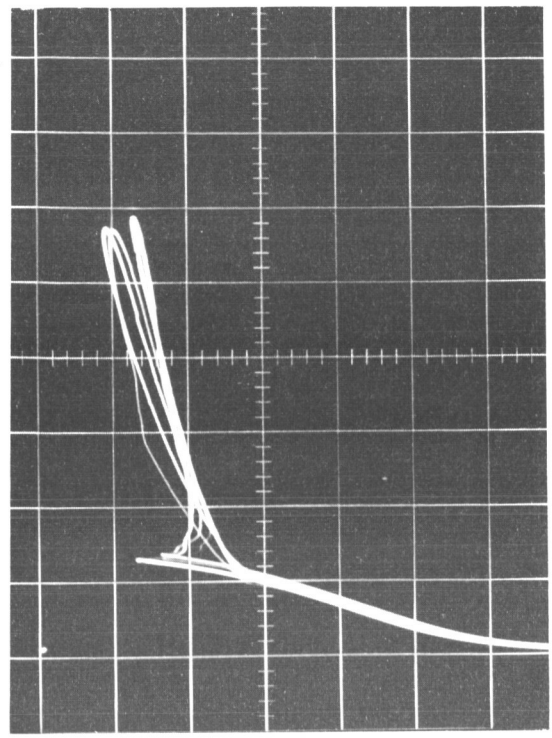


Figure 2-28(a), EX-9 at T_E = 1850°K and Several Cesium Temperatures

T_E = 1850°K
$T_{(Coll)}$ = 861°K
T_{Cs} = 617, 626, 635°K

5107

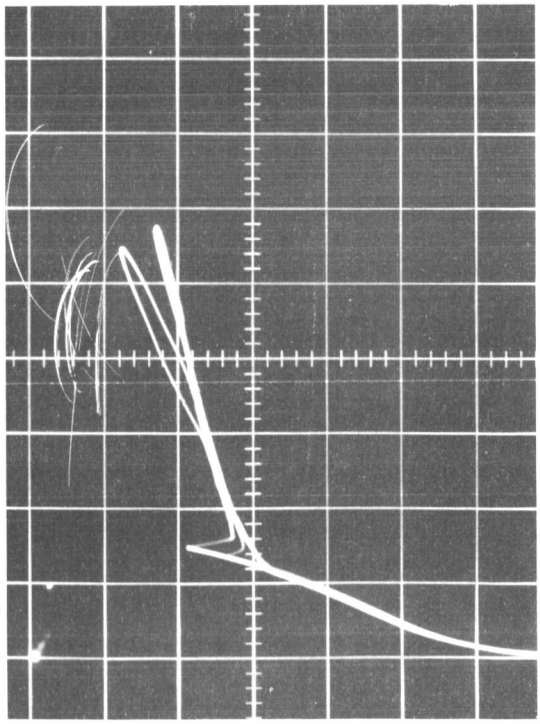


Figure 2-28(b), EX-8 at T_E = 1850°K and Several Cesium Temperatures

T_E = 1850°K
$T_{(Coll)}$ = 845°K
T_{Cs} = 614,623°K

5108

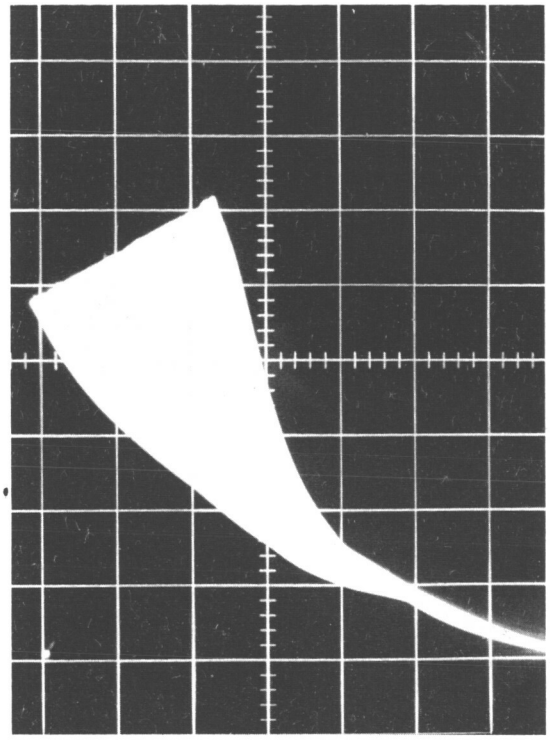


Figure 2-29(a), EX-8 at T_E = 1900°K

T_E = 1900°K

$T_{(Coll)}$ = 874°K

T_{Cs} = 597-647°K

5109

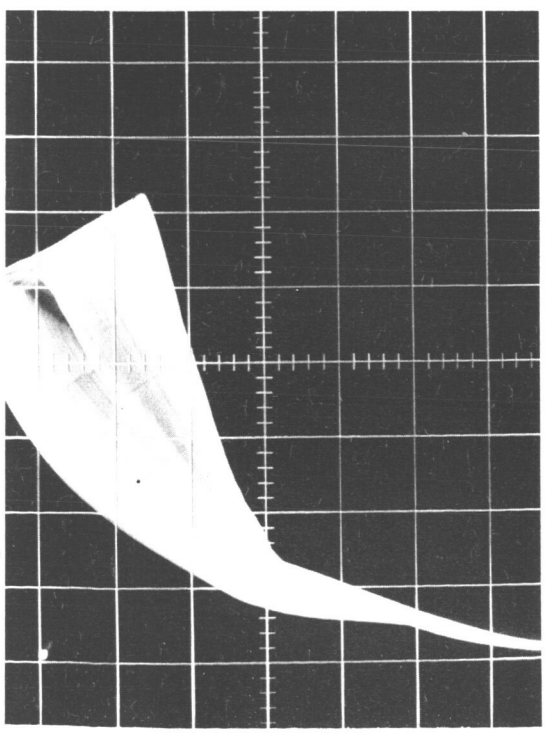


Figure 2-29(b), EX-9 at T_E = 1900°K

T_E = 1900°K

$T_{(Coll)}$ = 862°K

T_{Cs} = 577-649°K

5110

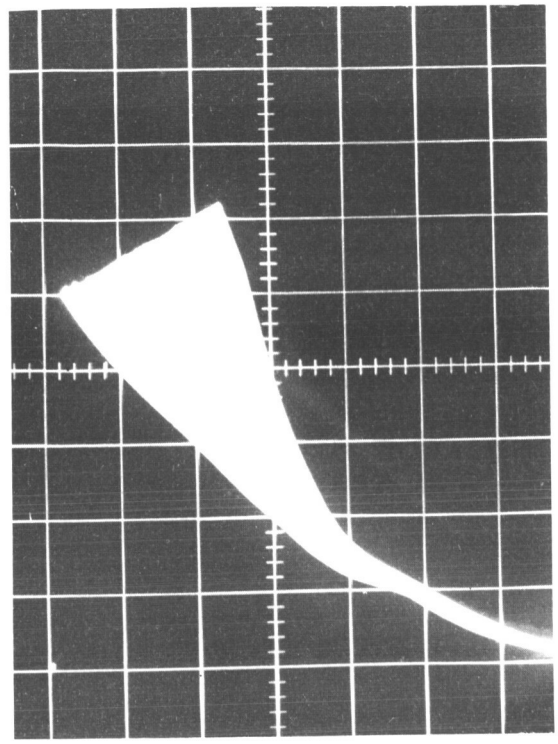


Figure 2-30(a), EX-8 at T_E = 1950°K

T_E = 1950°K
$T_{(Coll)}$ = 898°K
T_{Cs} ≐ 609-646°K

5111

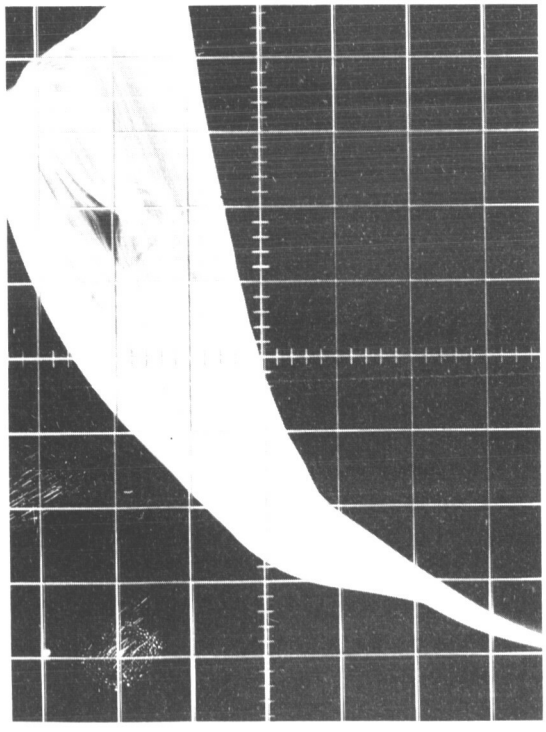


Figure 2-30(b), EX-9 at T_E = 1950°K

T_E = 1950°K
$T_{(Coll)}$ = 888°K
T_{Cs} = 590-649°K

5112

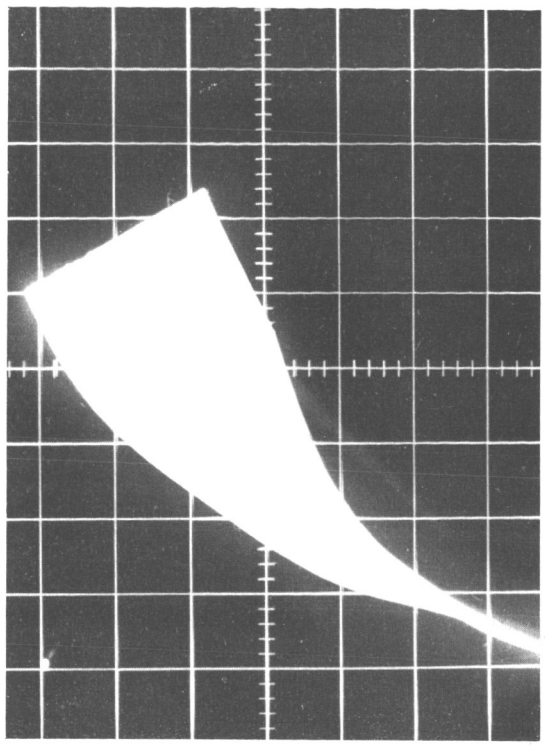


Figure 2-31(a), EX-8 at T_E = 2000°K

T_E = 2000°K

$T_{(Coll)}$ = 895°K

T_{Cs} = 602-645°K

5113

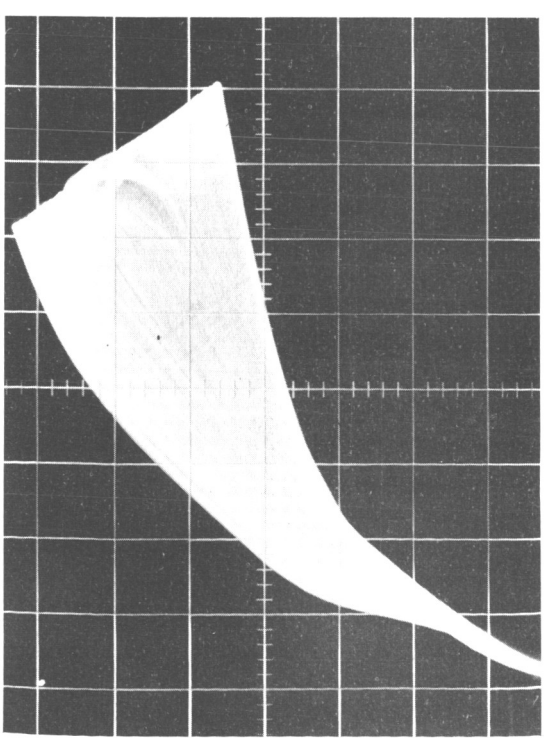


Figure 2-31(b), EX-9 at T_E = 2000°K

T_E = 2000°K

$T_{(Coll)}$ = 900°K

T_{Cs} = 597-649°K

CHAPTER 3

MAPPING OF EX-2 AND EX-6

3.1 INTRODUCTION

In addition to constructing the three new EX converters, two others, EX-2 and EX-6, that were constructed and delivered on a prior year's contract were returned to Thermo Electron for more extensive performance mapping. EX-6 used a tungsten emitter and tantalum collector. Earlier testing showed a performance well below both tantalum and rhenium converters and the new tests confirmed the earlier results.

The additional testing of EX-2 on the other hand resulted in very significant new information. The performance of EX-2 when carefully mapped and compared with EX-1 showed a very similar difference in performance to that between converters EX-8 and EX-9. Since EX-1 and EX-2 differ principally in that the former has a molybdenum collector and the latter's collector is tantalum, further support is given to the significance of the differences in performance of EX-8 and EX-9. Furthermore, the inference that a molybdenum collector produces better performance than one of tantalum is again suggested.

A detailed discussion of the performance testing of converters EX-2 and EX-6 follows.

3.2 TESTING OF EX-2

Figures (3-1) through (3-11) show the data taken in testing converter EX-2. As with EX-8 and EX-9, a wider range of collector temperatures could be scanned at the lower emitter temperatures. At the higher emitter temperatures it is possible that the optimum collector temperature was never reached due to

inadequate cooling. Figure 3-12 shows the temperature corrections applied to the observed emitter and collector temperatures to compensate for the temperature gradients. Figures 3-13 through 3-17 show the comparison of EX-1 and 2. The data at the most nearly equal emitter and collector temperatures have been chosen and in all cases the curves shown are the upper limit of the envelopes, i.e., the optimum performance at each output voltage. As can be seen from the data, EX-1 performance appears nearly identical to EX-2 in shape, but there is a shift to the right in output voltage. At 1850°K, the shift is between 80 and 110 millivolts. At 2050°K, the shift is about 50 millivolts. Since both converters were virtually identical except that EX-1 had a molybdenum collector and EX-2 a tantalum collector it is logical to infer that the difference in characteristics may be the result of the difference in materials. In further support of this conclusion is the nature of the performance differences, i.e., a shift in the curves parallel to the voltage axis. Such a shift might be expected if the collector work function of EX-1 were lower than that of EX-2 by the amount of the shift. Furthermore, the similarity of these results with those of EX-8 and 9 further supports the conclusion that the differences may be due to the collector material. These results are additional reason for constructing two or more carefully instrumented converters designed specifically to provide a definitive comparison of the effect of collector material over a wide range of operating parameters.

3.3 TESTING OF EX-6

Figures 3-18 through 3-22 show the performance of converter EX-6 which has a tungsten emitter and a tantalum collector. Like EX-2 it was constructed before the start of this program but its performance was not thoroughly mapped. A comparison of the performance of this converter with that of either rhenium or tantalum converters finds EX-6 lower in performance over its entire operating range.

However, a comparison of the data with Thermo Electron's data on tungsten research converters (Figures 3-23, 3-24, 3-25), with molybdenum collectors shows also a shift in performance somewhat similar to that between converters (EX-8 and EX-9) and (EX-1 and 2). Here again the difference may be due to the difference in collector materials. However, accurate comparisons between EX and research converters are more difficult than between two EX converters because of the difficulty in comparing accurately the true effective emitting areas in converters of significantly different design.

5114

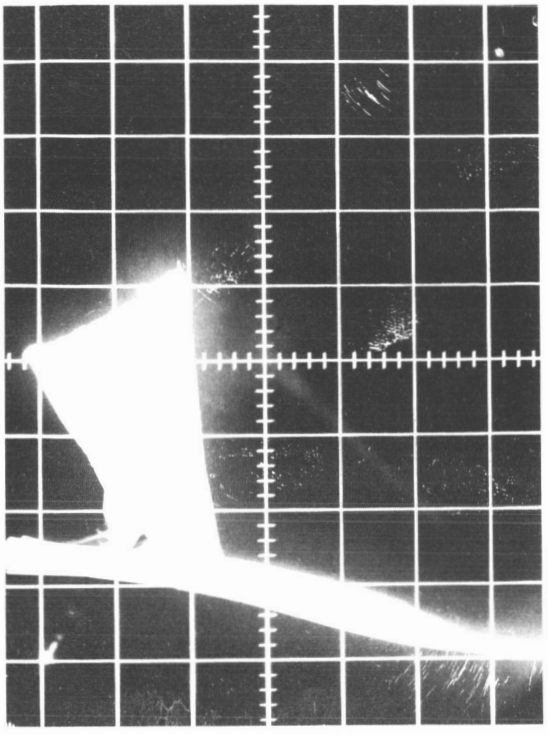


Figure 3-1(a), EX-2 at T_E = 1850°K

T_E = 1850°K

$T_{(Coll)}$ = 779°K

T_{Cs} 548-623°K

5115

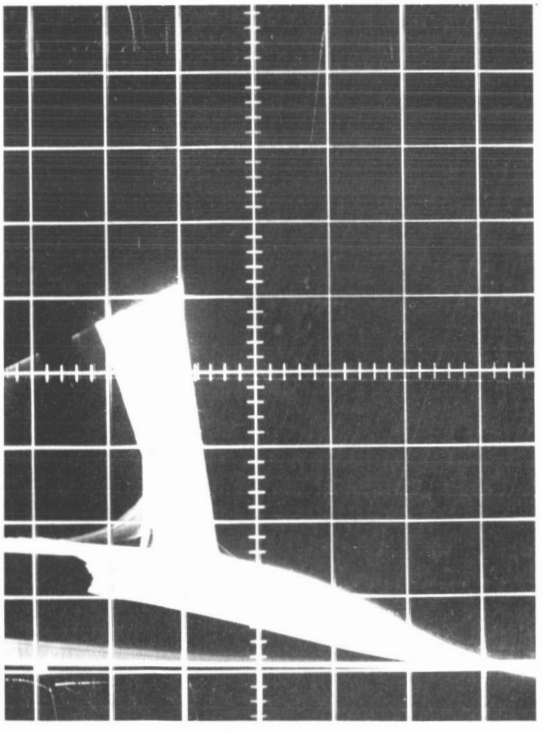


Figure 3-1(b), EX-2 at T_E = 1850°K

T_E = 1850°K

$T_{(Coll)}$ = 823°K

T_{Cs} = 556-563°K

5116

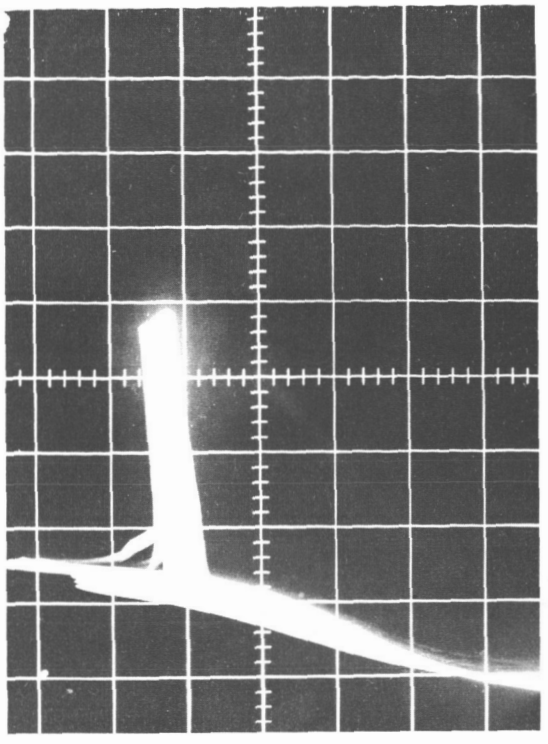


Figure 3-2(a), EX-2 at T_E = 1850°K

T_E = 1850°K
$T_{(Coll)}$ = 854°K
T_{Cs} = 576-633°K

5117

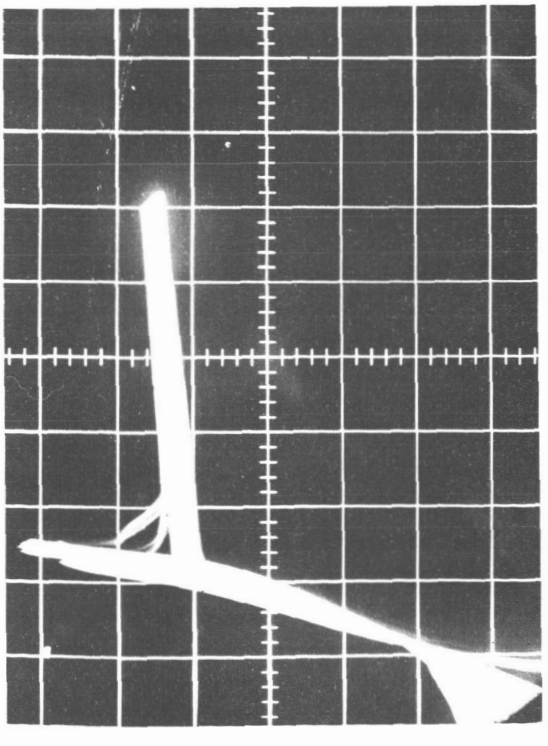


Figure 3-2(b), EX-2 at T_E = 1850°K

T_E = 1850°K
$T_{(Coll)}$ = 886°K
T_{Cs} = 593-633°K

5118

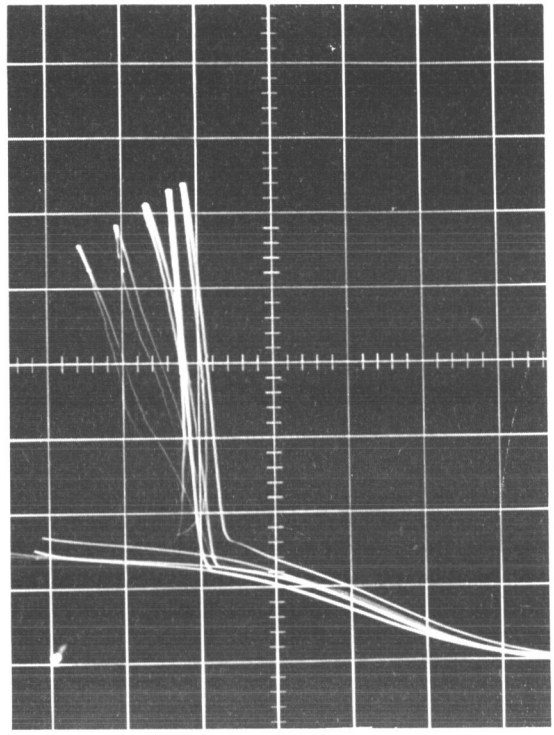


Figure 3-3, EX-2 at T_E = 1850°K

T_E = 1850°K

$T_{(Coll)}$ = 823°K

T_{Cs} = 558, 568, 578, 588, 598°K

5119

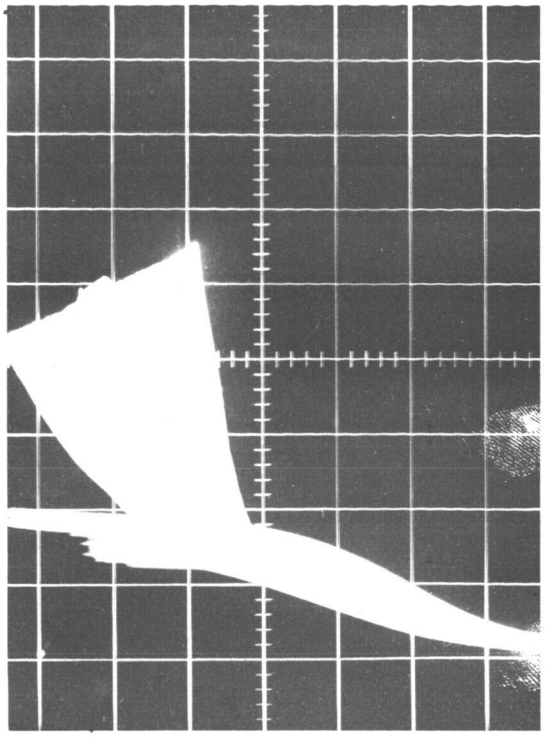


Figure 3-4(a), EX-2 at T_E = 1900°K

T_E = 1900°K
$T_{(Coll)}$ = 793°K
T_{Cs} = 551-623°K

5120

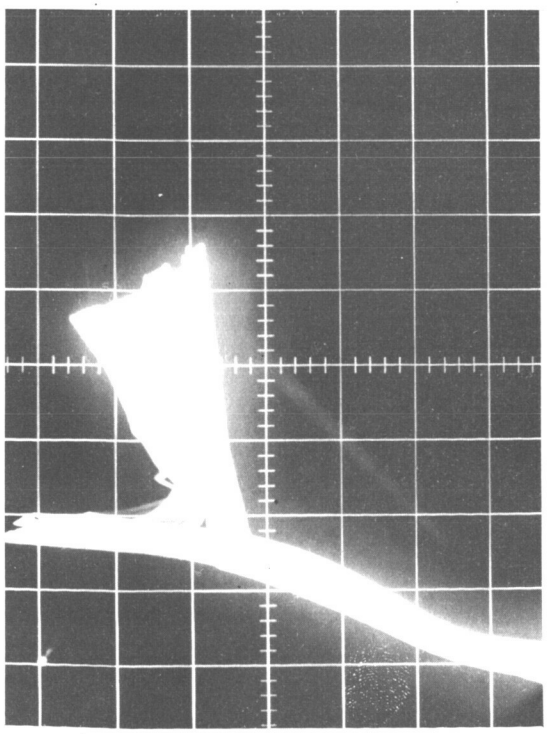


Figure 3-4(b), EX-2 at T_E = 1900°K

T_E = 1900°K
$T_{(Coll)}$ = 821°K
T_{Cs} = 563-623°K

5121

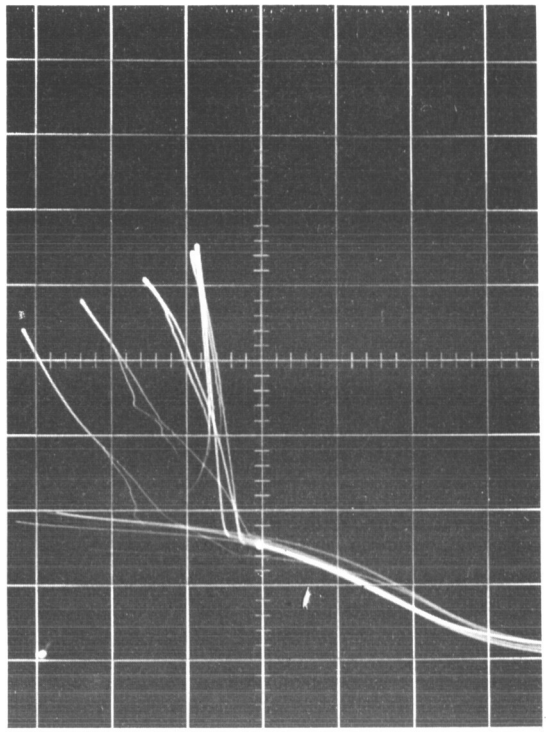


Figure 3-5, EX-2 at T_E 7 1900°K

T_E = 1900°K

$T_{(Coll)}$ = 794°K

T_{Cs} = 553, 563, 573, 583, 593°K

5122

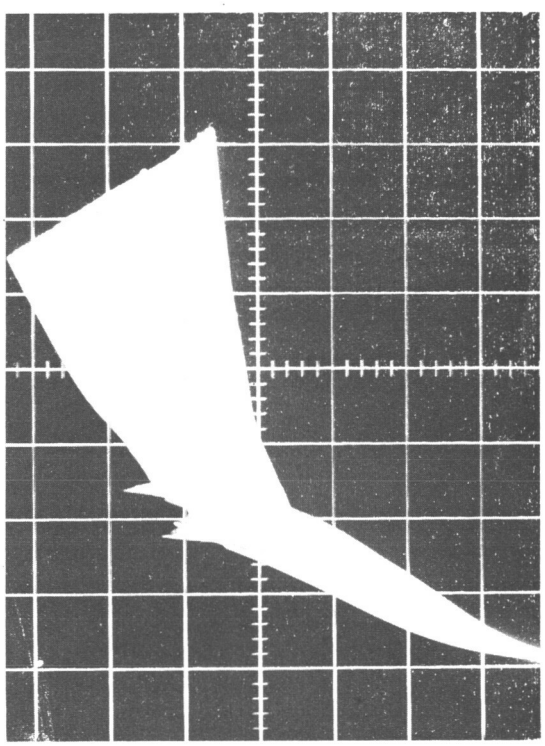


Figure 3-6(a), EX-2 at T_E = 1950°K

T_E = 1950°K
$T_{(Coll)}$ = 815°K
T_{Cs} = 553-623°K

5123

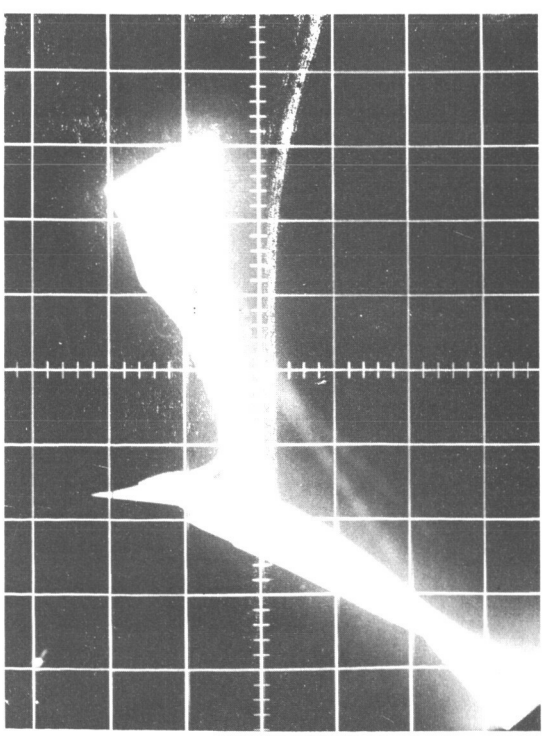


Figure 3-6(b), EX-2 at T_E = 1950°K

T_E = 1950°K
$T_{(Coll)}$ = 845°K
T_{Cs} = 568-623°K

5124

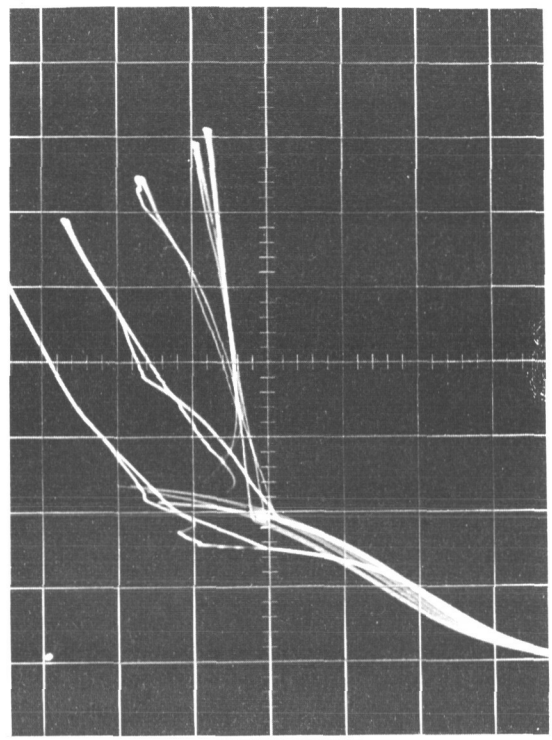


Figure 3-7(a), EX-2 at T_E = 1950°K

T_E = 1950°K

$T_{(Coll)}$ = 815°K

T_{Cs} = 553, 563, 573, 583, 593°K

5125

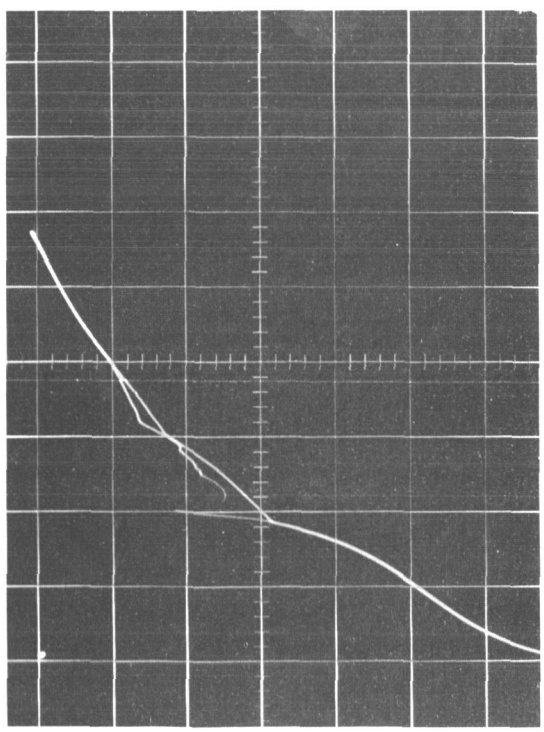


Figure 3-7(b), EX-2 at T_E = 1950°K

T_E = 1950°K

$T_{(Coll)}$ = 814°K

T_{Cs} = 568°K

5126

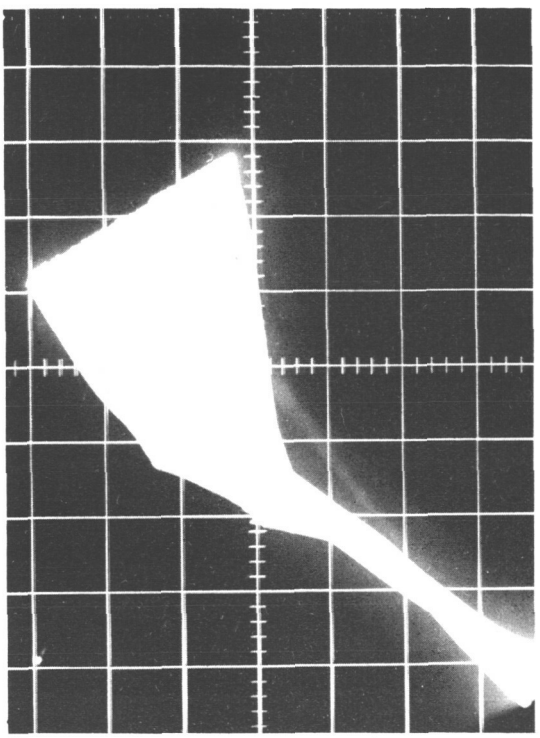


Figure 3-8, EX-2 at T_E = 2000°K

T_E = 2000°K
$T_{(Coll)}$ = 828°K
T_{Cs} = 565-623°K

5127

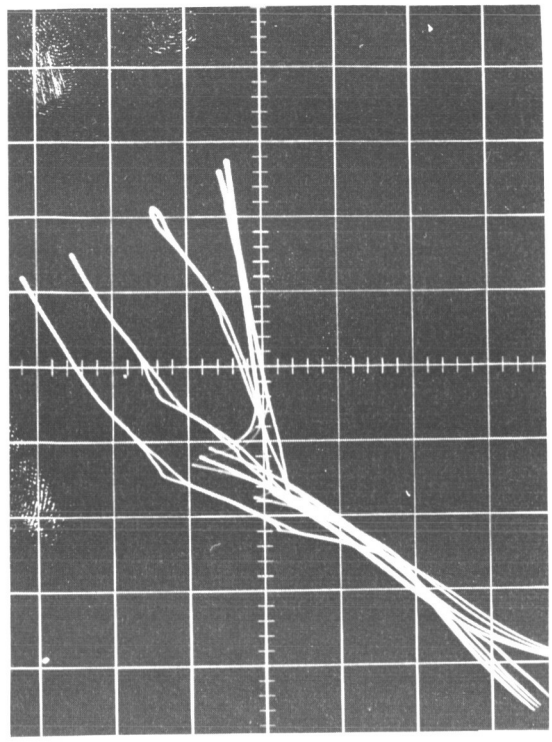


Figure 3-9(a), EX-2 at T_E = 2000°K

T_E = 2000°K

$T_{(Coll)}$ = 830°K

T_{Cs} = 565, 573, 583, 593, 603°K

5128

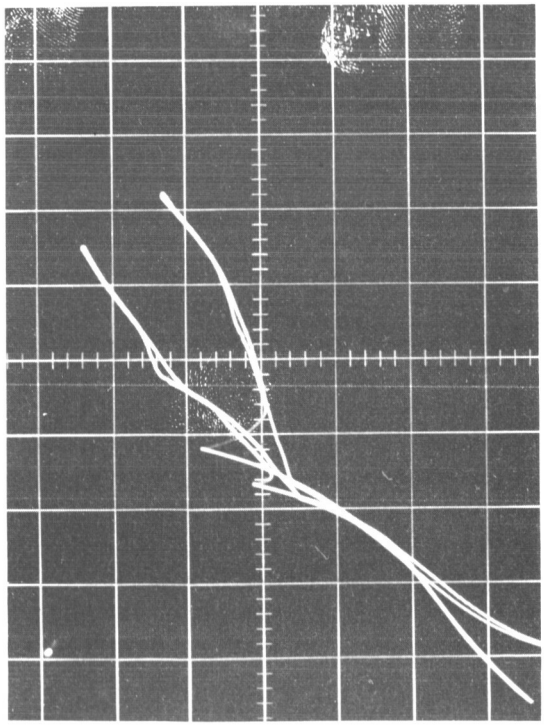


Figure 3-9(b), EX-2 at T_E = 2000°K

T_E = 2000°K

$T_{(Coll)}$ = 828°K

T_{Cs} = 573, 583°K

5129

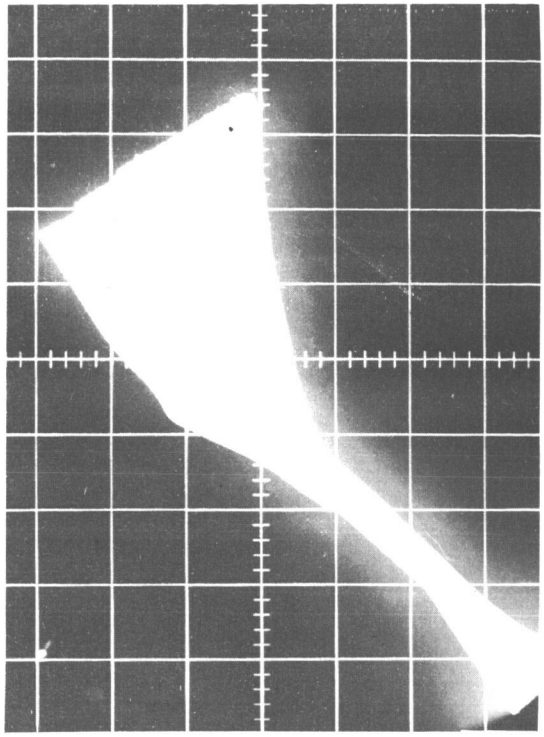


Figure 3-10(a), EX-2 at T_E = 2050°K

T_E = 2050°K

$T_{(Coll)}$ = 835°K

T_{Cs} = 573-623°K

5130

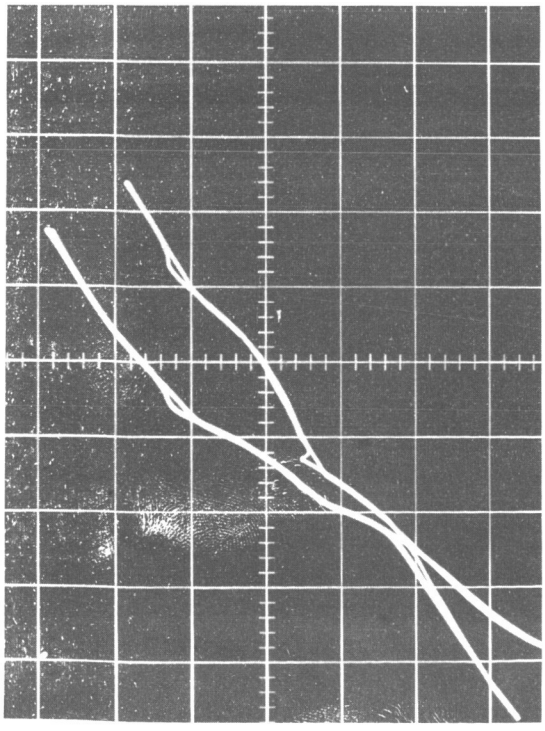


Figure 3-10(b), EX-2 at T_E = 2050°K

T_E = 2050°K

$T_{(Coll)}$ = 836°K

T_{Cs} = 573, 583°K

5131

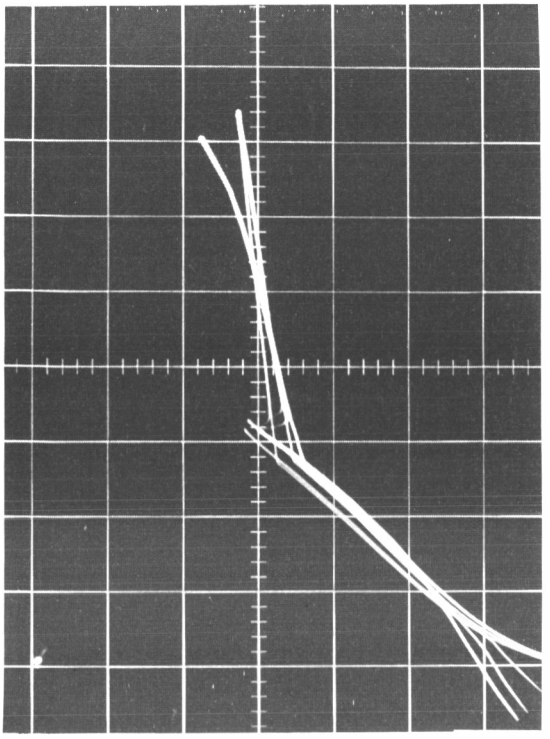


Figure 3-11(a), EX-2 at T_E = 2050°K

T_E = 2050°K

$T_{(Coll)}$ = 836°K

T_{Cs} = 593, 603, 613°K

5132

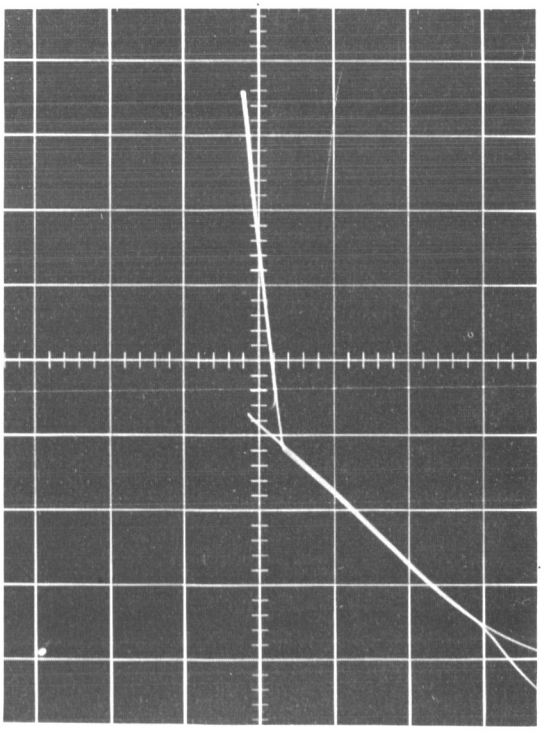


Figure 3-11(b), EX-2 at T_E = 2050°K

T_E = 2050°K

$T_{(Coll)}$ = 836°K

T_{Cs} = 613°K

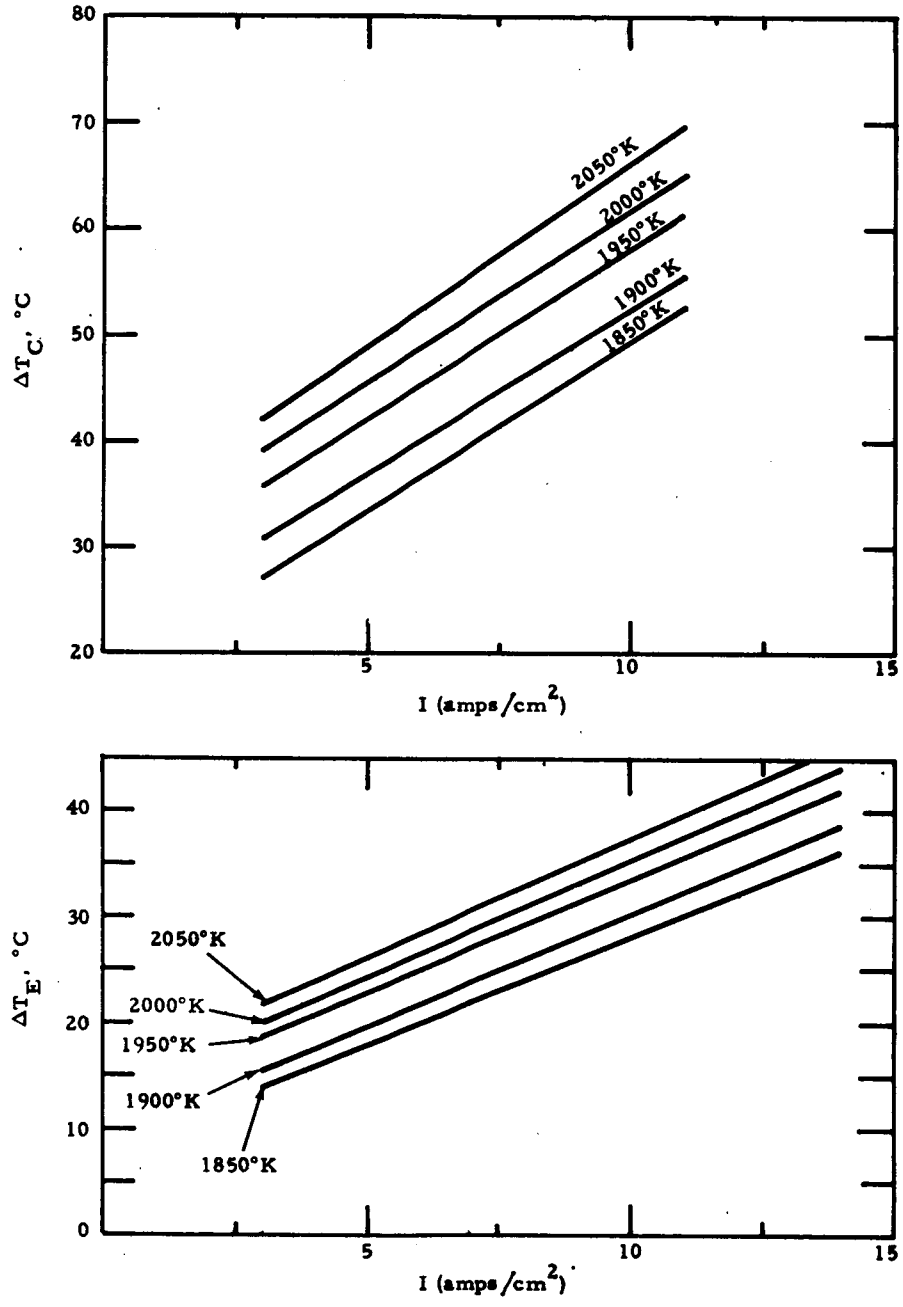


Figure 3-12. Emitter and Collector Temperature Drop Vs. Output Current Density for EX-2.

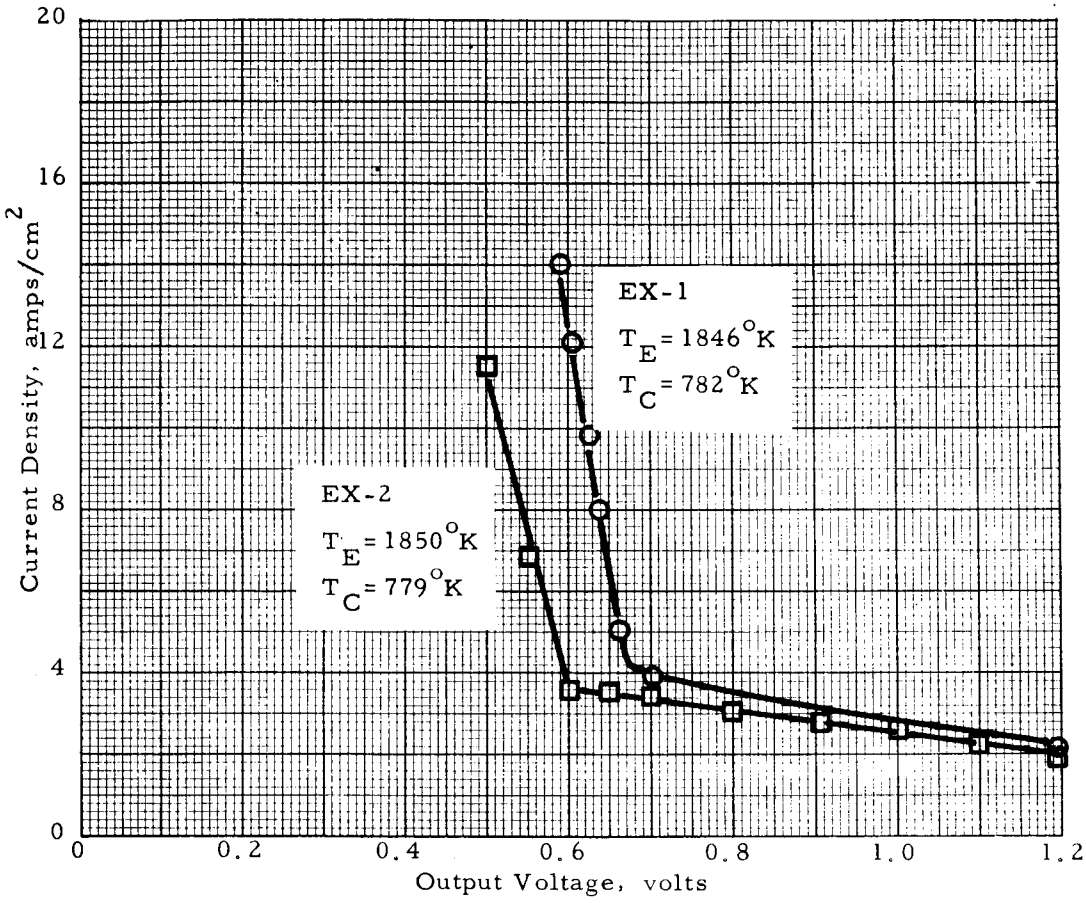


Figure 3-13. Comparison of EX-1 and EX-2 at T_E = 1850°K

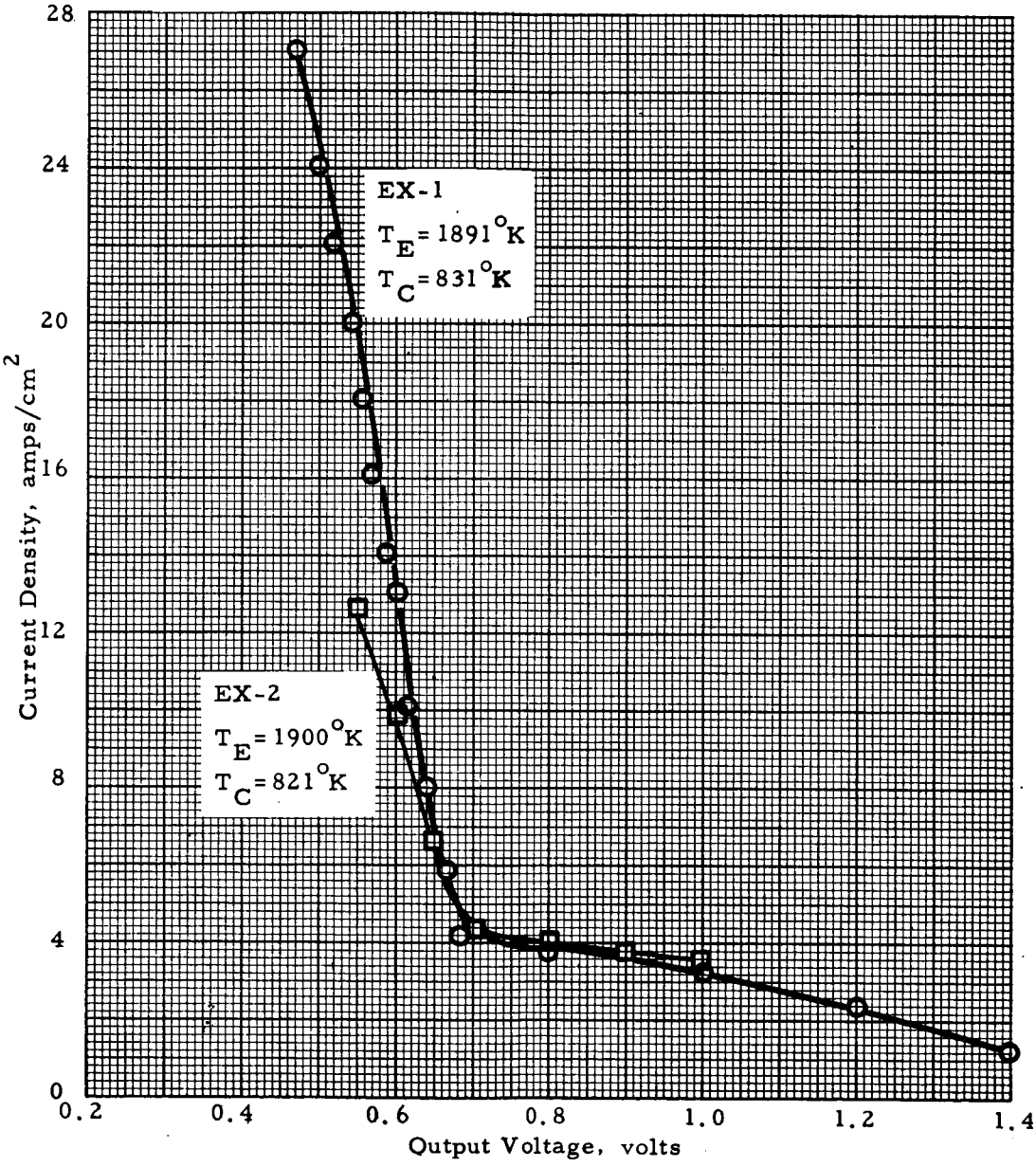


Figure 3-14. Comparison of EX-1 and EX-2 at T_E = 1900°K

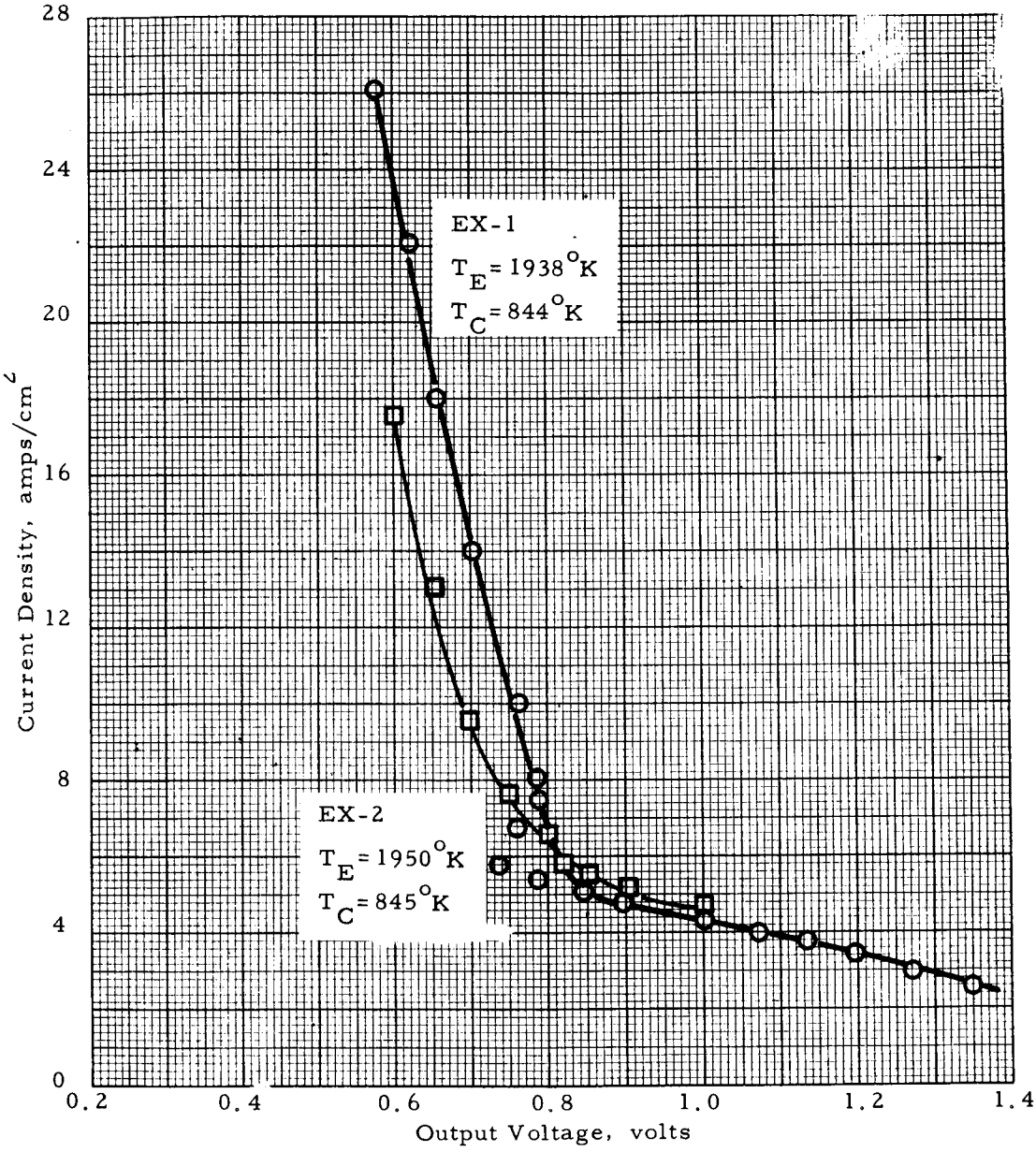


Figure 3-15. Comparison of EX-1 and EX-2 at T_E = 1950°K

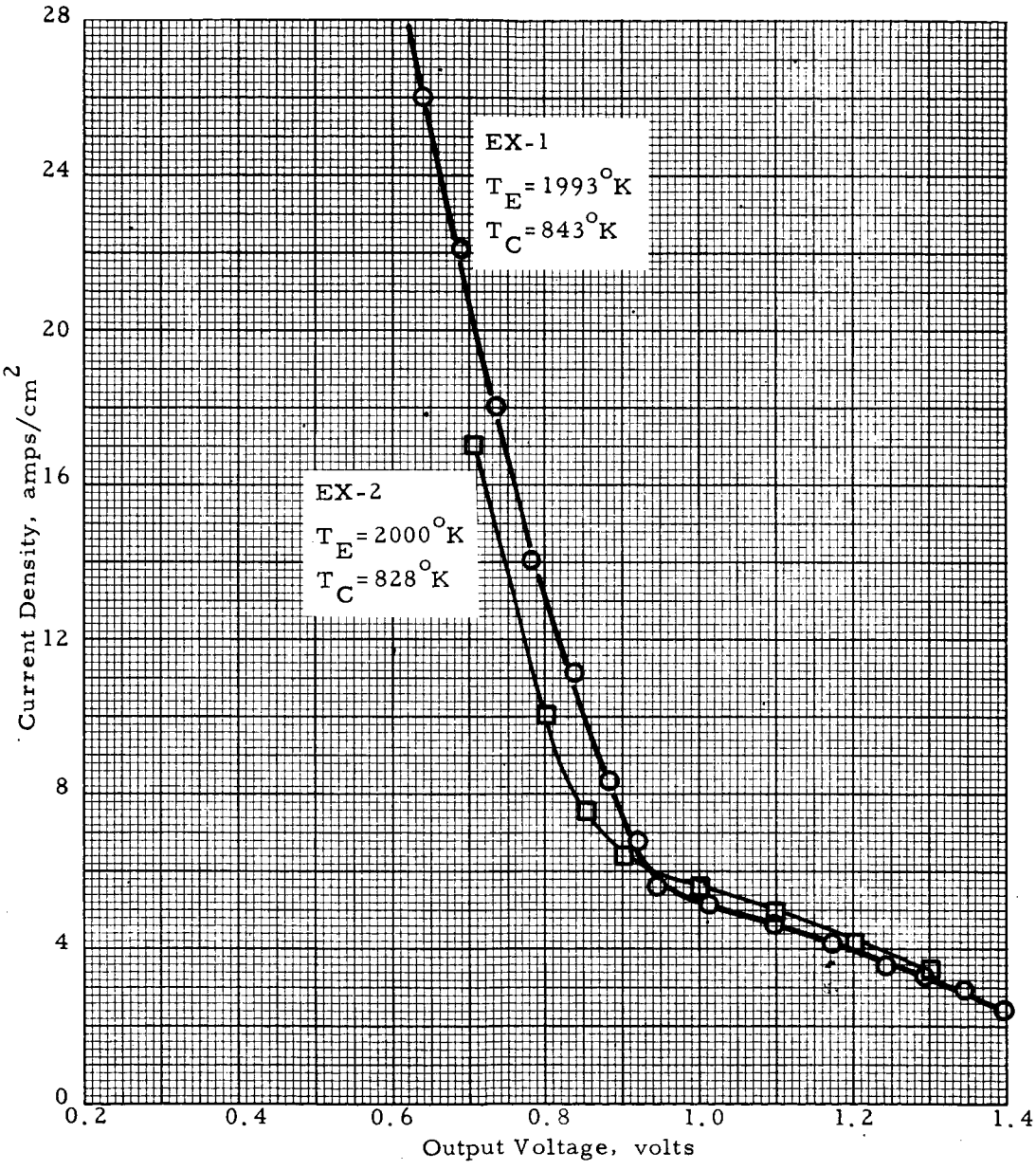


Figure 3-16. Comparison of EX-1 and EX-2 at T_E = 2000°K

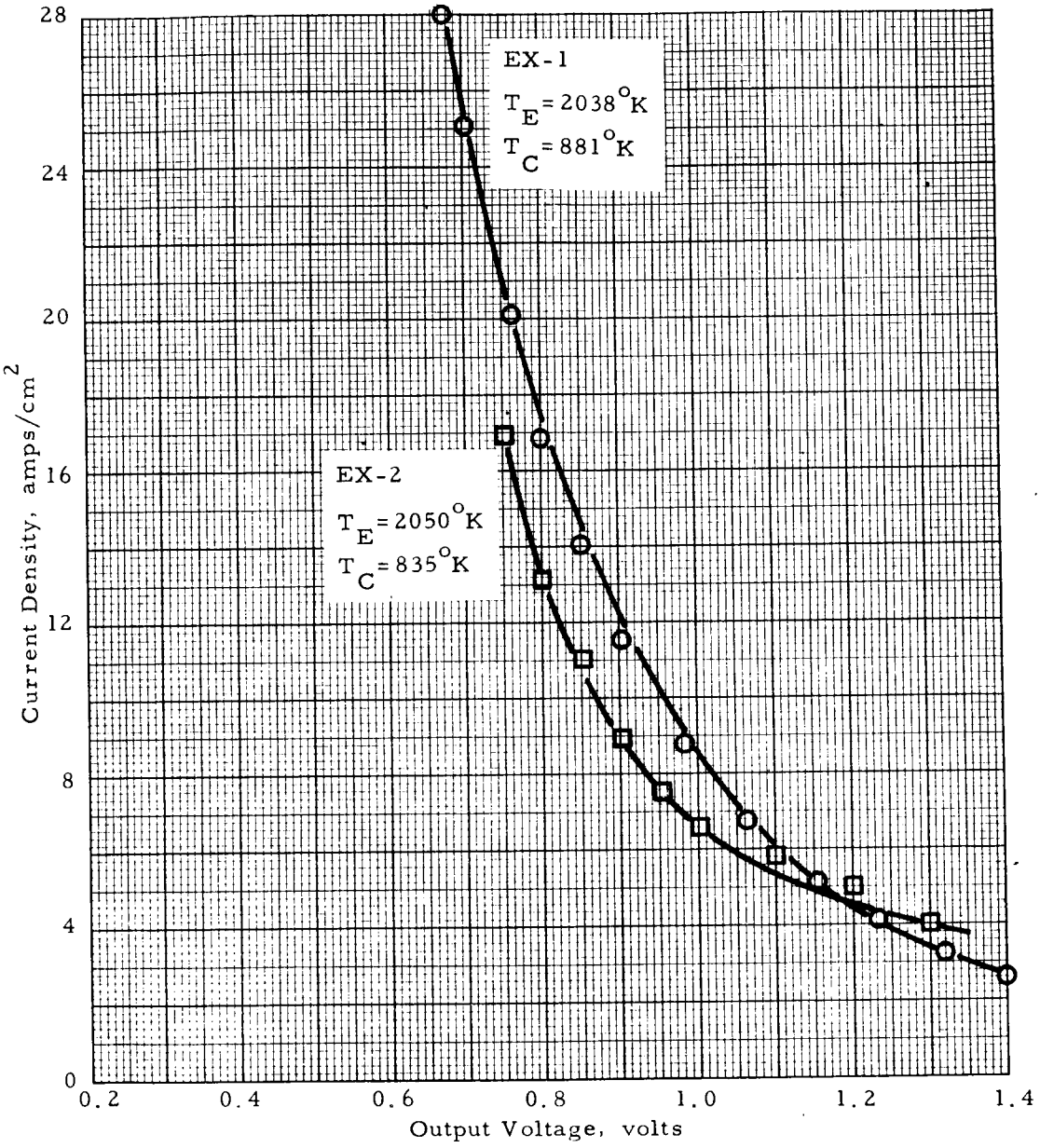


Figure 3-17. Comparison of EX-1 and EX-2 at T_E = 2050°K

5133

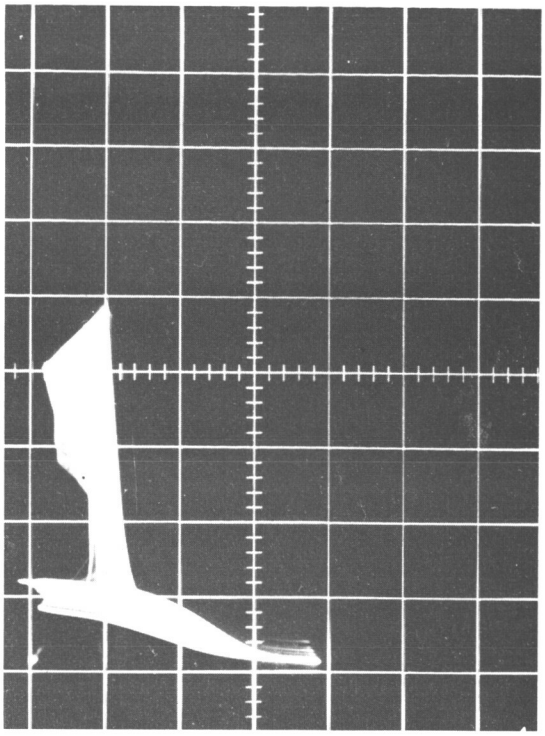


Figure 3-18(a), EX-6 at T_E = 1850°K

T_E = 1850°K

$T_{(Coll)}$ = 784°K

T_{Cs} = 548-633°K

5134

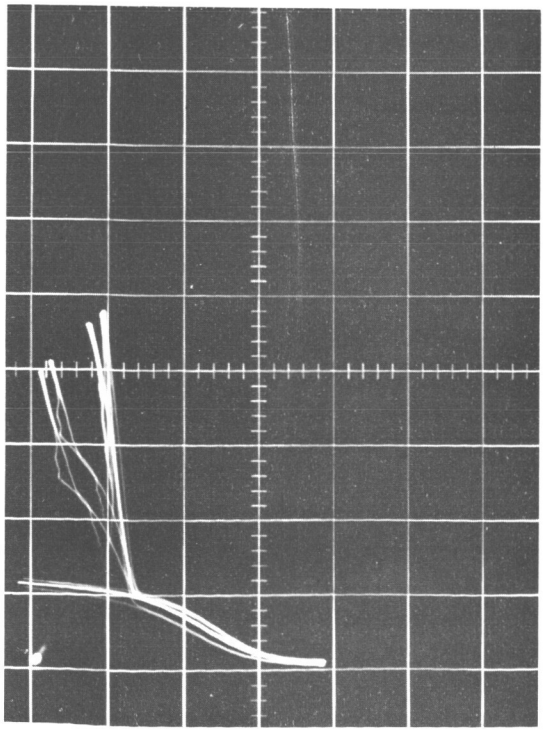


Figure 3-18(b), EX-6 at T_E = 1850°K

T_E = 1850°K

$T_{(Coll)}$ = 783°K

T_{Cs} = 548, 553, 563, 573, 583°K

5135

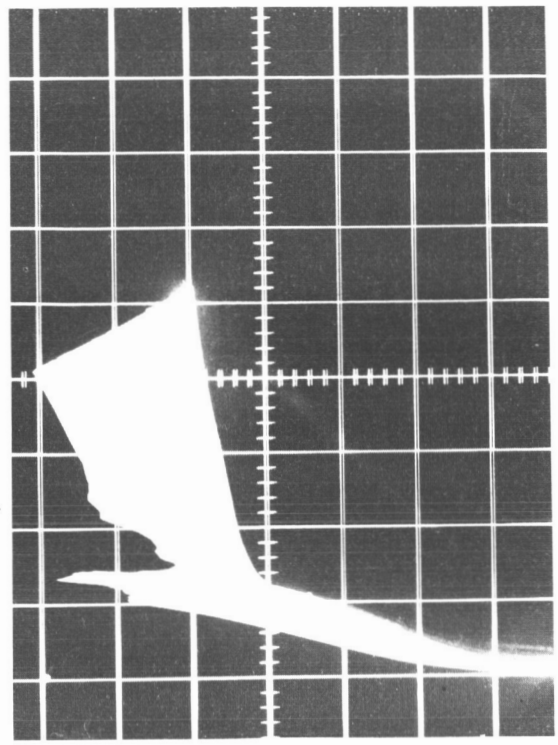


Figure 3-19(a), EX-6 at T_E = 1900°K

T_E = 1900°K
$T_{(Coll)}$ = 800°K
T_{Cs} = 548-633°K

5136

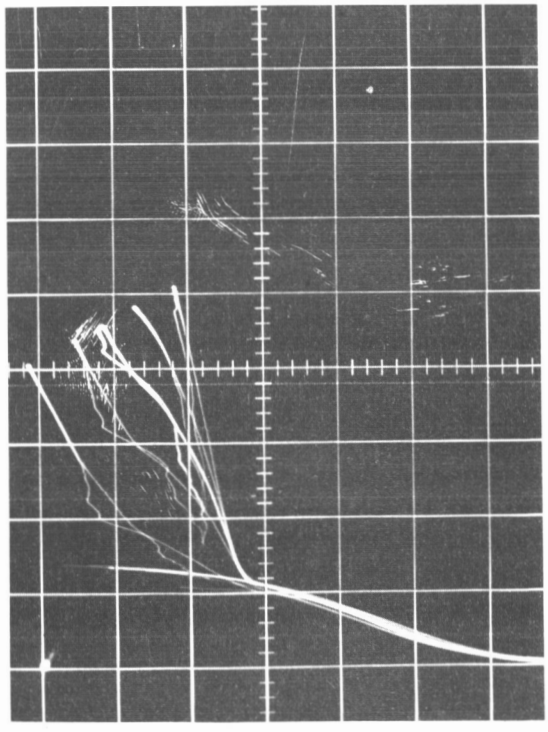


Figure 3-19(b), EX-6 at T_E = 1900°K

T_E = 1900°K
$T_{(Coll)}$ = 795°K
T_{Cs} = 548, 558, 563, 568, 578°K

5137

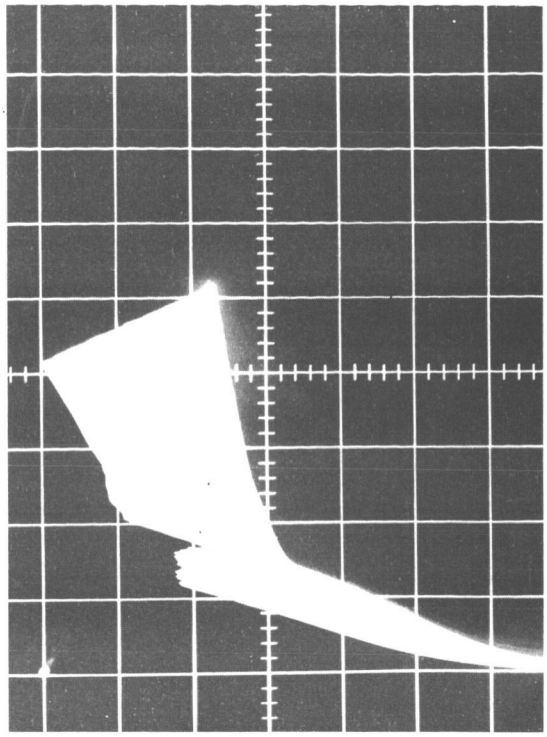


Figure 3-20(a), EX-6 at T_E = 1950°K

T_E = 1950°K
$T_{(Coll)}$ = 804°K
T_{Cs} = 553-633°K

5138

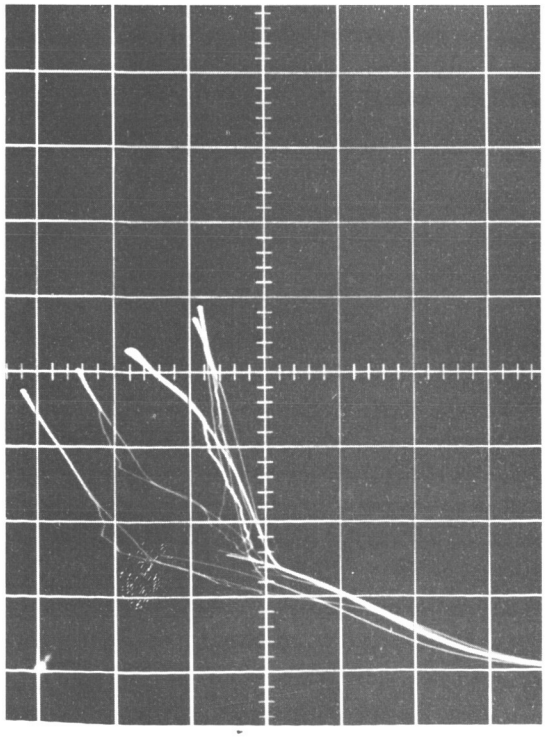


Figure 3-20(b), EX-6 at T_E = 1950°K

T_E = 1950°K
$T_{(Coll)}$ = 805°K
T_{Cs} = 548, 558, 568, 578, 588°K

5139

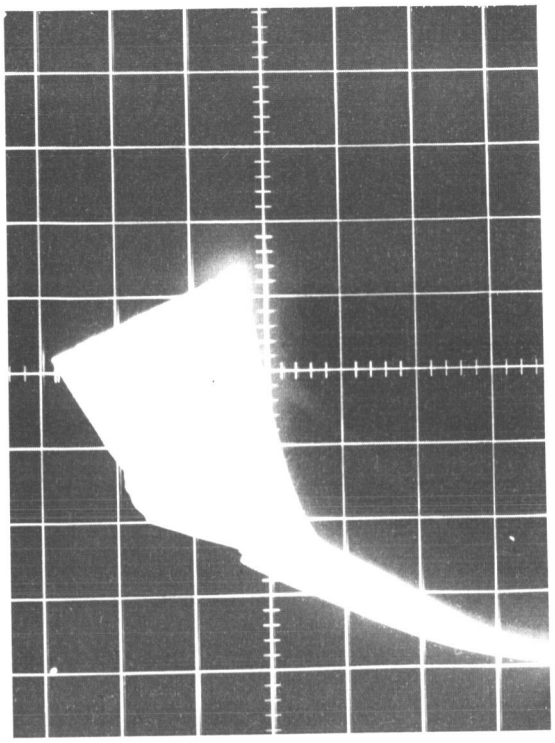


Figure 3-21(a), EX-6 at T_E = 2000°K

T_E = 2000°K
$T_{(Coll)}$ = 812°K
T_{Cs} = 633-653°K

5140

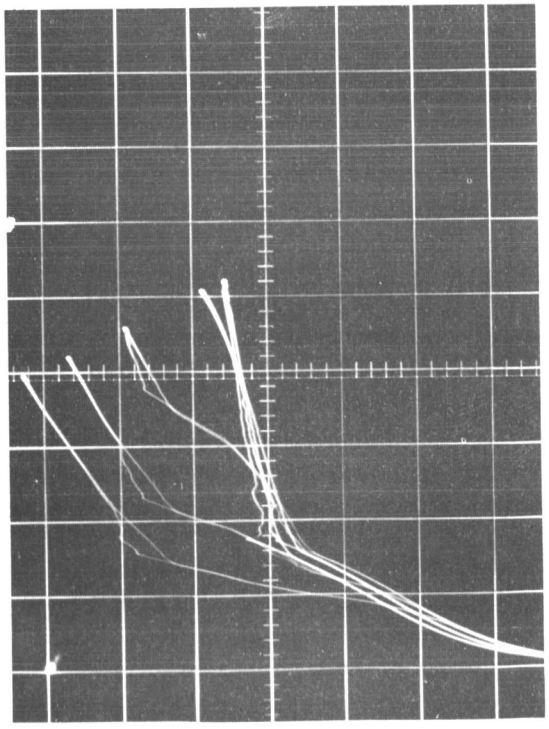


Figure 3-21(b), EX-6 at T_E = 2000°K

T_E = 2000°K
$T_{(Coll)}$ = 810°K
T_{Cs} = 548, 558, 568, 578, 588°K

5141

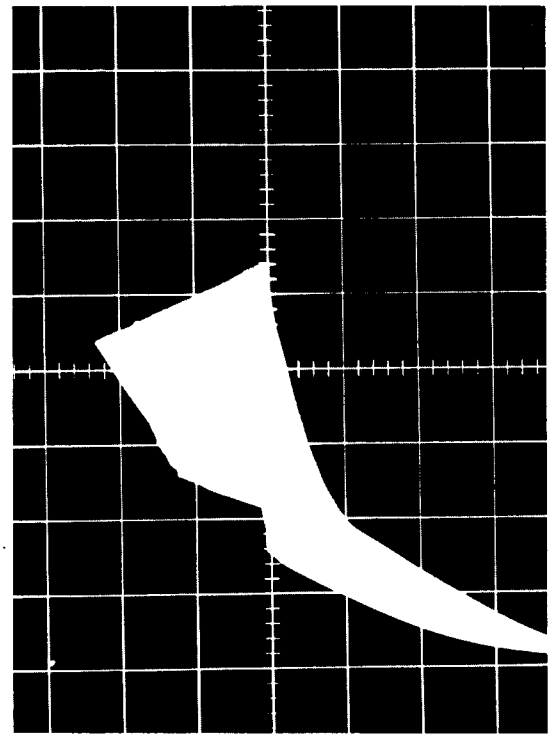


Figure 3-22(a), EX-6 at T_E = 2050°K

T_E = 2050°K

$T_{(Coll)}$ = 821°K

T_{Cs} = 563-653°K

5142

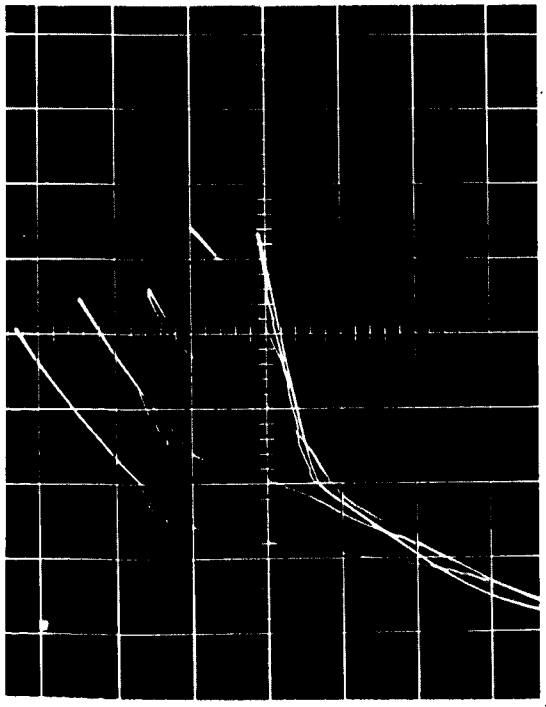


Figure 3-22(b), EX-6 at T_E = 2050°K

T_E = 2050°K

$T_{(Coll)}$ = 821°K

T_{Cs} = 553, 563, 573, 583, 593°K

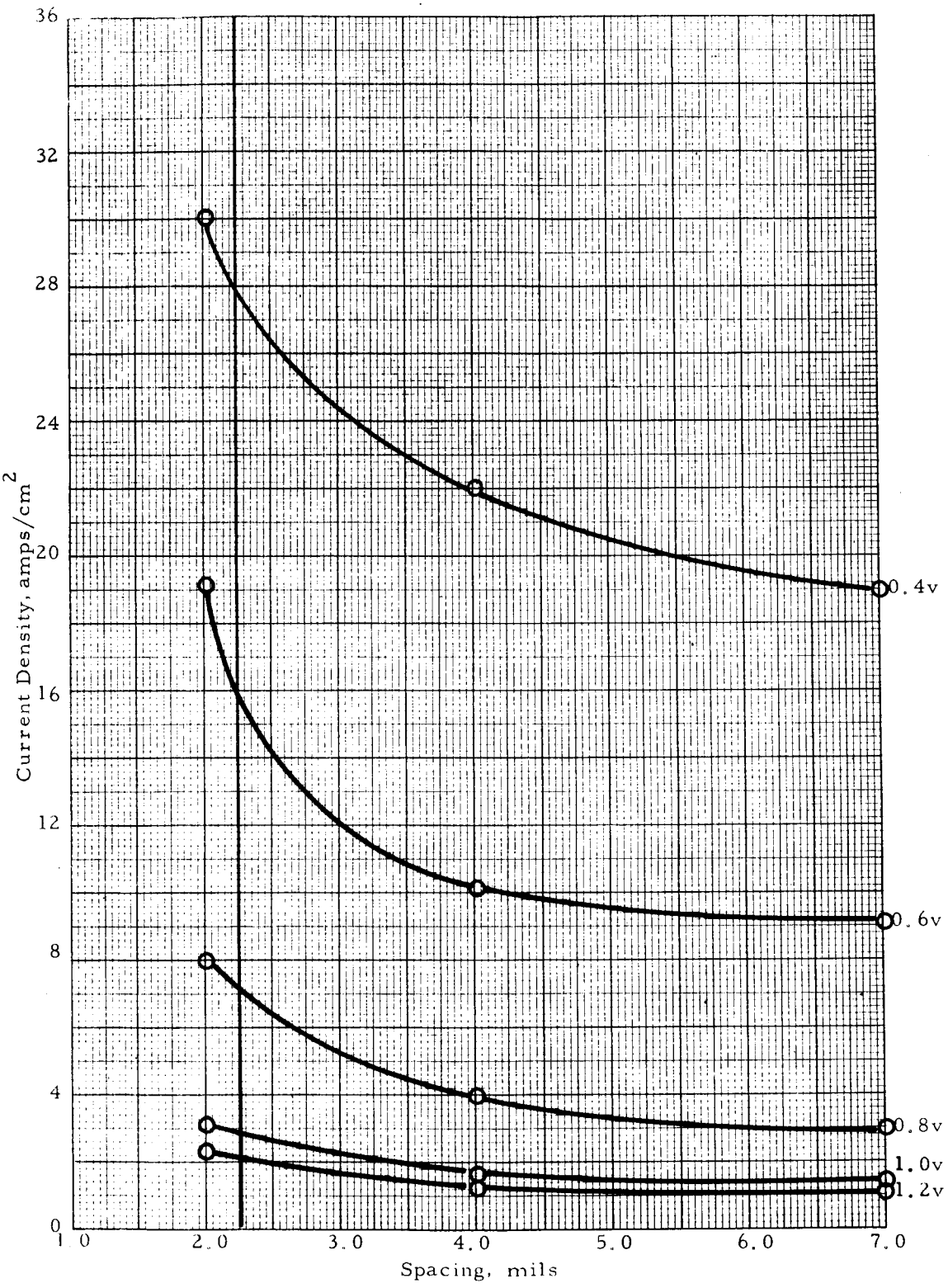


Figure 3-23. Current Density Vs. Spacing for a Rhenium Diode With an Emitter Temperature of 1950°K

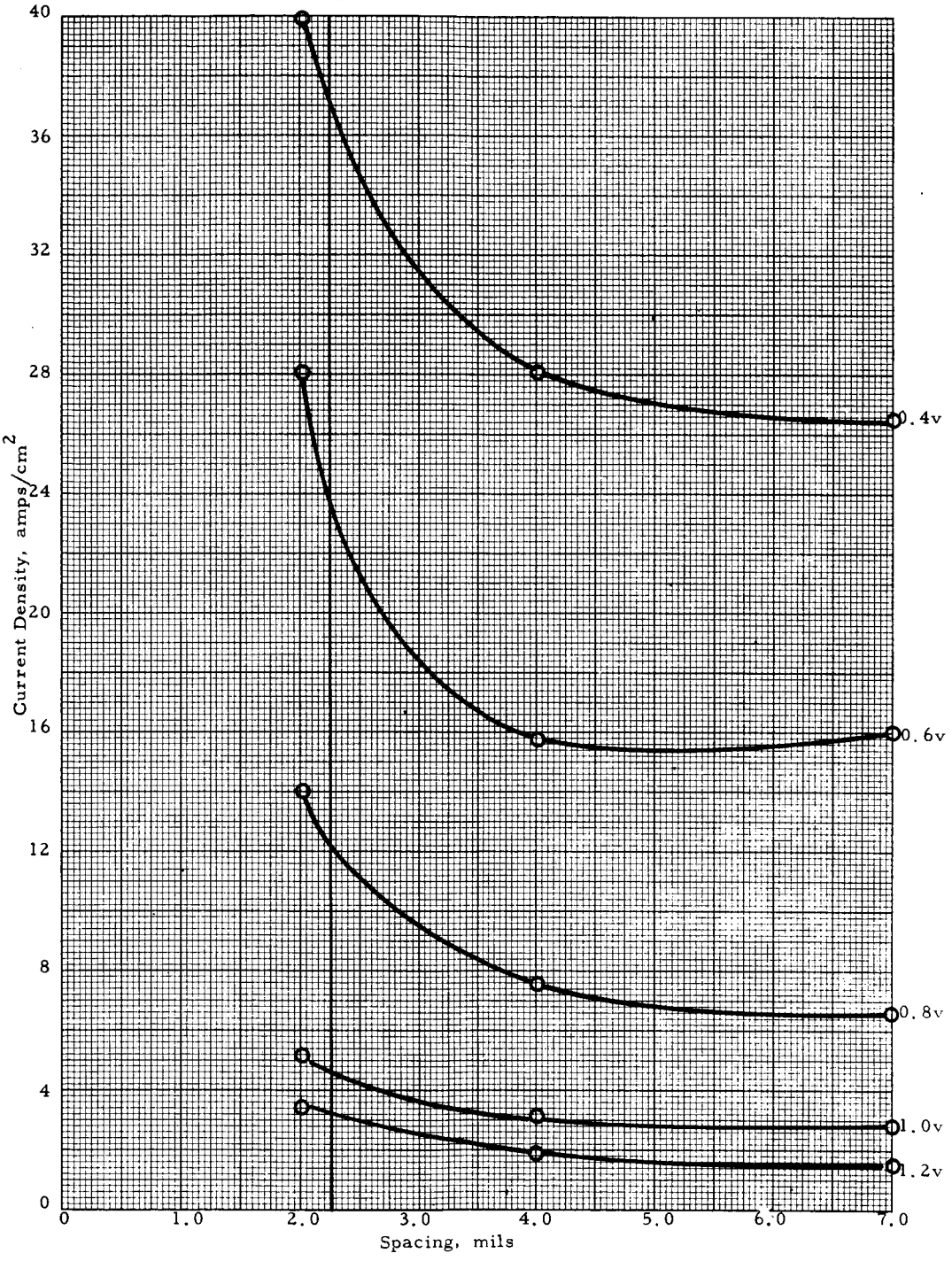


Figure 3-24. Current Density Vs. Spacing for a Rhenium Diode With an Emitter Temperature of 2050°K

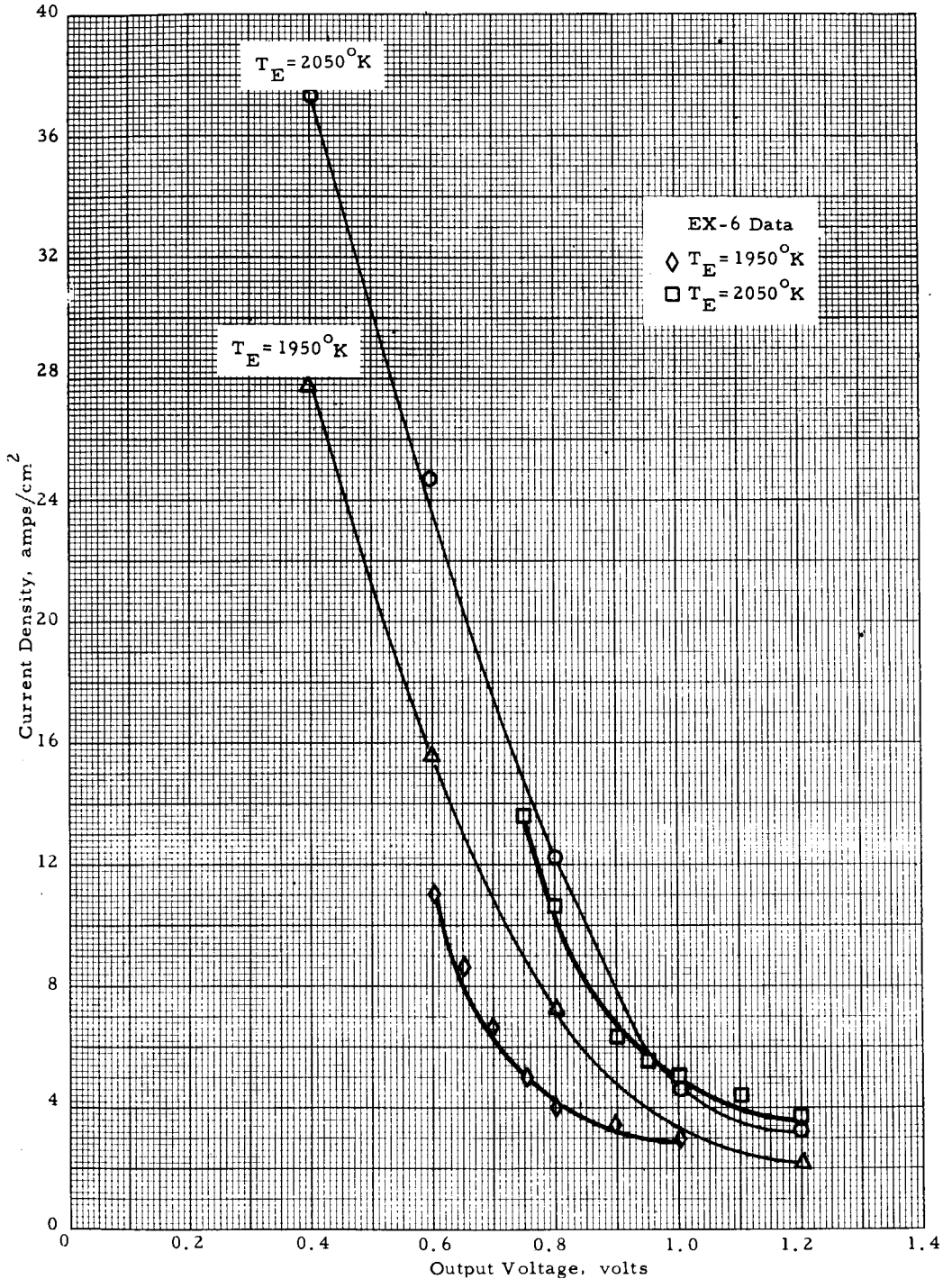


Figure 3-25. Performance of EX-6 Compared With That of a Research Diode.

CHAPTER 4

PROTOTYPE CONVERTER DEVELOPMENT

During the first three quarters, seven Series VII prototypes were built and tested. These converters are designated VII-P-1 through VII-P-7. Table 4-1 contains a summary of the Series VII prototype development listing major parts, changes, reason for changes, test data, post-mortem observations, and analyses performed. As a result of the prototype development, a design was frozen, and the layout drawing is shown in Figure(4-1). From these results, SET VII-S-4 and 5 were built, acceptance tested, and mounted for life testing.

The major problem encountered during the development of the prototypes was degradation of the power output with time. In all cases a black collector deposit was observed in those converters which deteriorated. This deposit, in addition to presenting an electrical resistance between the emitter and collector surfaces, increases the collector work function. Collector work function measurements were made on SET VII-P-3 and SET VI-S-11 and these were compared. The results (Figure(4-2)) of the work function determination demonstrated an increase of the collector work function by approximately 0.23 volt for VII-P-3 over SET VI-S-11 which had no record of degradation.

A preliminary analysis using semi-quantitative chemical analysis of the VII-P-2 collector deposit showed tantalum and cesium as the main constituents. (This prototype was cut open for examination prior to VII-P-1 prototype.) Since it was not known whether tantalum oxide or metallic tantalum or both were present on the collector, further tests were conducted on the collector deposit of VII-P-1 prototype, which visually appeared identical to VII-P-2, using the technique of sputtered ions from the surface. A large number of elements were found dominated by tantalum and cesium and including carbon, oxygen, sodium, aluminum, silicon,

molybdenum, copper, iron and nickel. These results clearly indicated the presence of oxygen previously not detectable with semi-quantitative means. The same collector then was submitted to X-ray diffraction analysis in an attempt to determine the compounds. This analysis revealed the presence on the collector of metallic tantalum, MoO_3 and three allotropic forms of tantalum oxide.

Because the evaporation of tantalum at 2000°K within the testing period could not account for the mass of deposit present, it became clear that a cyclic transport process was occurring. To remove a significant amount of tantalum from the emitter required the intercession of Ta_2O_5 as an intermediate component because Ta_2O_5 has the required ability to dissociate at emitter temperatures into a volatile component. Various reactions were considered leading to a tantalum transfer cycle. These are summarized in the form of a plot of free energy versus absolute temperature in Figure (4-3). To find a feasible transfer reaction, one seeks a pair of lines involving tantalum and crossing at a temperature between those of the emitter (2000°K) and the collector (1000°K). Such lines do not exist in Figure (4-3).

The closest approximation is the lines for $1/5\ Ta_2O_5 + 1/2\ SiO_2$, which show a tendency to converge at higher temperatures. The existence of silicon in the reaction mechanism is not improbable. Silicon has been observed spectroscopically in cesium samples and in collector deposits. Furthermore, diodes which contain glass cesium capsules in their tubulations for prolonged periods during outgassing, or which contain glass capsules at high temperatures, show more severe deposits on their collectors.

The only apparent explanation for the deposits, therefore, particularly of the metallic tantalum, invokes the reaction

$$2\text{-}1/2\ SiO_2 + 2\ Ta \underset{2000^\circ K}{\overset{1000^\circ K}{\rightleftharpoons}} 2\text{-}1/2\ Si + Ta_2O_5$$

and uses the small partial pressures of Si, SiO_2 and O_2 to explain the distribution of tantalum between Ta_2O_5 and metallic tantalum on the collector.

As a result of this explanation, steps were taken in the design, construction and outgassing of diodes VII-S-4 and 5 to further reduce capsule-cesium reactions. This was accomplished by incorporating a cesium reservoir and tubulation assembly which from experiments were known to allow the cesium capsule envelope to achieve a temperature during outgassing below the typical cesium distillation temperature of 250°C.

From the test results of VII-P-5, VII-P-6, and VII-P-7 (shown in Table 4-1) it appeared that degradation could also be decreased by operating the collector at a higher temperature.

In order to increase the collector temperature by 50°C it was necessary to neck down the collector diameter over a portion of its length as shown in Figure (4-4).

The data for the acceptance tests of VII-S-4 and 5 are included in Tables 4-2 and 4-3. At an observed emitter temperature of 1655°C in the pyrometer hole, VII-S-4 produced 15.4 watts at .8 volt and VII-S-5 produced 14.4 watts at .8 volt.

Although the minimum acceptance test requirement of 10 watts at .8 volt for converters VII-S-4 and 5 was exceeded by 5.4 watts and 4.4 watts respectively at

an observed temperature of 1655°C in the pyrometer hole, no information is presently available on the optimum performance of these converters. As will be seen in the discussion of the acceptance testing of converters VII-S-6 through VII-S-12, the collector temperature variation among converters appears to account for significant differences in diode output. With a limited acceptance test requirement, it was not possible to determine the maximum capability of the converter.

Figure 4-1. Layout Drawing of Series VII Prototype

(See Volume II)

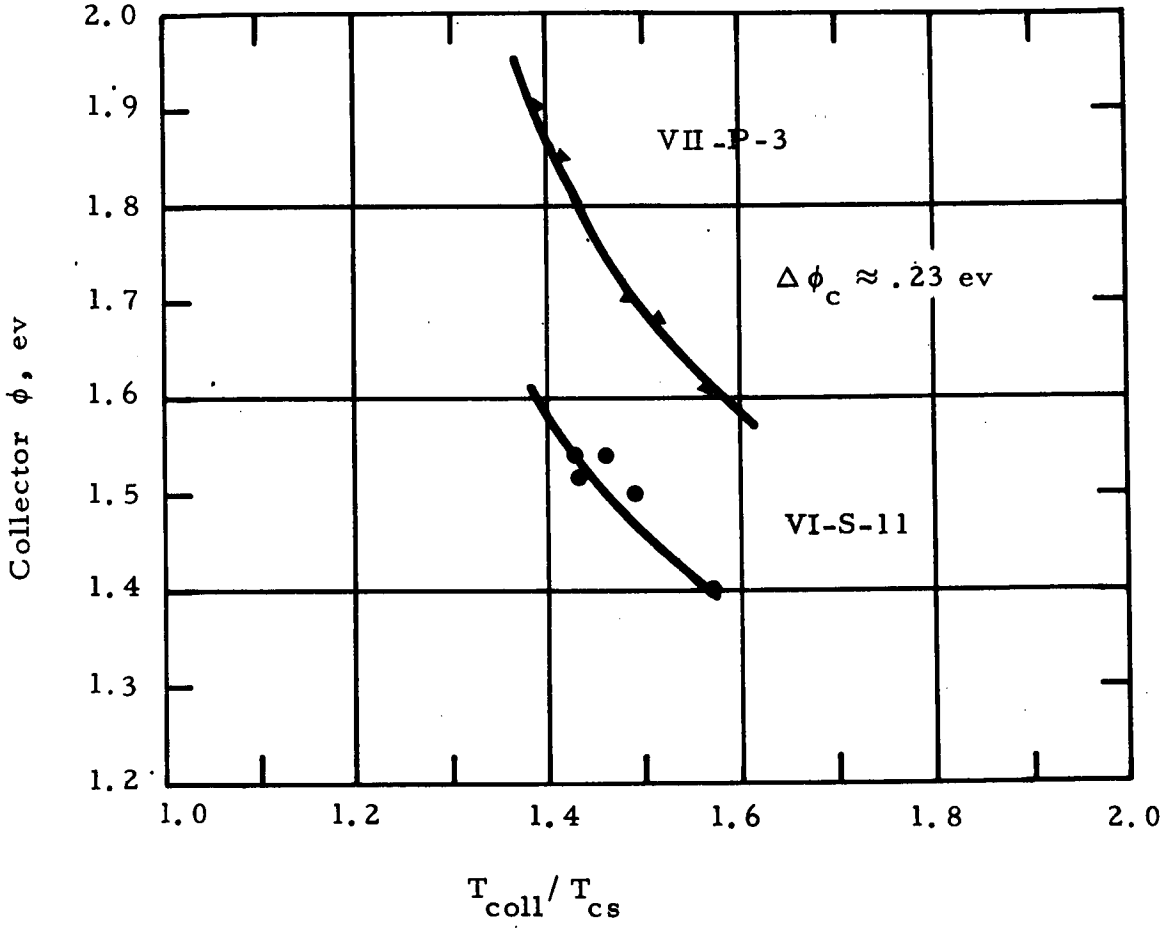


Figure 4-2. Results of Ten Diagnostic Experimental Runs for Collector Work Function Determination

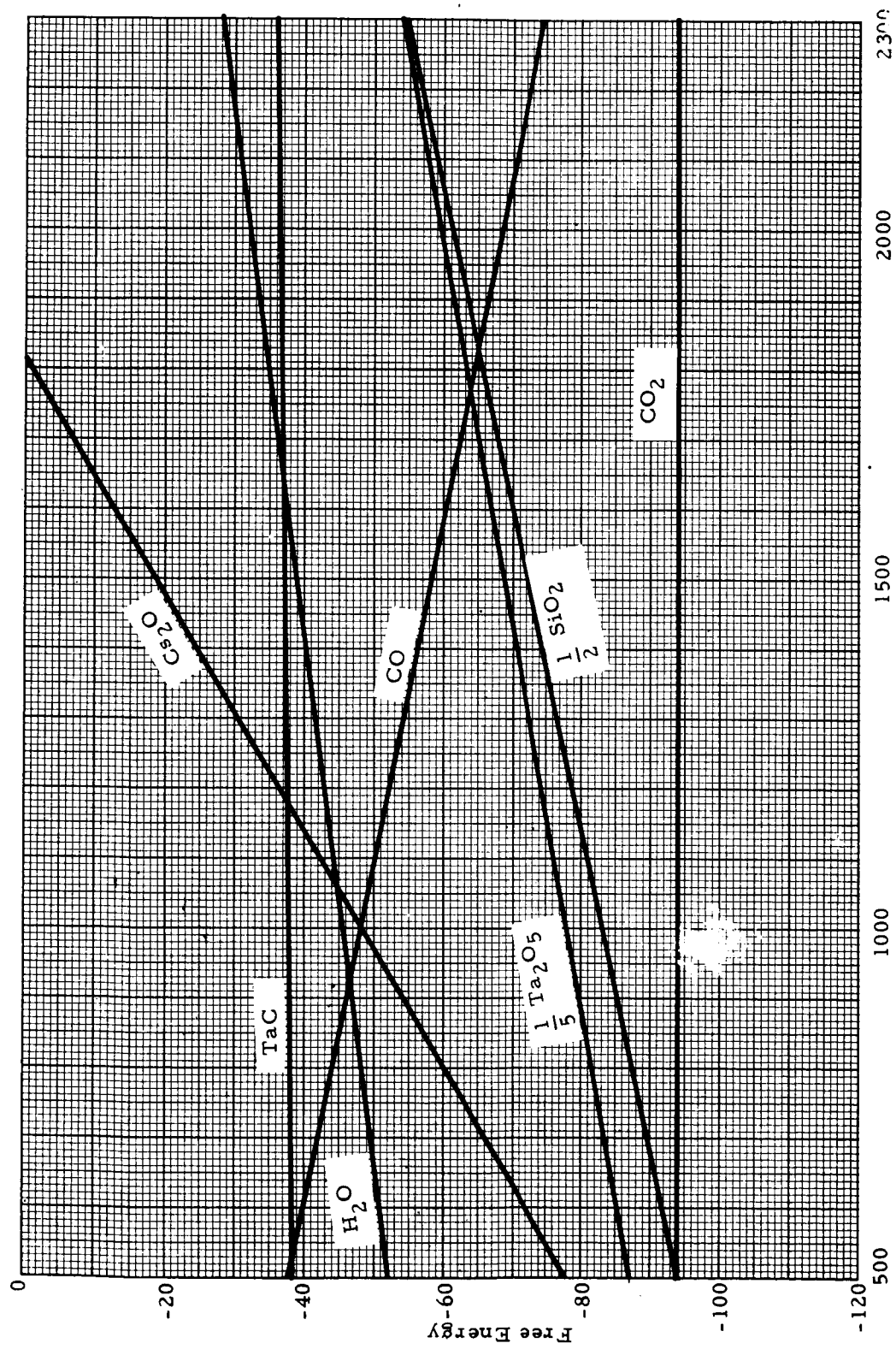


Figure 4-3. Free Energy Vs. Absolute Temperature

Figure 4-4. Detail Drawing of Series VII Collector

(See Volume II)

Table 4-1. Series VII Converter Prototype Program History.

	SET VII-P-1	SET VII-P-2	SET VII-P-3	SET VII-P-4	SET VII-P-5	SET VII-P-6	SET VII-P-7
Emitter: Change Reason	K Annealed Ta	Annealed Ta No Fabricated at time of SET VII-P-1.	Annealed Ta Yes Increased class "A" processing in an effort to remove oxygen.	Annealed No Same as SET VII-P-3.	Unannealed Ta Yes Less Nb and O_2 ppm than prev. annealed stock Increase firing 2050° C	Unannealed Ta No Same as SET VII-P-5.	Unannealed Ta Yes Increase firing to 2300°C further effort to remove impurities.
Collector: Change Reason	Moly	Moly No Fabricated at time of SET VII-P-1	Ta-Moly Yes Gettering ability of Ta. Evaporation of Ta from Emitter to collector face	Moly Yes No improvement in SET VII-P-3.	Ta-Moly Yes SET V and SET VI performance.	Ta-Moly No Performance of SET VII-P-5.	Ta-Moly Yes Change in design of collector to increase face temperatures to minimize accumulation of deposit
Cesium Reservoir: Change Reason	1/8" Kovar	1/8" Kovar No Fabricated at time of SET VII-P-1.	3/16" Nickel Yes Purity. Improve outgassing of converter.	3/16" Nickel No Same as SET VII-P-3.	3/16" High Purity Ta Yes Remove source of CO	3/16" High Purity Ta No Same as SET VII-P-5	3/16" Nickel Yes No major improvement. Simpler construction with nickel
Cesium: Change Reason	30 mg, 1720 glass then, 250 mg. 1720 glass Yes Degradation. Gettering ability of cesium.	250 mg. 1720 glass capsule Yes Results of SET VII-P-1	1720 glass capsule No Duplicate SET VII-P-2	Pyrex capsule Yes Successful application in other TEE converters.	Initially copper capsule, then 1720 glass capsule Yes Remove glass. Unsuccessful in breaking copper capsule.	1720 glass Yes Availability	1720 glass No Availability
Degradation: All data at 2000°K T.E.S.	Acc. Hours / Volt / Amp 0 / 1.0 / 11.7 -- / 0.8 / 25.0 48 / 1.0 / 11.7 -- / 0.8 / 19.0 60 / 1.0 / 9.2 77 / 0.8 / 7.5 Recharge with 250 mg Cs capsules 85 / 0.8 / 10.0	Acc. Hours / Volt / Amp 0 / 1.0 / 8.1 -- / 0.77 / 16.0 10 / 0.77 / 6.0	Acc. Hours / Volt / Amp 0 / 0.8 / 24.5 20 / 0.8 / 18.5 76 / 0.8 / 7.5	Acc. Hours / Volt / Amp 0 / 0.8 / 11.3 24 / 0.8 / 6.5	Acc. Hours / Volt / Amp 0 / 0.8 / 16.4 7 / 0.8 / 16.8 29 / 0.8 / 12.3 Shield radiator Heat collector 31 / 0.8 / 17.0 35 / 0.8 / 20.0 63 / 0.8 / 17.0 86 / 0.8 / 16.4	Acc. Hours / Volt / Amp 0 / 0.8 / 20.0 15 / 0.8 / 17.0 23 / 0.8 / 15.0	Acc. Hours / Volt / Amp 0 / 1.0 / 11.8 -- / 0.8 / 19.1 18 / 1.0 / 11.8 -- / 0.8 / 17.0 30 / 1.0 / 12.0 -- / 0.8 / 15.2 39 / 1.0 / 12.0 42 / 1.0 / 10.9 45 / 1.0 / 11.9 65 / 1.0 / 12.1 -- / 0.8 / 15.4
Post Mortem:	Black collector deposit.	Black collector deposit.	Not performed. Used as dummy converter for life tests.	Black collector deposit.	Black collector deposit. Not as heavy as previous (heating).	Black deposit on collector. Spacer failed during testing.	Medium deposit on collector. Spacer failed during testing.
Analysis:	Sputtered Ion Analysis and x-ray powder analysis of collector deposits	Semiquantitative chemical analysis of collector face, emitter face, and inner sleeve deposits	Work function of collector after running	Sent to JPL.	Sent to JPL.	Sent to JPL.	Sent to JPL.
Conclusion:	Metallic Ta on collector. Cesium impurities. Tantalum oxide.	Tantalum on face of molybdenum collector.	Work function increased by ≈ 0.21v over SET VI-S-11.			Poor vacuum during testing cause of failure.	

CHAPTER 5

FABRICATION AND ACCEPTANCE TESTING OF SERIES VII SET CONVERTERS

5.1 CONSTRUCTION

During the last quarter of the program, seven carefully constructed Series VII diodes were built and tested. The design was identical to VII-S-4 and VII-S-5 which were life tested. A materials survey of the critical diode components is listed in Table 5-1 which lists the various types of material and quality control identification numbers. The tube record of the emitters and outgassing information is included in Table 5-2. Figure (5-1) shows an over-all view of the SET VII converter which has been fabricated, outgassed, and acceptance tested. Figure (5-2) is a close-up of the emitter and sleeve of the same converter. The exceptionally clean appearance of the tantalum may be noted. Figure (5-3) shows seven SET VII diodes which were fabricated while Figure (5-4) shows the SET VII diode and an exploded view of the various components of the converter in a typical assembly area (dust free hood). Figure (5-5) shows a close-up of the various diode components. During fabrication, no complications were encountered in brazing the various components. During the construction of the seven converters, only one braze out of 80 failed. During the fabrication and outgassing, special care was given to carefully follow the specifications and maintain the quality control inspection adopted during the prototype development. The cleanliness achieved as a result of this outgassing is clearly demonstrated by Figures (5-1) and (5-2).

5.2 ACCEPTANCE TESTING

The results of the acceptance tests are listed in Table 5-3. As can be seen from these data, the performance of the diodes varied. The differences in power

densities at one volt between the highest and the lowest performance diodes is 2.7 watts/cm^2.

Only limited test data are available on these diodes because the program called only for measuring the output power at an output voltage of one volt and an observed emitter temperature of 1700°C with the cesium temperature optimized. Also no means were available for varying the collector temperature.

The wide variation in these tests results between various diodes was very surprising in view of the extremely careful control that was exercised during the construction and processing of the diodes. Consequently, a careful analysis of the test results of the diode design and construction was made to try to determine the cause of the variation. This analysis indicates that the probable cause was variation in collector surface temperature. As pointed out above, the collector temperature of these diodes was not optimized during testing because a heater and cooling arrangement is not included with the diodes. To verify that the collector surface temperature was the cause of the variations in performance, Diode VII-S-7 was again placed on test with a cooling strap added to the radiator which reduced the temperature by 16° C, as read by the thermocouple at the bottom of the collector. When this diode was retested at optimum cesium pressure at 1700° C observed emitter temperature and at one volt, its performance with the lower radiator collector temperature increased by one-half watt per cm^2. When the collector temperature was subsequently lowered even further by 50° C, the performance of the diode increased even further to 8.7 watts/cm^2, making it very close in performance to the best of these Series VII diodes. This variation in performance with collector temperature could, of course, be expected. However, whatever the historical reasons for the collector differences, there are many good reasons for testing these Series VII diodes more extensively than was called for in the original contract.

As can be seen from Table 5-1, in addition to having variations in output performance, there also exist wide variations in power input to the diodes. The bulk of this variation is most likely due to leakage from the electron bombardment gun to a shield used around the emitter spacer(to reduce reflections to the pyrometer) and thence through the ceramic seal to ground. This has been partially verified by replacing the original shield with a new shield made of much thinner material and noting that the power input to that particular diode dropped significantly. The wide variations from diode to diode, even though the same emitter shield was used, were most probably caused by variations in the leakage across the ceramic, which placed the shield at various potentials with respect to the electron bombardment gun and to ground, thus causing a variation in the bombardment of the shield. Additional verification of this latter phenomenon has been the fact that on those diodes requiring very high input powers, the emitter shield also operated at a very high temperature. In future testing, this problem can be virtually eliminated by using one or several very thin tantalum shields which have very low conductivity along the length and consequently cannot conduct much heat into the seal structure. A test has recently been conducted on a Series VII diode to confirm this.

TABLE 5-1

MATERIAL SURVEY SET VII

Part No.	Part Name	Mat'l	VII-S-1 QC No.	VII-S-2 QC No.	VII-S-3 QC No.	VII-S-4 QC No.	VII-S-5 QC No.	VII-S-6 QC No.	VII-S-7 QC No.	VII-S-8 QC No.
1	Emitter Spacer	Ta	422	422	422	422	422	422	422	422
2	Collector Base	Mo	426	426	426	426	426	426	426	426
4	Support Flange	Nb	249	249	249	249	249	249	249	249
5	Ceramic Insulators	Al_2O_2	500	500	500	500	500	500	500	500
6	Emitter Flange	Nb	272	272	272	272	272	272	272	272
7	Collector Flange	Nb	369	369	369	369	369	369	369	369
8	Radiator	OFHC Cu	412	412	412	412	412	412	412	412
9	Cesium Tube	Ni	349	349	349	349	349	349	349	349
10	Adapter Tube	Ni	179	179	179	179	179	179	179	179
11	Cesium Reservoir	Ni	276	276	276	276	276	276	276	276
13	Thermocouple Wire	Alumel	257	257	257	257	257	257	257	257
14	Thermocouple Wire	Chromel	258	258	258	258	258	258	258	258
15	Pinch off Tubulation	OFHC Cu	362	362	362	362	362	362	362	362
16	Thermocouple Wire	Alumel	257	257	257	257	257	257	257	257
23	Collector Face	Ta	422	422	422	422	422	422	422	422
24	Thermocouple Wire	Chromel	258	258	258	258	258	258	258	258
25	Thermocouple Wire	Alumel	257	257	257	257	257	257	257	257
26	Thermocouple Wire	Chromel	258	258	258	258	258	258	258	258
27	Thermocouple Wire	Chromel	258	258	258	258	258	258	258	258
28	Thermocouple Wire	Alumel	257	257	257	257	257	257	257	257
2001	Braze Washer	Cu	416	416	416	416	416	416	416	416
2002	Braze Ring	Cu	419	419	419	419	419	419	419	419
2003	Braze Ring	Cu	419	419	419	419	419	419	419	419
2004	Braze Washer	Ti	140	140	140	140	140	140	140	140
2005	Braze Ring	Cu	127	127	127	127	127	127	127	127
2006	Braze Ring	Cu	419	419	419	419	419	419	419	419
2007	Braze Ring	Cu	127	127	127	127	127	127	127	127
2009	Braze Washer	75 EE	138	138	138	138	138	138	138	138
2010	Braze Washer	Cu	187	187	187	187	187	187	187	187
2012	Braze Disc	Ni	346	346	346	346	346	346	346	346

TABLE 5-2

TUBE RECORD VII-S

		6	7	8	9	10	11	12
1.	Emitter Identification	1	2	3	4	5	6	8
2.	Emitter QC No.	422	422	422	422	422	422	422
3.	Emitter Spacer Material	Ta	Ta	Ta	Ta	Ta	Ta	Ta
4.	Flatness (inches)	$\pm$ .0001	.0001	.0004	.0001	.0001	.0001	.0001
5.	Concave (Cv) or Convex(Cx)	Cv	Cx	Cx	Cv	Cx	Cx	Cv
6.	Average Thin Wall Thickness (inches)	.00335	.0029	.0034	.0034	.0033	.0034	.00335
7.	RMS Finish O. D. (μinches)	28-30	18-20	16-19	10-14	15-18	13-15	15-18
8.	Overall Quality Rating	Good	Good	Good	Good	Good	Good	Good
9.	Outgassing							
10	Total Time @ 1700/1750°C (hours)	21	27	20	20-1/4	27	26	26
11	Interruptions	0	1	1	0	0	0	0
12	Final Internal Pressure at 1700° C (mm Hg)	2×10^{-7}	7×10^{-8}	8×10^{-8}	4×10^{-7}	1.4×10^{-7}	1.5×10^{-7}	8.8×10^{-8}
13	External Pressure with Liquid Nitrogen (mm Hg)	8×10^{-7}	7×10^{-7}	1.1×10^{-6}	6×10^{-7}	4.2×10^{-7}	5×10^{-7}	3.5×10^{-7}

THERMO ELECTRON ENGINEERING CORPORATION

TABLE 5-3

SUMMARY OF DIODE ACCEPTANCE TEST RESULTS

		VII-S -6	VII-S -7	VII-S -8	VII-S -9	VII-S -10	VII-S -11	VII-S -12
1	Amperage at 1 volt 1700° C	14.4	13.0	15.5	12.0	12.0	17.3	17.4
2	Tcs °C	395	393	398	372	367	384	380
3	Trad °C	583	569	581	575	600	589	584
4	Tseal °C	678	740	649	694	737	685	682
5	Tcol °C	628	652	628	623	649	631	637
6	EB Power (watts) 1700° C	292	450	292	300	410	315	304

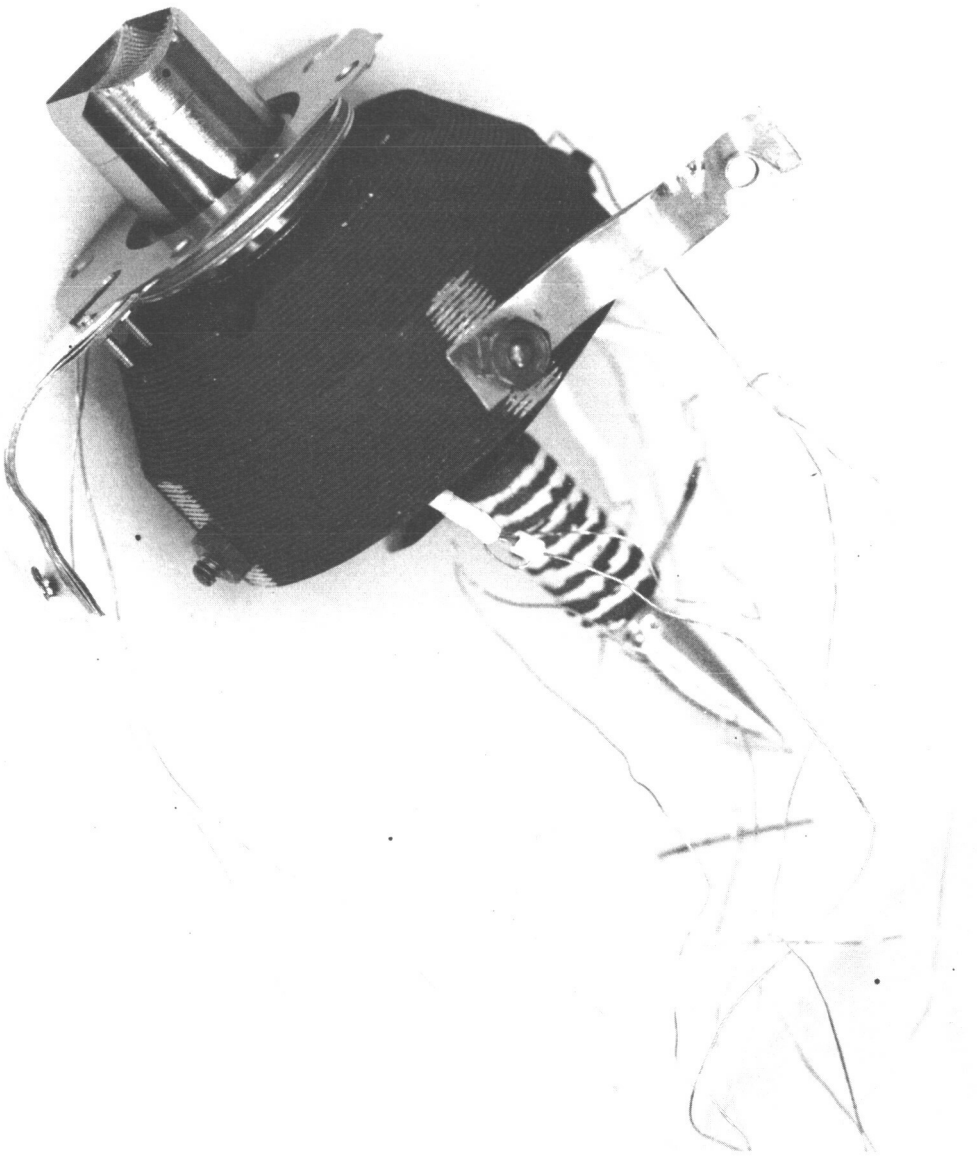


Figure 5-1. SET VII Diode

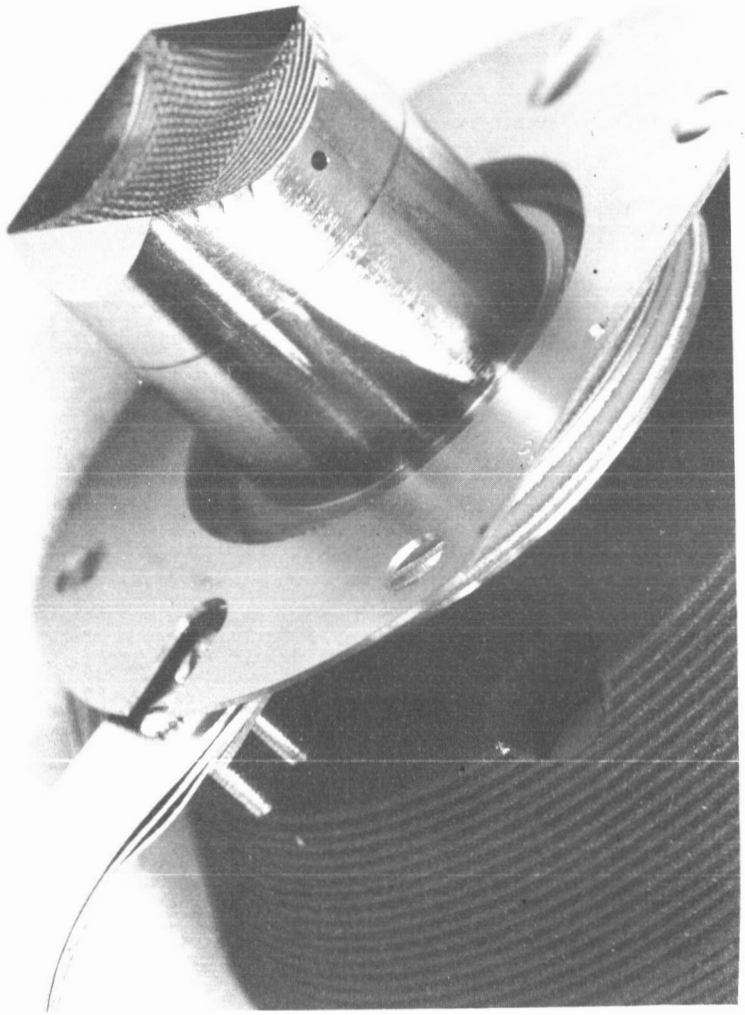


Figure 5-2. SET VII Spacer

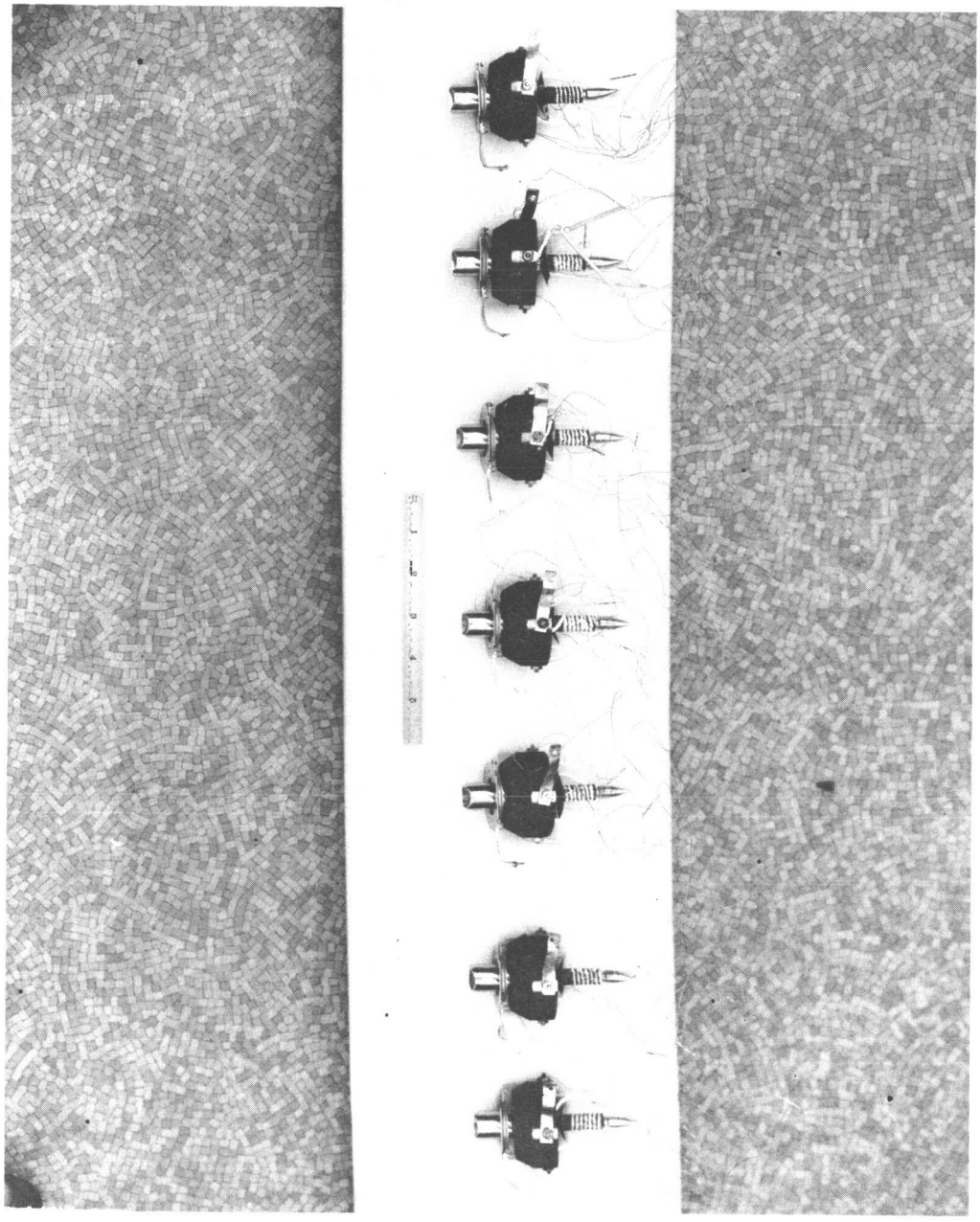


Figure 5-3. Seven SET VII Diodes

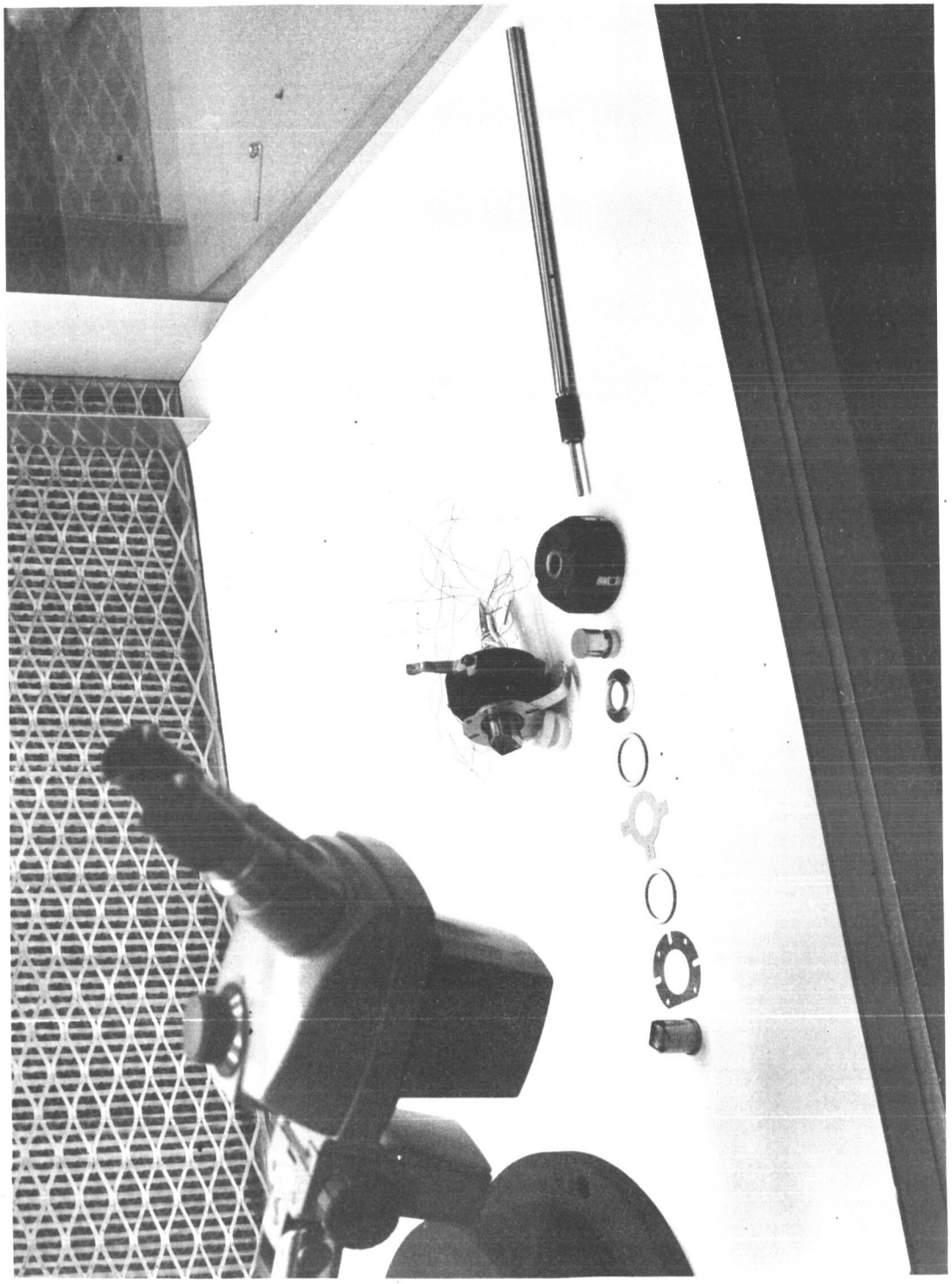


Figure 5-4. Dust Free Hood, Microscope, Exploded View SET VII Parts and SET VII Diode

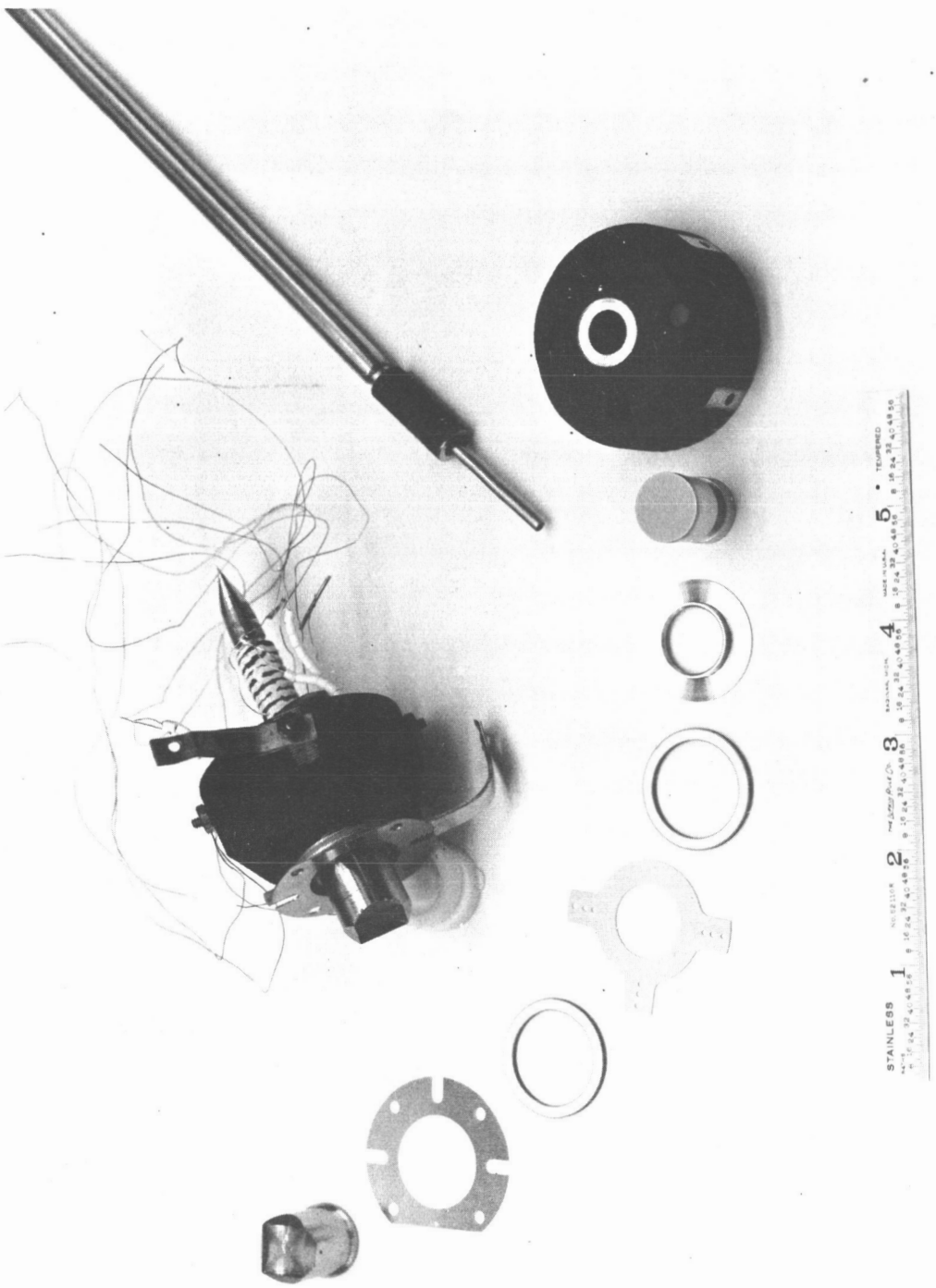


Figure 5-5. Exploded View of SET VII Parts and SET VII Diode

CHAPTER 6

LIFE AND RELIABILITY TEST

6.1 LIFE TEST EQUIPMENT

6.1.1 Introduction

Since the beginning of this program considerable time and effort was expended in the design and fabrication of five life test units to ensure that the vacuum environment, the method of heating, and the method of testing would not jeopardize the life of a diode. From component and prototype development, very high quality vacuum was found to be indispensable for meaningful converter testing. For this reason, Thermo Electron has designed and fabricated five special systems for life testing of solar converters. These units include vacuum chamber, electron gun, electron gun power supply, gun power supply regulator, cesium reservoir heater and power supply, elapsed time at temperature recorder and ion type vacuum pump and power supply. All controls are on a single console which can be locked to prevent any adjustments by unauthorized personnel. The results of life testing which will be discussed in this chapter showed that the units were basically well designed and operated well. There follows a description of the major components of the life test system.

6.1.2 Vacuum Chamber

The vacuum chamber is a 304 stainless steel cylinder 10.48" i.d. x 20" high. An oxidized, OFHC copper coil is mounted inside the bell jar, Figure (6-1) to adsorb the heat thrown off by the converter and the gun. The coil is water cooled. This type of arrangement avoids the necessity of cooling the stainless walls and presents a uniform radiation environment to the converter radiators. The cooling water outlet contains a pressure sensitive switch which upon sensing

insufficient water pressure opens. This switch is interlocked with the electron gun power supply and when it opens all heater power is automatically cut off, thus providing a fail safe arrangement with respect to the cooling of the unit. The switch does not affect the ion pump, however, thus maintaining the vacuum in the chamber while the converter cools down.

A 2" window with a Kovar to Pyrex housekeeper seal is used for pyrometer observations. The window is protected against deposits by a nickel gate which is pivoted out of the line of sight during observations with the aid of a small permanent magnet. The window assembly (Fig. 6-8) is heliarced to a stainless steel coupling which is welded to a grindable steel flange on the bell jar. This design permits easy replacement of the window if damage occurs, or if the nickel gate requires adjustment.

A Parker Gask-O-Seal, which has negligible sublimation at 10^{-8} mm Hg and a relative leak rate which is small in comparison with the stainless steel, is used to seal the chamber to the base plate. The base plate is made of stainless steel. Leadthroughs are heliarc welded to the base plate. The welds are grindable and easily accessible for convenient replacement should they be damaged. All feedthroughs are of metal-ceramic construction and are welded internally to the base plate. All welds on leadthroughs are made internally to avoid virtual gas loads. After the chamber has been mechanically pumped below 10 microns, a 50/liter/sec (Ultek Corporation) ion pump takes over. Roughing is accomplished through a stainless steel bellows valve which has a Teflon seat rather than a standard elastomer seal. Thermocouple lead wires pass through the feedthrough insulator uninterrupted. Connections are made inside the vacuum chamber mechanically, except for thermocouples which are tack-welded according to accepted standard practice. The connections outside

the chamber are made at a terminal board to avoid handling of loose wires, thus eliminating the danger of bending and pulling on the leads which connect to the relatively fragile feedthroughs.

Converters have been operated in these chambers, Figure (6-2) for more than 15,000 hours, at an emitter temperature of 2000° K and all units have operated in the low 10^{-7} or high 10^{-8} torr range without difficulty. During checkout, one unit was opened between tests more than 20 times and did not encounter any pumpdown difficulties.

6.1.3 Electron Gun and Converter Support Structure

The heat source for the diode is a Pierce type electron gun which delivers the required power uniformly distributed to a target area approximately 1/2" in diameter. The electron source consists of 0.030" diameter tungsten filament. The electron flow is accelerated by a plate potential of about 2000 volts and is shaped and controlled by a grid at a negative potential of about 400 volts. The gun was designed, developed, fabricated and tested by Thermo Electron especially for bombardment of converters of solar configuration.

6.1.4 Power Supplies and Regulator

The electron gun is operated by a Thermo Electron designed and fabricated power supply. The self-contained unit provides a maximum of 50 amperes at 10 volts ac to the filament. This current is regulated by a control circuit which has eliminated shutdowns due to power supply drift, where earlier units had encountered shutdowns from this cause averaging one every 48 hours. The unit also provides 0-2000 volts dc for the accelerating potential and 0-750 volts dc for the grid. Each of the three supplies is independently

controllable from the front panel of the console. The operation of the unit requires both single phase 220 volts ac and 100 volts ac (from neutral line of 220 volt supply).

The life test base plate is shown in Figure (6-3); the base plate with its Gask-O-Seal is shown in Figure (6-4), the bell jar with its protected pyrometer window is shown in Figure (6-5). Figure (6-6) depicts the Pierce type electron gun. The instrument panel and chamber of a complete life test unit is shown in Figure (6-8). Dummy testing of converters in the life test equipment did not reveal any major difficulties; therefore, no further changes were made in the equipment prior to converter life testing.

6.1.5 Instrumentation

Figure (6-7) shows the connections made to the various elements in the vacuum chamber while Figure (6-8) shows the front view of a life test unit.

6.1.5.1 Emitter Temperature Measurement

As explained in the description of the vacuum chamber, the emitter temperature measurement is made by means of an optical pyrometer sighting through a clean pyrex window. The reflection and transmission losses of the window were measured with an NBS calibrated tungsten ribbon lamp. The average correction in the 2000° K range was 20° K.

6.1.5.2 Thermocouples

The thermocouple terminals are located to the rear of the cabinet. These are of the plug-in type and can readily be connected by means

of thermocouple extension wire to the switching and cold-reference location where the temperatures for all five test units are recorded.

6.1.5.3 Diode Load and Cesium Reservoir Heater Panel

The top panel combines the diode load instruments and the power supply for the cesium reservoir heater. The diode load is a rheostat in series with an ammeter; the panel also carries a voltmeter to measure the potential developed at the diode terminals by means of suitable voltage taps.

6.1.5.4 Elapsed Time Meter

This meter records the time a converter is operating at a predetermined emitter temperature. The meter is actuated by a relay switch connected to a Zener diode. The terminals of the relay switch are shorted until the bombardment current reaches a value corresponding to the required emitter temperature at which point the Zener diode unshorts the relay terminals and the relay actuates the meter. The threshold value of bombardment current is set by means of a rheostat.

6.1.5.5 Chamber Pressure

The ion pump is provided with a power unit with provision for measuring the internal chamber pressure.

6.1.6 Protection Features

The unexpected conditions that should be examined are the following:

1. Loss of electrical power – All heat sources and the ion pump will turn off, water circulation will remain. Sudden cooling of the diode is

unavoidable, most likely the chamber vacuum will remain excellent at least during the cooling period. The power supply has a relay disconnect which prevents it from turning on again; should the main electrical power be re-established, manual re-start is required. No other equipment in the plant is used in the same fused circuit.

2. Loss of water circulation — To protect the diode from water shut-off, a water flow sensor is placed in the water line. When the water flow decreases below the minimum flow rate of 2 gpm, a command is given to the power supply to shut-off. The ion pump is kept under power.

3. Vacuum chamber leak — Loss of vacuum will eventually result in an electrical discharge on the emitter structure. To prevent this, a sensor is provided in the pressure measurement circuit of the power supply which actuates the power supply shut off in case the chamber pressure exceeds 5×10^{-5} mm Hg. The sensor also actuates the ion pump power supply shut-off and the cesium reservoir heater shut-off so as to protect all components from the presence of excessive amounts of gas in the chamber.

4. Ion pump or ion pump power supply failure — This occurrence is so unlikely that no protection features are incorporated in the event of ion pump shut-off. The vacuum in the chamber will slowly deteriorate until the electron gun discharges and the power supply shuts off.

5. Filament "burn out" in electron gun — The electron gun power will be interrupted. The diode will cool and no other damage will result.

6. Excessive emitter temperature or excessive electron bombardment

A relay meter commands power supply shut-off should the bombardment current

exceed a pre-adjusted level. Thus, the diode is protected against excessive electron bombardment and excessive emitter temperature due to excessive electron bombardment. There are no provisions incorporated to shut off when the emitter rises because of other causes than excessive electron bombardment such as loss of cesium. This is because in such events, it is almost certain that the diode will have failed and protection against over-temperature is then less essential.

7. Low emitter temperature – No damage results but there is a threshold level below which life-hours should no longer be counted. No adjustment made during start-up of the life test and described in the operating procedure permits stopping the lapsed time indicator when the bombardment current decreases below a set level. A light signal on the exterior of the cabinet is then also turned off to call attention of the laboratory personnel. Decreases in emitter temperature due to other causes than decreased electron bombardment are not detected until the data is taken; the chance of this happening is very unlikely since experience has indicated that, under constant electron bombardment power, if a tendency for the emitter temperature to decrease exists, it manifests itself extremely slowly.

8. Line voltage fluctuations – As already mentioned in the description of the design of the power supply, the electron bombardment current is maintained constant by means of a saturable choke. All other components should remain uneffected by normal voltage fluctuations.

9. Cesium leak from the diode – The vacuum will deteriorate and the chamber pressure sensor will command total power shut-off.

10. Changes in adjustment by unauthorized personnel — To protect against this possibility, the front panel of the cabinet is locked by means of a locked door that closes over it. Only the technicians in charge of running the test will have a key for access to the panels. In order to detect shut-off, a "power on" light is mounted on the outside of the cabinet.

6.1.7 Operation Procedure for the Power Supply

The operating procedure for the power supply is as follows; (Refer to Figure (6-8).

Automatic:

It is assumed that all the bell jar connections have been made, that a SET converter prototype of either Series VI or VII is mounted on the test structure, that the bell jar has been evacuated and its water cooling connections are ON.

1. Turn all 5 knobs on the power supply fully counterclockwise.
2. Depress the "Manual-Automatic" switch to the Automatic position.
3. Turn the "Power" switch on.
4. Push the "Start" button. Red light next to "Start" button should to on to indicate that connection to power line is established.
5. Allow two minutes for warm-up. The "Control Current" meter should indicate approximately 50 to 100 mA.
6. Adjust the accelerating voltage to 2000 volts.
7. Adjust the grid bias voltage to 400 volts.
8. Set the red pointer on the bombardment current meter to 300 mA.
9. Slowly turn the Filament Current knob fully clockwise. Notice that bombardment will begin to occur at a filament current of about 26 amperes. If this is the first time the chamber elements are brought

up to temperature since exposure to atmosphere, watch the pressure indication given by the vac-ion control unit. This pressure should not be allowed to exceed 1 x 10^{-5} mm Hg at any time during power supply start-up. As the "Filament Current" knob is turned further clockwise, a bombardment current level of approximately 150 mA will be reached at a filament current of approximately 28.5 amperes. Further clockwise turning of the knob will not produce more bombardment current because the control circuit takes over at this point.

10. Correct the accelerating voltage setting to maintain a meter reading of 2000 volts.
11. Turn the "Control Current" knob clockwise until the desired level of bombardment current is achieved. Repeat steps 10 and 11 as often as required while adjusting the cesium temperature and converter load.
12. Adjust the "Timer On" knob to trigger the "elapsed time at temperature" indicator. Calibrate this setting by causing deliberate variations in bombardment current (by moving the "Control Current" knob) until the drop off point is at the desired emitter temperature. This completes the start-up.

Manual:

To switch from automatic to manual operation, i.e., to by-pass the control circuit, use the following procedure. (To avoid burning out the filament, never switch from automatic to manual when the filament is carrying current.)

1. Reduce filament current to zero by means of the "Filament Current" knob.

2. Depress "Manual-Automatic" switch to the manual position.
3. Increase filament current with "Filament Current" knob, to the value that gives the desired bombardment current.

Shut-Down:

From automatic or manual operation, follow these steps:

1. To avoid sudden cooling of converter, gradually decrease the bombardment current by turning counterclockwise the "Filament Current" knob.
2. Reduce the accelerating voltage to zero.
3. Reduce the grid bias voltage to zero.
4. Shut-off the "Power" switch.

6.2 LIFE TEST OF FIVE CONVERTERS

The object of testing three Series VI (VI-TEP-1, VI-S-14*, and VI-S-18) and two Series VII converters (VII-S-4 and VII-S-5) was to demonstrate that a life of 2000 hours at 2000° K emitter temperature could be achieved in a hardware type solar thermionic converter without significant deterioration of output with time. Extraneous limitations which had been encountered in previous life testing of SET converters such as reaction of hot structures with a harmful environment or localized bombardment of emitter with non-focused electron gun were virtually eliminated with a careful design of the life test equipment.

From earlier system considerations, the SET VI diodes were acceptance and life tested at 1 volt at 1655° C observed while more recent considerations led to testing the SET VII diodes at 0.8 volt. Neither voltage represents either the maximum power or efficiency point. The acceptance test data is summarized in Table 6-1. With these results, each converter was placed in a life test chamber (shown in Figure (6-8)) and was set initially at a value as close as possible to the initial conditions. The initial starting points for life testing are shown in Table 6-2. When steady-state conditions had been achieved, each converter was then maintained at constant heat input to simulate solar heating.**

---

* Of the five life test converters, four were constructed during the present program, while VI-S-14 had been constructed approximately one year earlier.

** After approximately 465 hours of running, the bombardment filament of VI-S-14 burned out and was replaced. When the converter was restarted, the heat input was adjusted to give the same output as recorded previous to shutdown. The new value of power input was 378 watts as compared to the starting value of 344 watts. From this time forward, the power input was maintained constant. Because converter VI-TEP-1 required substantially less power input than the other four converters, and, because the ensuing value of bombardment current was in low range of the control unit during the first several hundred hours of testing, difficulty was encountered in maintaining power input at its original value. However, an adjustment was made in the control circuit and the power input was reset at the original value of 300 watts, and maintained there during the balance of life testing.

The following data was taken at intervals defined in the statement of work: emitter temperature, seal temperature, collector temperature, radiator temperature, cesium reservoir temperature, electron bombardment power (including grid voltage and control current setting), output voltage, output current, pressure in vacuum chamber, date, time, cesium heater current, and observer. Data was not recorded until the cesium pressure had been optimized for a particular converter. During the course of testing, no difficulty was encountered in manipulating the magnetic shield which protected the pyrometer window. Because the pyrometer hole in the diode emitters of VI-S-14 and VI-TEP-1 were not perfectly concentric with the holes in the anodes of the electron guns, it was more difficult to obtain measurements on these units than with the others.

The majority of shut-downs encountered were directly attributable to failures of electron tubes in the high-voltage power supply.

The actual life test data sheets are included in Tables 6-3 through 6-22 (see Volume II). Weekly summaries of this data are included in Tables 6-23 through 6-42. These later tables include the day, time, accumulated running time, output current and voltage, power density, power input, chamber pressure, cesium, radiator, collector, seal temperatures, and observed emitter temperatures. Since converters VI-S-14 and VI-TEP-1 did not have collector thermocouples, no values are recorded. During testing, various thermocouples from time to time would give erroneous readings (due to touching other thermocouples, heaters, etc.) and for this reason were not recorded on the original data sheets.

Figures (6-10) through (6-14) show plots of power input, power output, and observed emitter temperature versus time. Table 6-43 lists for each converter, output power density, power input, cesium temperature, seal temperature, and observed emitter temperature at starting conditions, 1000-hour

level, 2000-hour level, and 3000-hour level. From this later table, it is interesting to note that, for all five converters, the seal temperatures ranged from 630° C to 660° C with no major changes occurring during testing.

For converter VI-S-18, which accumulated a life of 3342 hours without failure, the average order of change between initial and final operating conditions was 10%, while for VII-S-4, over 3212 hours without failure, it was less than 2%, for VII-S-5, over 3185 hours without failure, it was 12%, for VI-S-14 over 3013 hours without failure, it was less than 25%, and for VI-TEP-1, 3010 hours without failure, it was of the order of 40%.

The converter with maximum change, VI-TEP-1, likewise had a recorded emitter temperature 20° C lower than its initial value for the last 2000 hours of testing suggesting a change in heat input to the converter.

Figure (6-15) shows VII-S-5 mounted in the electron gun after 3000 hours of testing prior to removal and delivery to JPL, while Figure (6-16) shows VII-S-5 removed,* and Figure (6-17) shows an exploded view of the gun after testing. An overall view of the life test converters removed from the life test units is shown in Figure (6-18) while Figures (6-19) through (6-23) show views of each converter before and after life testing. These latter photographs show no major perceptible changes in the diode components after 3000 hours, especially in the emitter area.

The results of this program suggest that, in order to interpret changes in performance with time more accurately, it is necessary to implement more versatile measurements such as complete I-V characteristics at various time

*No difficulty was encountered in removing the stainless steel screws which held VII-S-4 and VII-S-5 in the electron gun after 3000 hours of testing.

intervals. From properly taken I-V data, one could measure such information as collector work function or shifts in I-V curves.

In order to achieve this with the present life test units, it would be necessary to add provisions for dynamic testing. This feature could be added to each unit or be provided by a master panel with necessary equipment which could be moved from unit to unit.

Further, since the emitter temperature is such an important parameter in testing, operation at constant-heat input demands that the measured power inputs be truly representative of the actual energy going into the converter and does not include extraneous heat to support structures or anything in proximity to the diode which might vary with time. Since the life test converters were mounted to the anode sections of the electron guns, and since for focusing purposes it was necessary to maintain this portion of the gun at the same potential as the emitter, a portion of the measured heat input is actually bombardment power to the gun. Recent experience with testing converters VII-S-6 through VII-S-12 has shown this type of leakage to be significant portions of the total heat input and that the leakage need not stay constant. Moreover, if practical, it would be desirable to make reliable efficiency measurements.

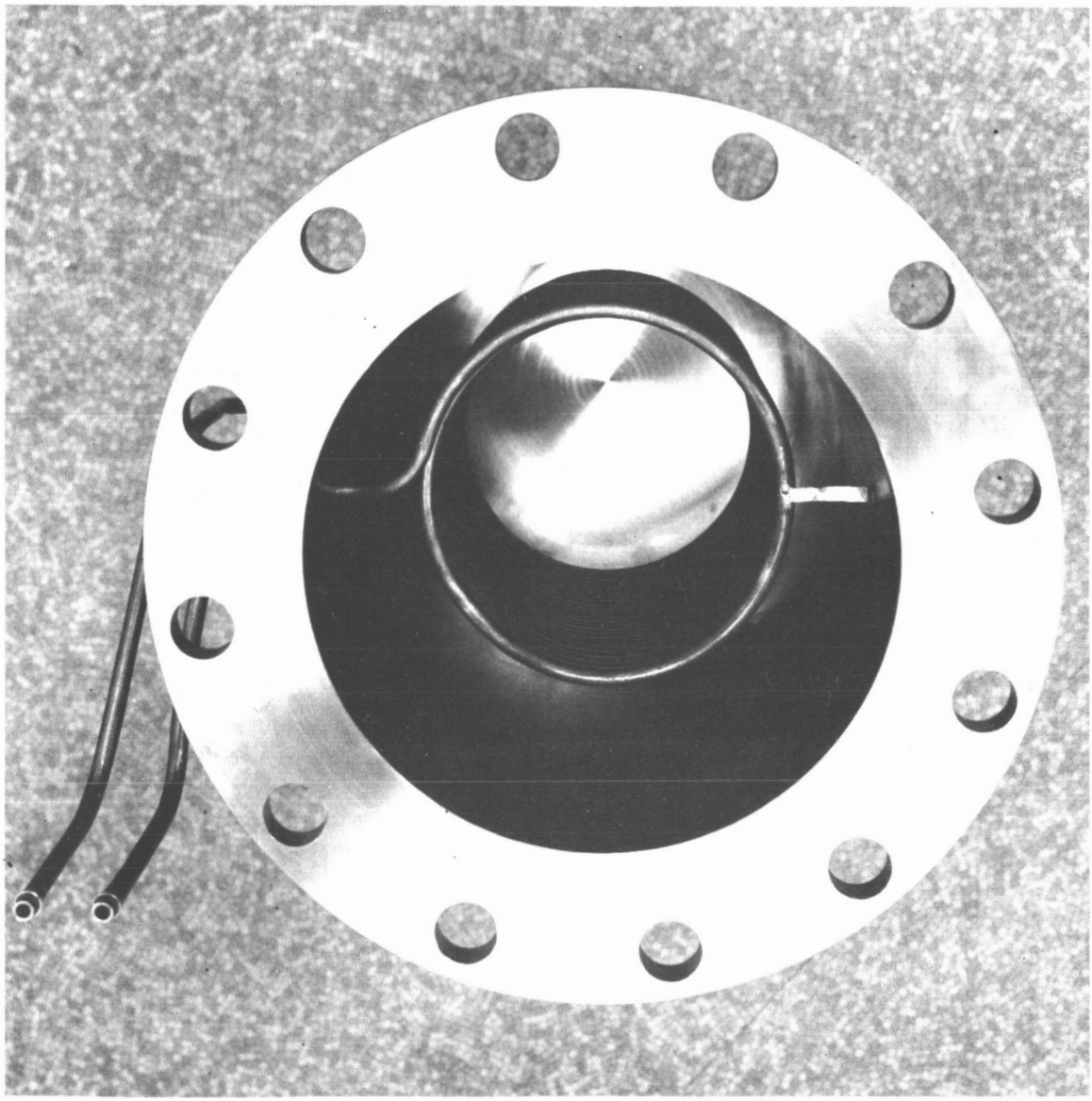


Figure 6-1. Cooling Coil in Life Test Chamber



Figure 6-2. Five Life Test Units.

5183

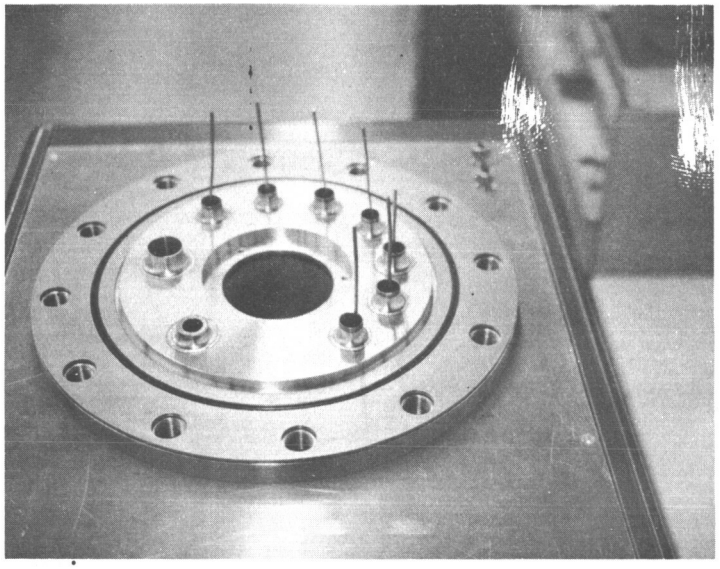


Figure 6-3. Life Test Base Plate

5184

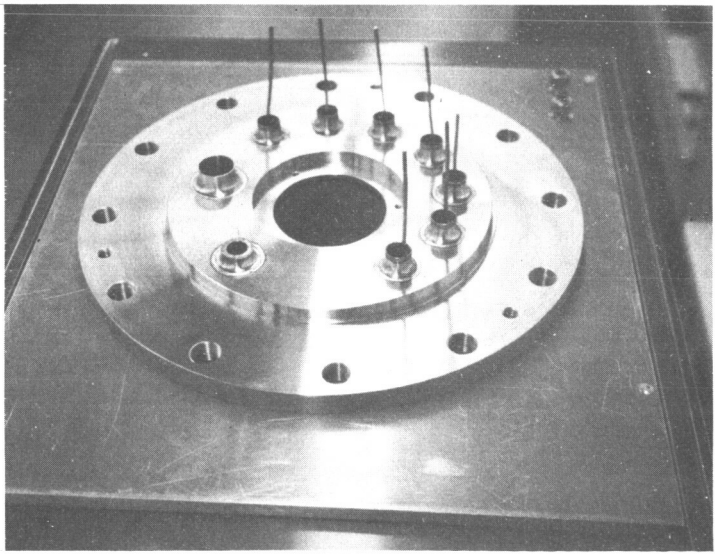


Figure 6-4. Base Plate Gask-O-Seal

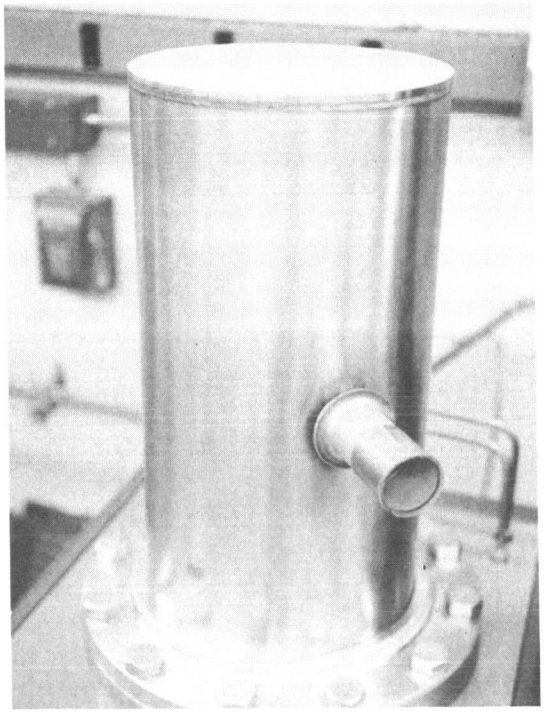


Figure 6-5. Bell Jar with Protective Pyrometer Window

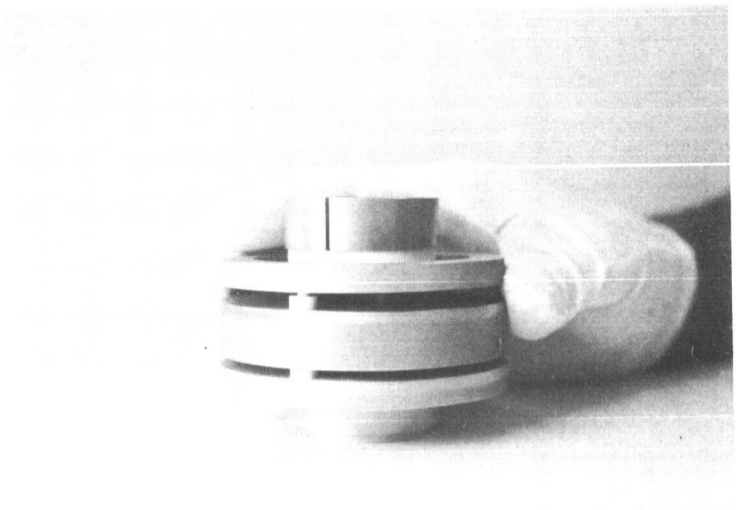


Figure 6-6. Pierce Type Electron Gun.

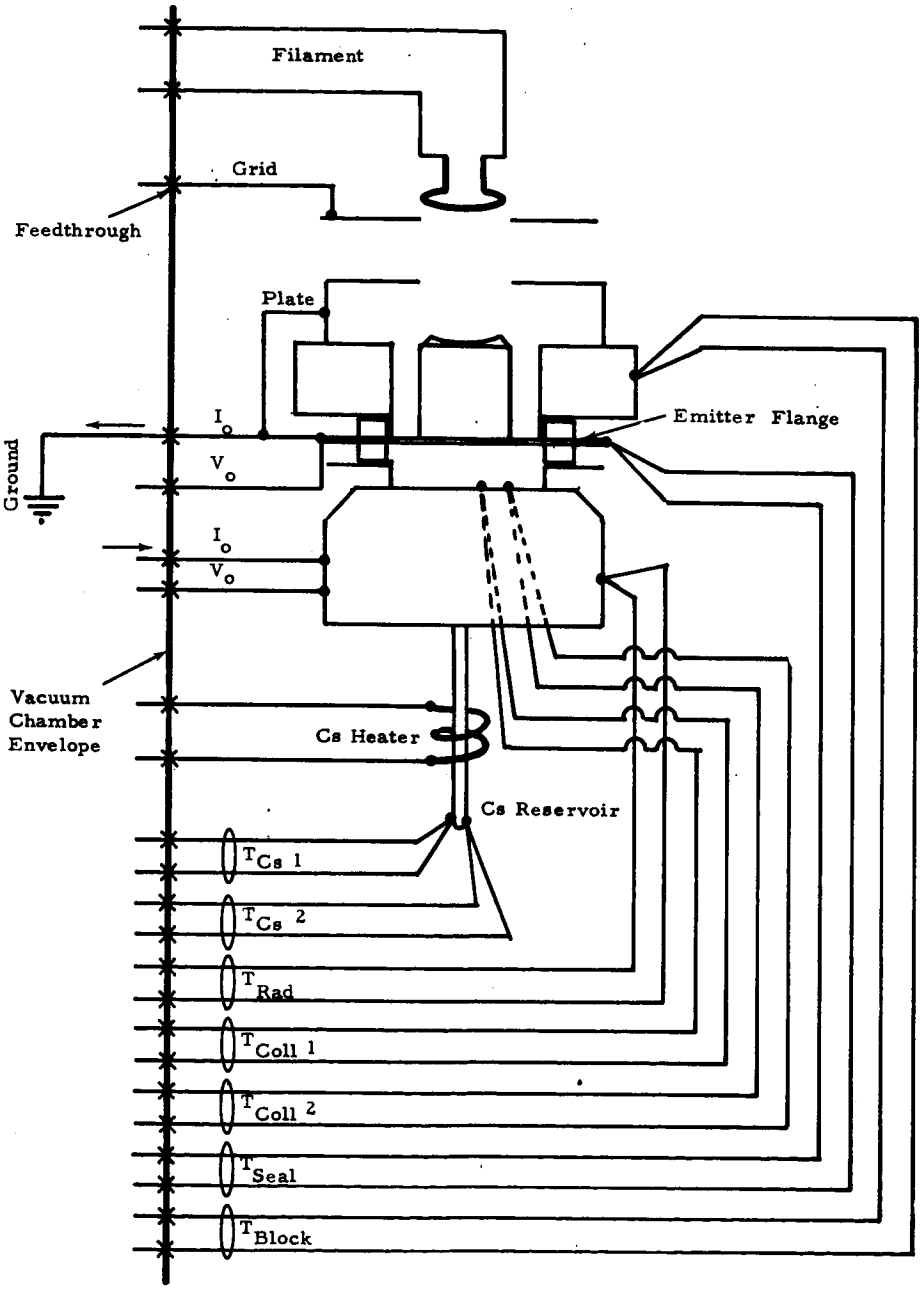


Figure 6-7. Vacuum Chamber with Connections to Elements

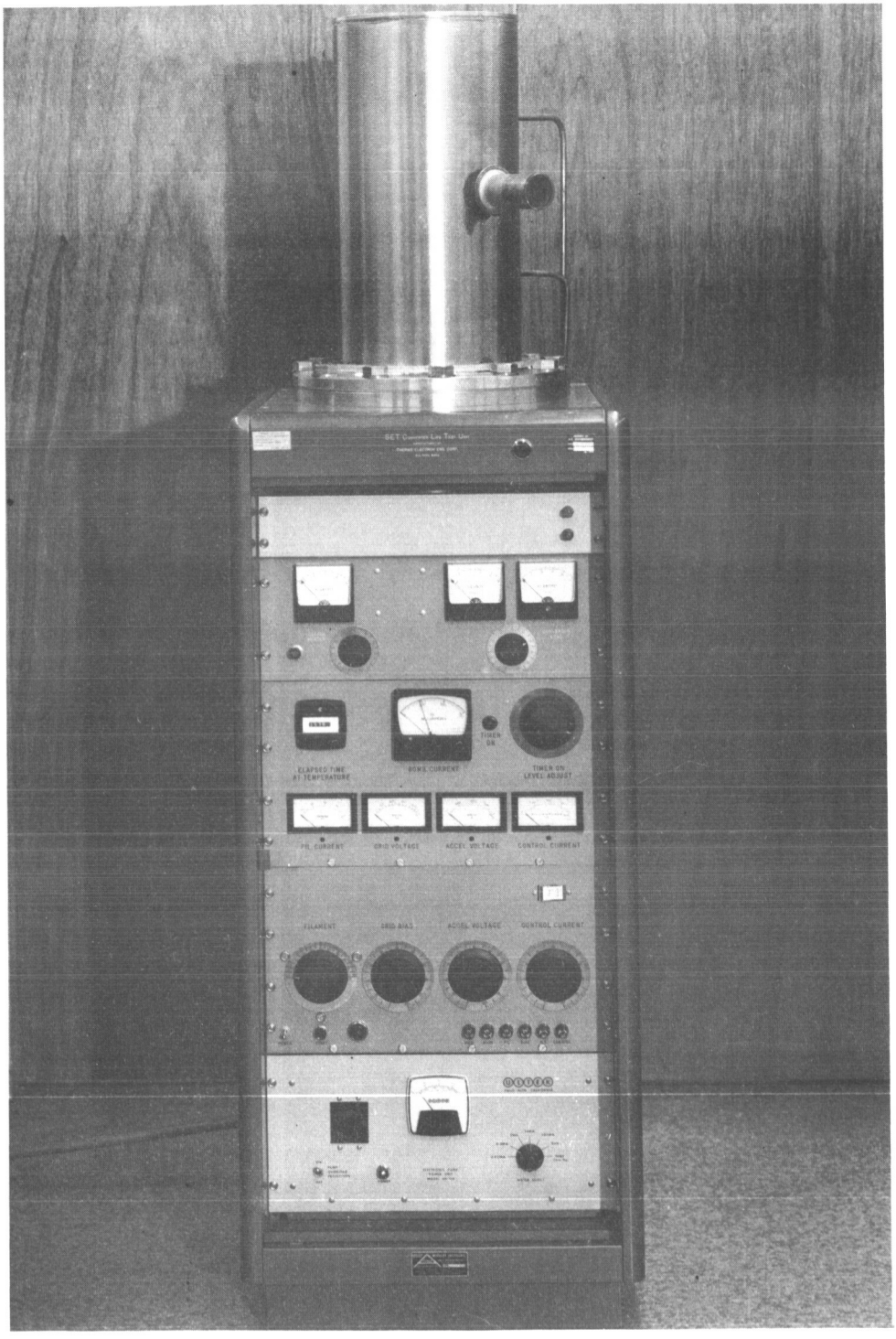


Figure 6-8. Instrument Panel and Chamber of a Complete Life Test Unit

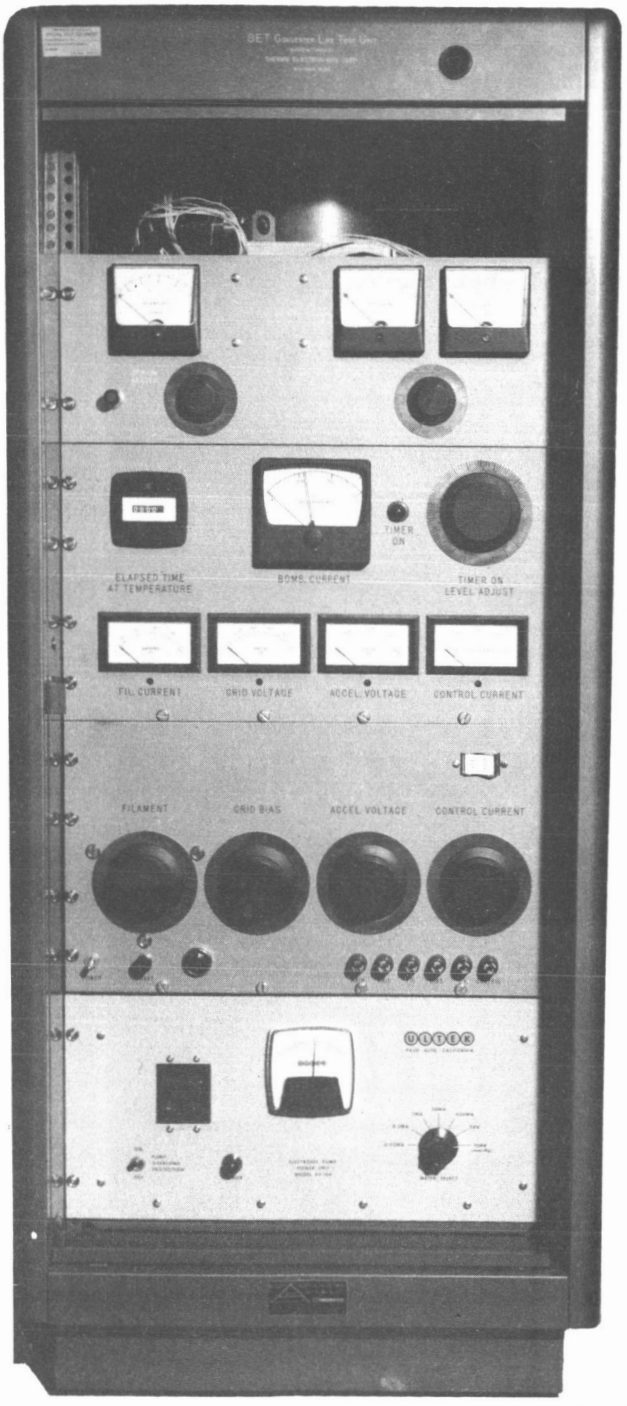


Figure 6-9. Instrument Panel of a Complete Life Test Unit

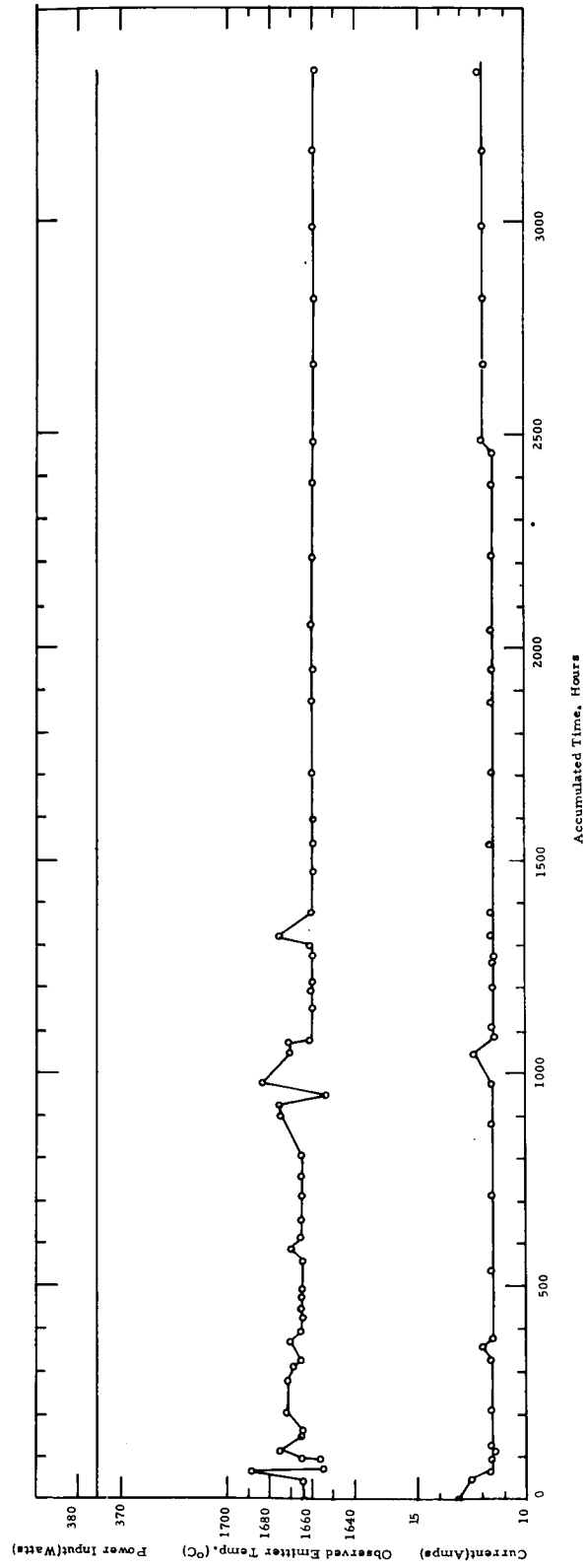


Figure 6-10. Converter VI-S-18, Power Input, Power Output, and Observed Emitter Temperature Vs. Time

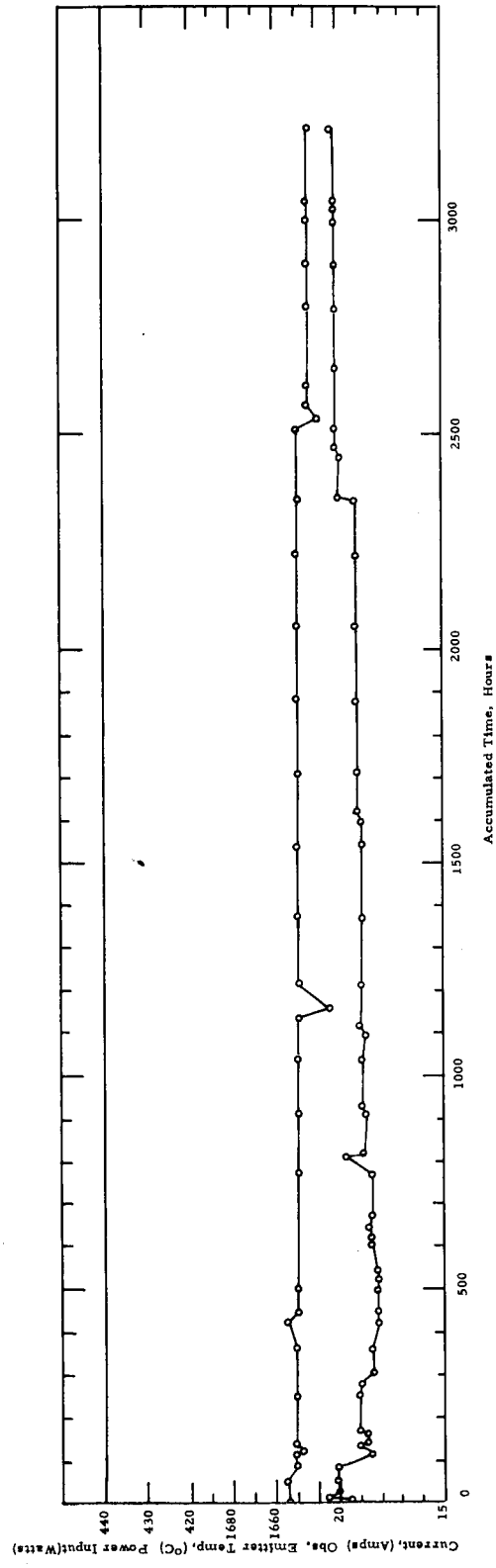


Figure 6-11. Converter VII-S-4, Power Input, Power Output and Observed Emitter Temperature Vs. Time

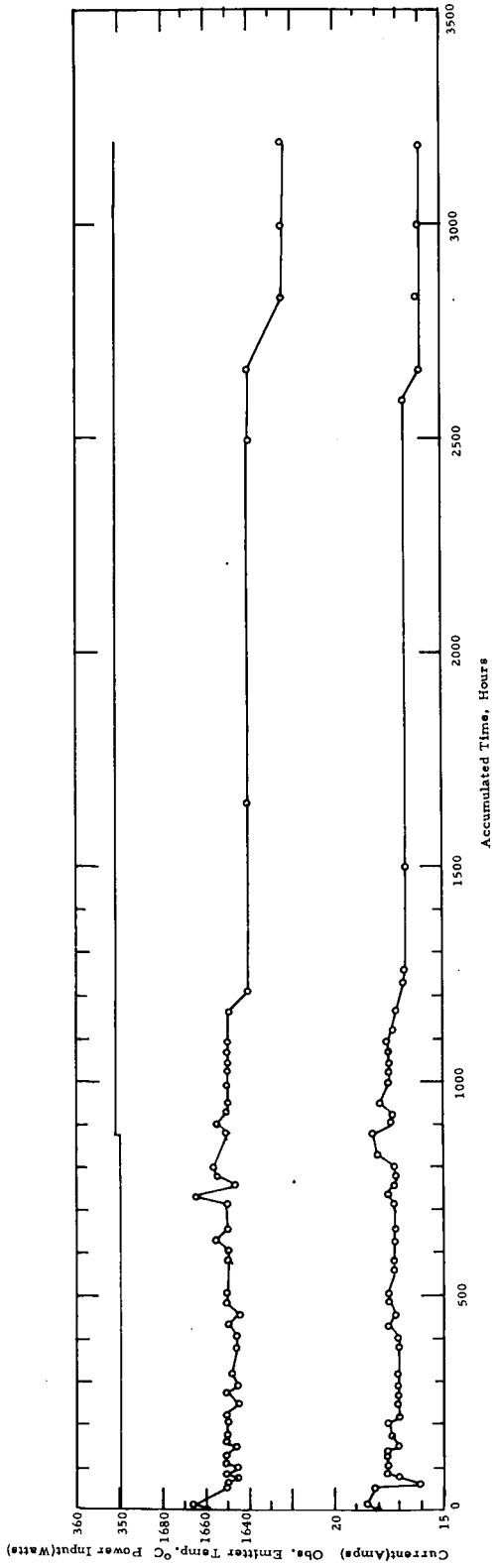


Figure 6-12. Converter VII-S-5, Power Input, Power Output and Observed Emitter Temperature Vs. Time

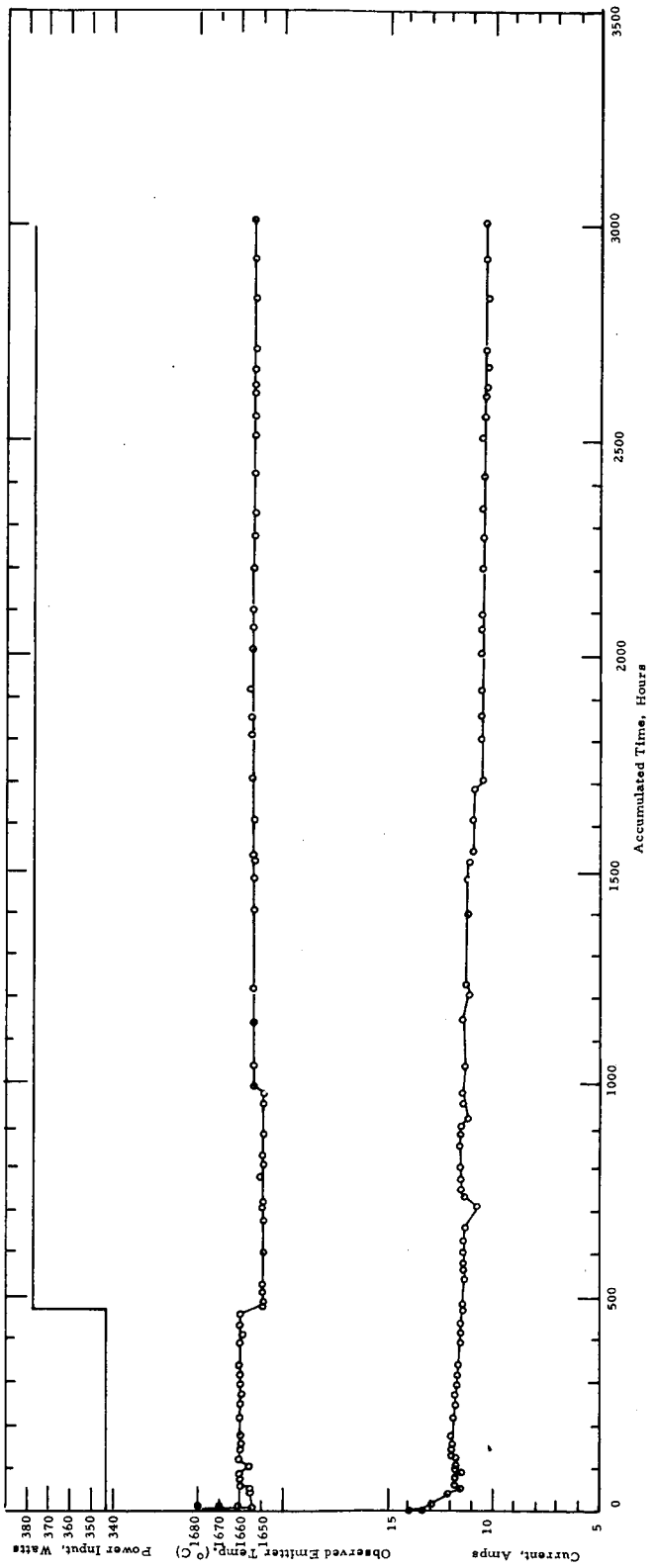


Figure 6-13. Converter VI-S-14, Power Input, Power Output and Observed Emitter Temperature Vs. Time

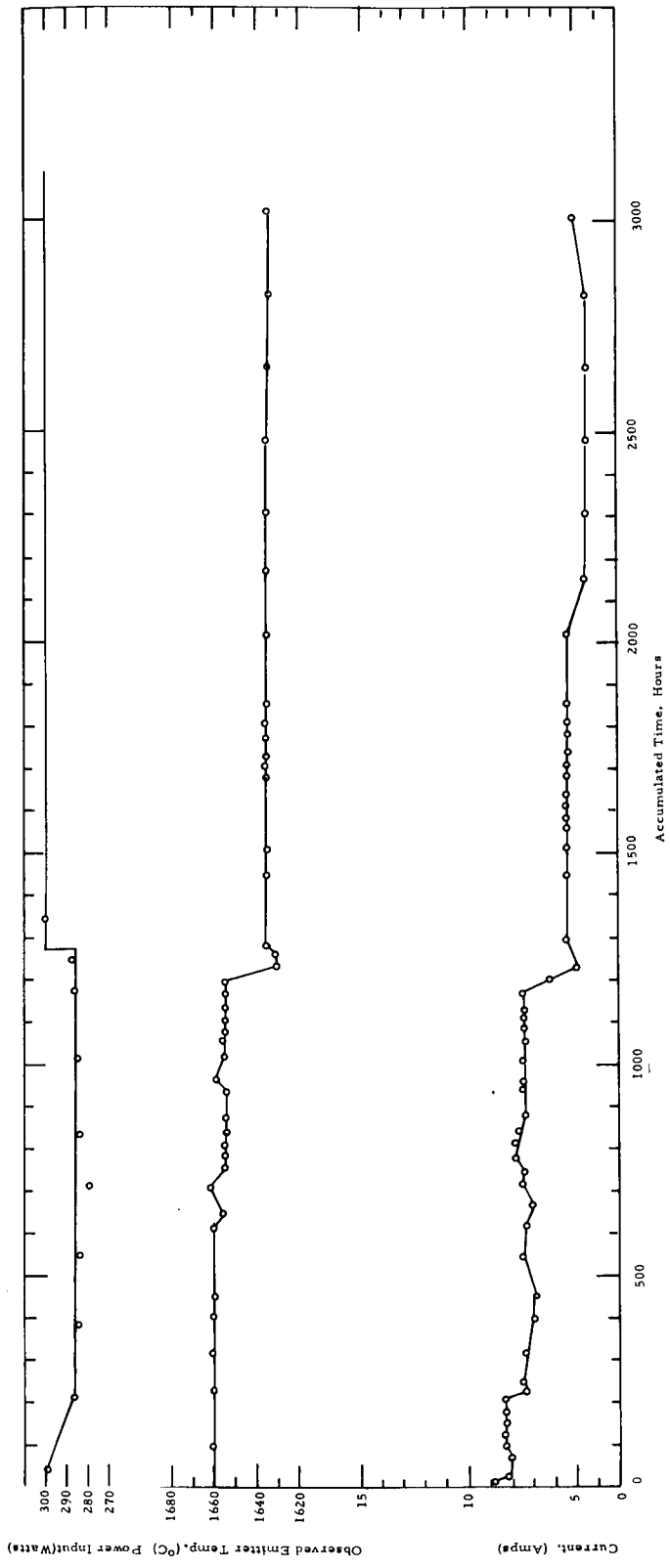


Figure 6-14. Converter VI-TEP-1, Power Input, Power Output and Observed Emitter Temperature Vs. Time

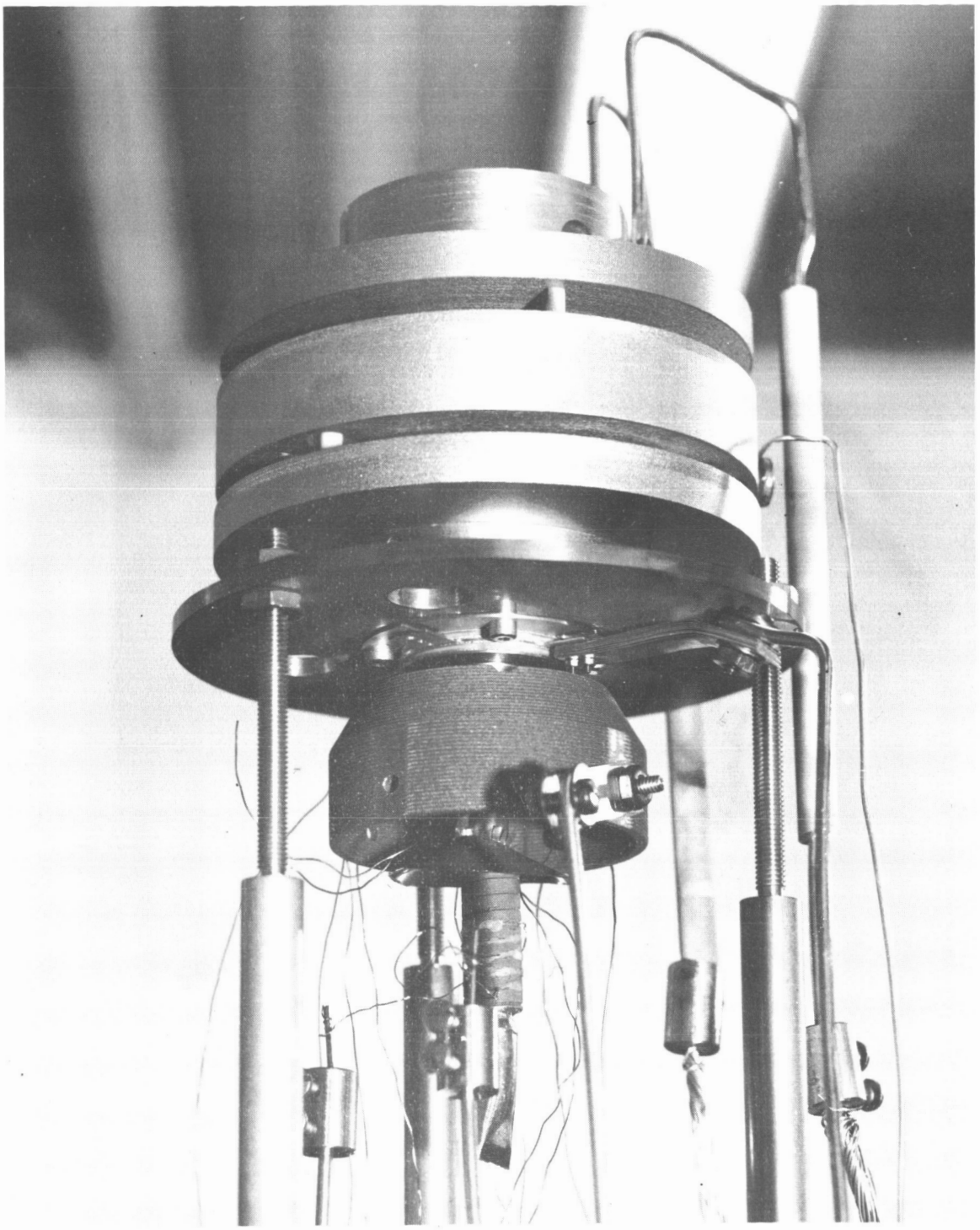


Figure 6-15. SET VII-S-5 Mounted in Electron Gun

Figure 6-16. SET VII-S-5 Removed after 3000 hours of Operation

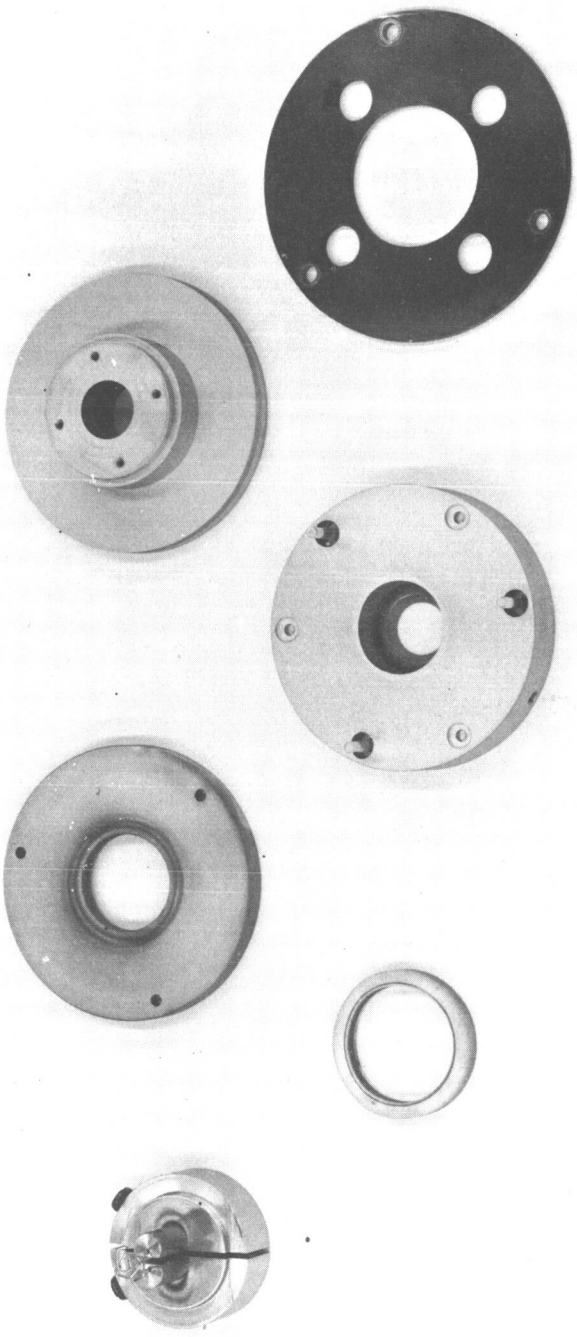


Figure 6-17. Exploded View of Electron Gun After Testing

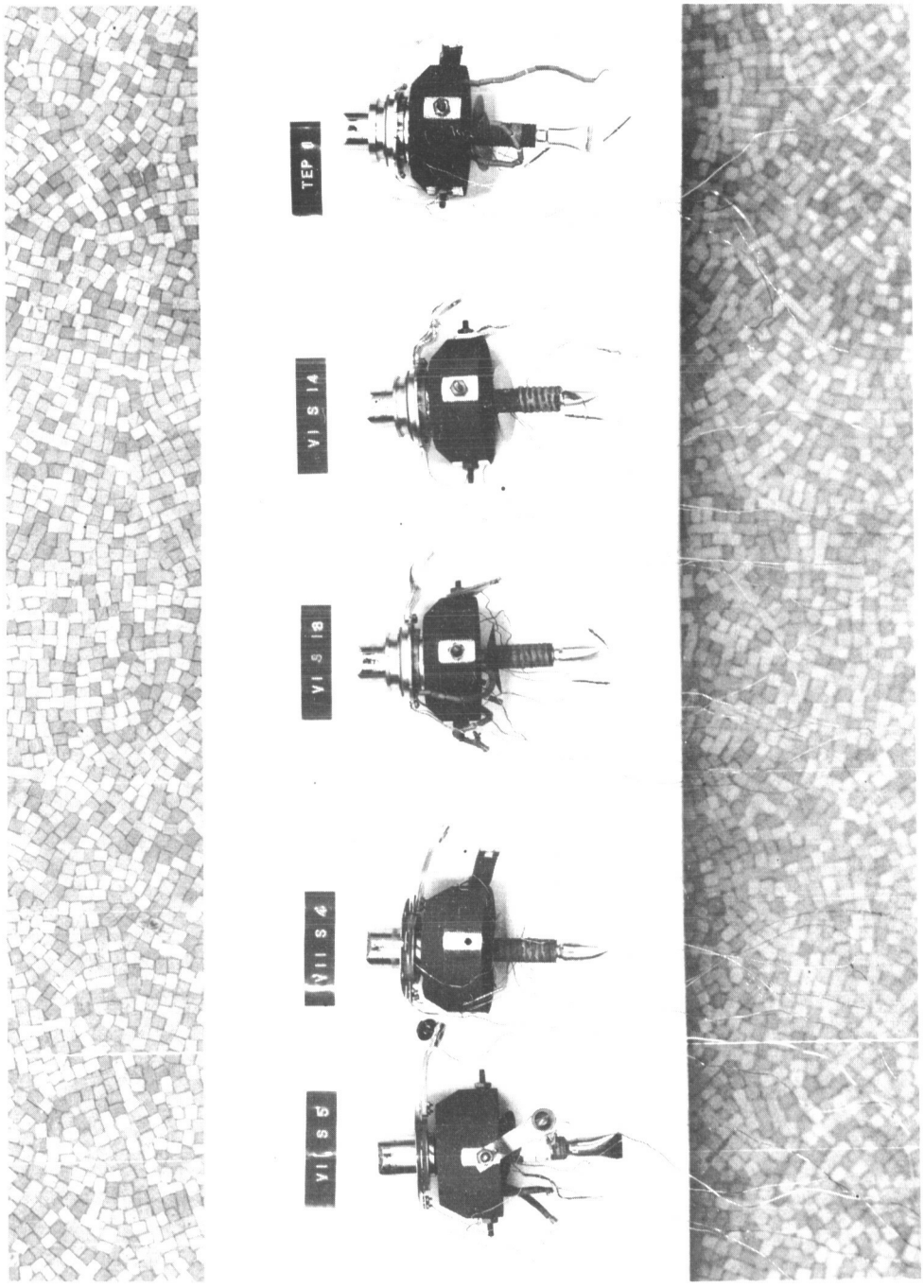
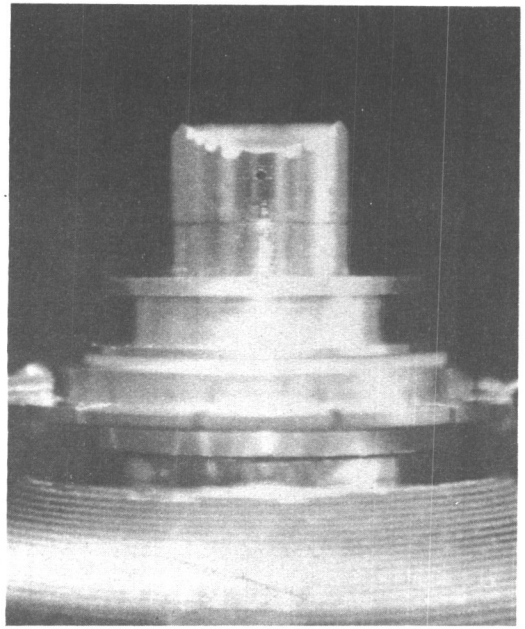


Figure 6-18. Five Life Test Diodes after 3000 Hours of Operation

5194

5195



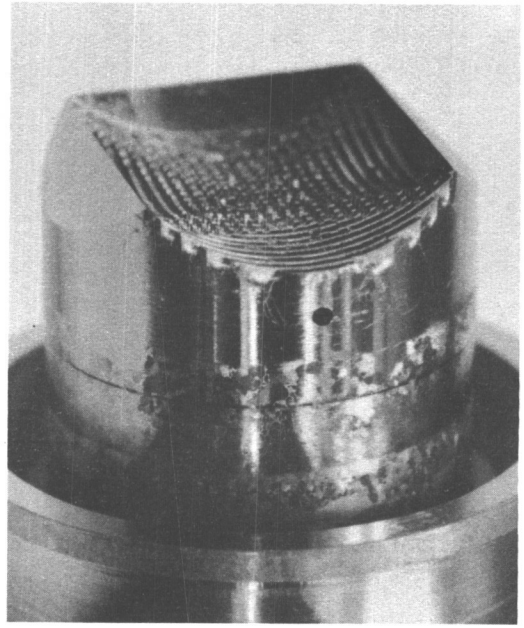
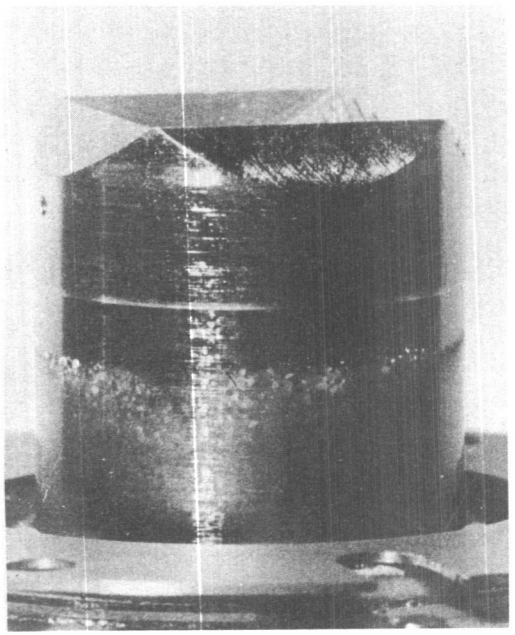


Figure 6-19. VI-S-18, View of Converter before and after Life Testing

THERMO ELECTRON ENGINEERING CORPORATION

5196



5197

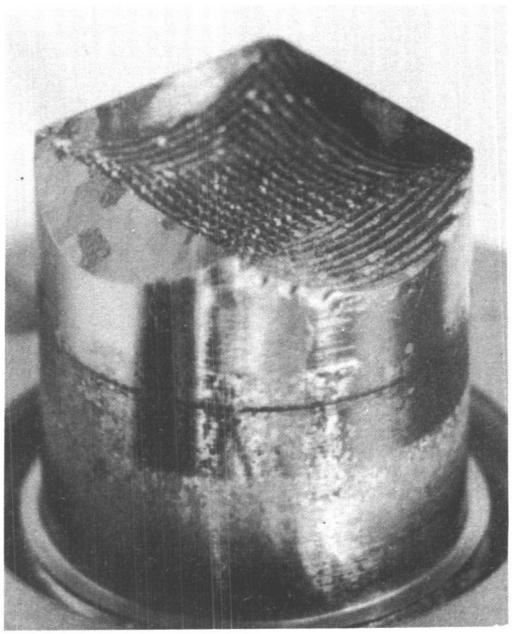
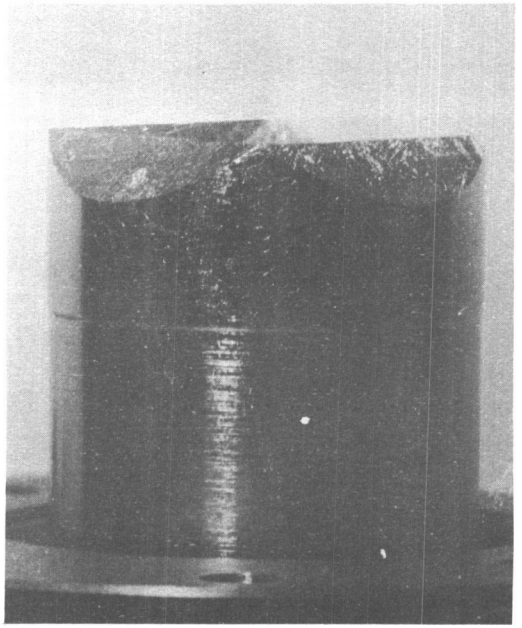


Figure 6-20. VII-S-4, View of Converter before and after Life Testing

THERMO ELECTRON
ENGINEERING CORPORATION

5198

5199



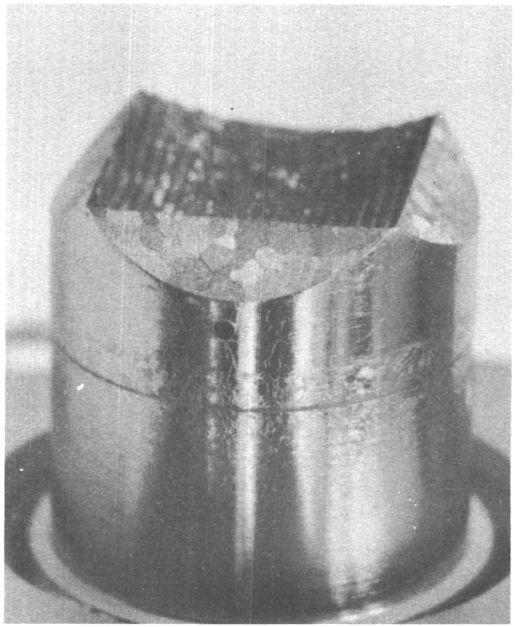
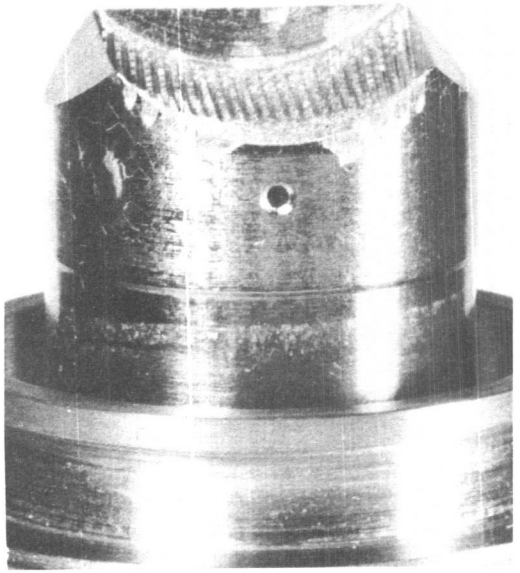


Figure 6-21. VII-S-5, View of Converter before and after Life Testing

THERMO ELECTRON ENGINEERING CORPORATION

5200



5201

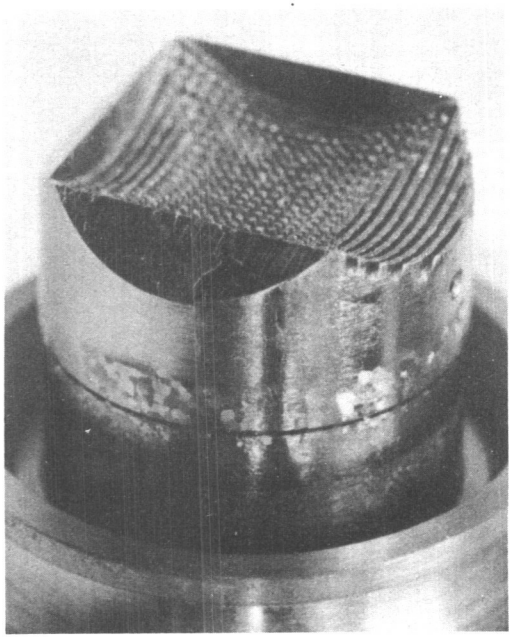
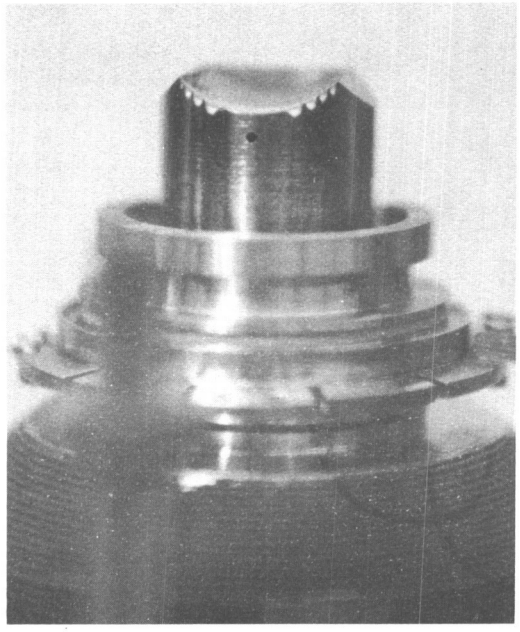


Figure 6-22. VI-S-14. View of Converter before and after Life Testing

THERMO ELECTRON ENGINEERING CORPORATION

5202



5203

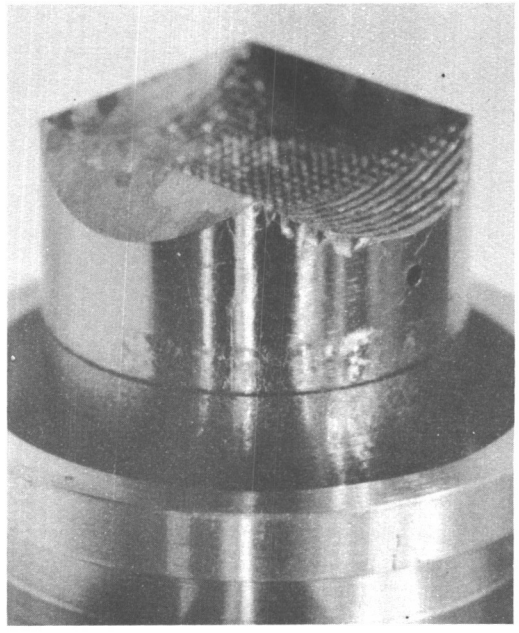


Figure 6-23. VI-TEP-1. View of Converter before and after Life Testing

TABLE 6-1

SUMMARY OF DIODE ACCEPTANCE TEST RESULTS

	VII-S -4	VII-S -5	VI-S -18	VI-Tep. -1
Date of Testing	6/3/63	5/22/63	7/13/63	7/17/63
Output Voltage (volts)	0.8	0.8	1.0	1.0
Output Current (amps)	19.1	18.0	13.5	8.5
Output Power Density (w/cm^2)	7.64	7.2	6.75	4.25
Power Input (watts)	335	365	328	310
Cesium Temperature (°C)	368	345	374	367
Radiator Temperature (°C)	551	540	572	564
Collector Temperature (°C)	590	583		
Seal Temperature (°C)	697	692	654	661
Observed Emitter Temperature (°C)	1655	1655	1655	1655

TABLE 6-2

REPORT OF INITIAL LIFE TEST RESULTS

PARAMETER	VI-S -18	VII-S -4	VII-S -5	VI-S -14	VI-Tep. -1
Date of Observation (day)	7/20/63	7/24/63	7/23/63	7/30/63	8/3/63
Time of Observation (hours)	14:00	15:30	16:00	15:30	11:00
Total Running Time (hours)	00.0	00.0	00.0	00.0	00.0
Output Voltage (volts)	1.0	0.8	0.8	1.0	1.0
Output Current (amps)	13.3	19.5	18.0	14.0	8.8
Output Power Density (w/cm^2)	6.65	7.8	7.2	7.0	4.4
Power Input (watts)	370	430	350	344	300
Chamber Pressure (mm Hg)	1×10^{-6}	3×10^{-6}	2×10^{-6}	1.5×10^{-6}	5×10^{-6}
Cesium Temperature (°C)	360	357	345	355	348
Radiator Temperature (°C)	573	579	555	583	566
Collector Temperature (°C)	623		595		
Seal Temperature (°C)	670	642	659	614	634
Observed Emitter Temperature (°C)	1665	1655	1660	1655	1655

TABLES 6-3 through 6-22

(See Volume II)

TABLE 6-23

REPORT OF LIFE TEST RESULTS AS OF MONDAY, 29 JULY 1963

PARAMETER	VI-S -18	VII-S -4	VII-S -5	VI-S -14	VI-Tep. -1
Time of Observation (hours)	08:40	08:30	08:30	14:30	
Total Running Time (hours)	210.7	88.6	53.0	00.0	
Output Voltage (volts)	1.0	0.8	0.8	1.0	
Output Current (amps)	11.6	20.0	18.1	14.5	
Output Power Density (w/cm^2)	5.8	8.0	7.3	7.3	
Power Input (watts)	376	430	350	340	
Chamber Pressure (mm Hg)	2.5×10^{-7}	2×10^{-7}	3.5×10^{-7}	1.5×10^{-6}	
Cesium Temperature (°C)	354		347	355	
Radiator Temperature (°C)	560	579	557	588	
Collector Temperature (°C)			604		
Seal Temperature (°C)	685	633	653	600	
Observed Emitter Temperature (°C)	1670	1650	1650	1655	

TABLE 6-24

REPORT OF LIFE TEST RESULTS AS OF MONDAY, 5 AUGUST 1963

PARAMETER	VI-S -18	VII-S -4	VII-S -5	VI-S -14	VI-Tep. -1
Time of Observation (hours)	09:05	09:35	09:25	09:10	08:45
Total Running Time (hours)	374.6	257.6	221.5	50.2	45.75
Output Voltage (volts)	1.0	0.8	0.8	1.0	1.0
Output Current (amps)	11.6	19.0	17.0	11.5	8.8
Output Power Density (w/cm^2)	5.8	7.6	6.8	5.8	4.4
Power Input (watts)	376	430	350	344	300
Chamber Pressure (mm Hg)	2×10^{-7}	1.2×10^{-7}	1.8×10^{-7}	1.2×10^{-7}	1×10^{-6}
Cesium Temperature (°C)	350	532	349	355	
Radiator Temperature (°C)	555	576	551	578	576
Collector Temperature (°C)	348	288	595		
Seal Temperature (°C)	661	629	637		
Observed Emitter Temperature (°C)	1670	1650	1645	1655	1650

TABLE 6-25

REPORT OF LIFE TEST RESULTS AS OF MONDAY, 12 AUGUST 1963

PARAMETER	VI-S -18	VII-S -4	VII-S -5	VI-S -14	VI-Tep. -1
Time of Observation (hours)	09:15	09:35	09:45	09:20	09:30
Total Running Time (hours)	542.75	425.6	383.8	218.1	210.65
Output Voltage (volts)	1.0	0.8	0.8	1.0	1.0
Output Current (amps)	11.6	18.2	17.0	11.9	8.1
Output Power Density (w/cm^2)	5.8	7.3	6.8	6.0	4.05
Power Input (watts)	376	430	350	344	287
Chamber Pressure (mm Hg)	2×10^{-7}	9×10^{-8}	2×10^{-7}	9×10^{-8}	3×10^{-7}
Cesium Temperature (°C)	348		355	352	
Radiator Temperature (°C)	554	575	552	578	571
Collector Temperature (°C)	614		597		
Seal Temperature (°C)	661	628	637		
Observed Emitter Temperature (°C)	1665	1655	1645	1660	1660

TABLE 6-26

REPORT OF LIFE TEST RESULTS AS OF MONDAY, 19 AUGUST 1963

PARAMETER	VI-S -18	VII-S -4	VII-S -5	VI-S -14	VI-Tep. -1
Time of Observation (hours)	15:10	15:30	15:35	15:20	15:25
Total Running Time (hours)	715.7	599.5	557.5	392.1	382.2
Output Voltage (volts)	1.0	0.8	0.8	1.0	1.0
Output Current (amps)	11.6	18.5	17.2	11.6	7.4
Output Power Density (w/cm^2)	5.8	7.4	6.8	5.8	3.7
Power Input (watts)	376	430	350	344	284
Chamber Pressure (mm Hg)	1.8×10^{-7}	1×10^{-7}	1.5×10^{-7}	6×10^{-8}	2.5×10^{-7}
Cesium Temperature (°C)	350		355	355	
Radiator Temperature (°C)	543	578	551	579	567
Collector Temperature (°C)	590		597		
Seal Temperature (°C)	649	628	637		
Observed Emitter Temperature (°C)	1665	1650	1650	1660	1660

TABLE 6-27

REPORT OF LIFE TEST RESULTS AS OF MONDAY, 26 AUGUST 1963

PARAMETER	VI-S -18	VII-S -4	VII-S -5	VI-S -14	VI-Tep. -1
Time of Observation (hours)	17:06	16:55	16:43	17:14	17:19
Total Running Time (hours)	885.6	768.9	717.2	546.0	549.2
Output Voltage (volts)	1.0	0.8	0.8	1.0	1.0
Output Current (amps)	11.6	18.5	17.2	11.4	7.3
Output Power Density (w/cm^2)	5.8	7.4	6.9	5.7	3.7
Power Input (watts)	376	430	350	378	284
Chamber Pressure (mm Hg)	1.8×10^{-7}	6×10^{-8}	1.2×10^{-7}	1×10^{-7}	2.2×10^{-7}
Cesium Temperature (°C)	330	504	356	359	
Radiator Temperature (°C)	551	573	551	585	547
Collector Temperature (°C)	579	278	594		
Seal Temperature (°C)	646	625	637	643	
Observed Emitter Temperature (°C)	1665	1650	1650	1650	1660

TABLE 6-28

REPORT OF LIFE TEST RESULTS AS OF MONDAY, 2 SEPTEMBER 1963

PARAMETER	VI-S -18	VII-S -4	VII-S -5	VI-S -14	VI-Tep. -1
Time of Observation (hours)	13:00	13:15	13:20	13:25	13:35
Total Running Time (hours)	1049.5	924.7	876.3	710.0	713.4
Output Voltage (volts)	1.0	0.8	0.8	1.0	1.0
Output Current (amps)	12.4	18.8	18.2	10.9	7.5
Output Power Density (w/cm^2)	6.2	7.5	7.3	5.5	3.8
Power Input (watts)	376	430	370	378	279
Chamber Pressure (mm Hg)	1.6×10^{-7}	8×10^{-8}	1.1×10^{-7}	7×10^{-8}	2.5×10^{-7}
Cesium Temperature (°C)	316	272	362	364	
Radiator Temperature (°C)	559	573	564	588	564
Collector Temperature (°C)	477	503	612		
Seal Temperature (°C)	653	620	646	644	
Observed Emitter Temperature (°C)	1670	1650	1650	1650	1660

TABLE 6-29

REPORT OF LIFE TEST RESULTS AS OF MONDAY, 9 SEPTEMBER 1963

PARAMETER	VI-S -18	VII-S -4	VII-S -5	VI-S -14	VI-Tep. -1
Time of Observation (hours)	13:40	13:30	13:35	13:43	09:00
Total Running Time (hours)	1207.7	1043.1	997.6	878.3	839.1
Output Voltage (volts)	1.0	0.8	0.8	1.0	1.0
Output Current (amps)	11.6	19.0	17.5	11.5	7.5
Output Power Density (w/cm^2)	5.8	7.6	7.0	5.8	3.8
Power Input (watts)	376	430	351	378	284
Chamber Pressure (mm Hg)	1.3×10^{-7}	1.5×10^{-7}	3×10^{-6}	7×10^{-8}	2.3×10^{-7}
Cesium Temperature (°C)		362	374	357	
Radiator Temperature (°C)	537	579	555	579	557
Collector Temperature (°C)		630	602		
Seal Temperature (°C)	640	661	642	647	
Observed Emitter Temperature (°C)	1660	1650	1650	1650	1655

TABLE 6-30

REPORT OF LIFE TEST RESULTS AS OF MONDAY, 16 SEPTEMBER 1963

PARAMETER	VI-S -18	VII-S -4	VII-S -5	VI-S -14	VI-Tep. -1
Time of Observation (hours)	13:50	13:30	13:35	13:55	14:03
Total Running Time (hours)	1376	1210.6	1165.7	1046.6	1016.8
Output Voltage (volts)	1.0	0.8	0.8	1.0	1.0
Output Current (amps)	11.6	19.0	17.2	11.4	7.3
Output Power Density (w/cm^2)	5.8	7.6	6.88	5.7	3.65
Power Input (watts)	376	430	351	378	284
Chamber Pressure (mm Hg)	1.5×10^{-7}	7×10^{-8}	1×10^{-7}	5×10^{-8}	1.5×10^{-7}
Cesium Temperature (°C)	354	360	379	360	348
Radiator Temperature (°C)	553	578	555	586	560
Collector Temperature (°C)	623	640	597		
Seal Temperature (°C)	647	661	636	644	637
Observed Emitter Temperature (°C)	1660	1650	1650	1655	1655

TABLE 6-31

REPORT OF LIFE TEST RESULTS AS OF MONDAY, 23 SEPTEMBER 1963

PARAMETER	VI-S -18	VII-S -4	VII-S -5	VI-S -14	VI-Tep. -1
Time of Observation (hours)	09:42	09:19	09:11	09:35	09:26
Total Running Time (hours)	1539.7	1374.9	1329.2	1210.2	1176.1
Output Voltage (volts)	1.0	0.8	0.8	1.0	1.0
Output Current (amps)	11.6	19.0	16.7	11.3	7.4
Output Power Density (w/cm^2)	5.8	7.6	6.7	5.7	3.7
Power Input (watts)	376	430	351	378	287
Chamber Pressure (mm Hg)	1.5×10^{-7}	6×10^{-8}	9×10^{-8}	4×10^{-8}	1.4×10^{-7}
Cesium Temperature (°C)		359	371	360	
Radiator Temperature (°C)	536	574	552	583	560
Collector Temperature (°C)		628	596		
Seal Temperature (°C)	634	654	630	642	
Observed Emitter Temperature (°C)	1660	1650	1640	1655	1655

TABLE 6-32

REPORT OF LIFE TEST RESULTS AS OF MONDAY, 30 SEPTEMBER 1963

PARAMETER	VI-S -18	VII-S -4	VII-S -5	VI-S -14	VI-Tep. -1
Time of Observation (hours)	13:45	13:55	14:00	13:47	13:52
Total Running Time (hours)	1711.7	1547.0	1504.0	1382.4	1346.5
Output Voltage (volts)	1.0	0.8	0.8	1.0	1.0
Output Current (amps)	11.6	19.0	16.7	11.3	5.3
Output Power Density (w/cm^2)	5.8	7.6	6.68	5.65	2.7
Power Input (watts)	376	430	351	378	300
Chamber Pressure (mm Hg)	1.2×10^{-7}	6×10^{-8}	9×10^{-8}	3.5×10^{-8}	1.4×10^{-7}
Cesium Temperature (°C)	354	359	373	360	348
Radiator Temperature (°C)	539	576	555	583	560
Collector Temperature (°C)		637	597		
Seal Temperature (°C)	635	654	629	643	
Observed Emitter Temperature (°C)	1660	1650	1640	1655	1635

TABLE 6-33

REPORT OF LIFE TEST RESULTS AS OF MONDAY, 7 OCTOBER 1963

PARAMETER	VI-S -18	VII-S -4	VII-S -5	VI-S -14	VI-Tep. -1
Time of Observation (hours)	11:30	11:35	08:30	09:54	11:30
Total Running Time (hours)	1877.5	1712.7	1647.9	1517.8	1514.2
Output Voltage (volts)	1.0	0.8	0.8	1.0	1.0
Output Current (amps)	11.6	19.2	16.7	11.3	5.3
Output Power Density (w/cm^2)	5.8	7.68	6.68	5.65	2.65
Power Input (watts)	376	430	351	378	300
Chamber Pressure (mm Hg)	1.2×10^{-7}	7×10^{-8}	8×10^{-8}	3.5×10^{-8}	1×10^{-7}
Cesium Temperature (°C)	354	360	372	363	348
Radiator Temperature (°C)	536	576	551	586	560
Collector Temperature (°C)	623	630	597		
Seal Temperature (°C)	637	654	637	652	637
Observed Emitter Temperature (°C)	1660	1650	1640	1655	1635

TABLE 6-34

REPORT OF LIFE TEST RESULTS AS OF MONDAY, 14 OCTOBER 1963

PARAMETER	VI-S -18	VII-S -4	VII-S -5	VI-S -14	VI-Tep. -1
Time of Observation (hours)	13:20	13:28	13:30	13:50	13:25
Total Running Time (hours)	2047.4	1882.8	1820.0	1685.5	1684.1
Output Voltage (volts)	1.0	0.8	0.8	1.0	1.0
Output Current (amps)	11.6	19.2	16.7	11.0	5.3
Output Power Density (w/cm^2)	5.8	7.68	6.68	5.5	2.65
Power Input (watts)	376	430	351	378	300
Chamber Pressure (mm Hg)	1×10^{-7}	7×10^{-8}	7×10^{-8}	3×10^{-8}	1×10^{-7}
Cesium Temperature (°C)	354	361	372	364	348
Radiator Temperature (°C)	537	576	550	583	560
Collector Temperature (°C)	623	629	594		
Seal Temperature (°C)	633	652	637	640	637
Observed Emitter Temperature (°C)	1660	1650	1640	1655	1635

TABLE 6-35

REPORT OF LIFE TEST RESULTS AS OF MONDAY, 21 OCTOBER 1963

PARAMETER	VI-S -18	VII-S -4	VII-S -5	VI-S -14	VI-Tep. -1
Time of Observation (hours)	14:05	14:07	14:10	14:00	14:00
Total Running Time (hours)	2216.0	2051.2	1988.7	1854.0	1856.0
Output Voltage (volts)	1.0	0.8	0.8	1.0	1.0
Output Current (amps)	11.6	19.2	16.7	10.6	5.3
Output Power Density (w/cm^2)	5.8	7.68	6.68	5.3	2.65
Power Input (watts)	376	430	351	378	300
Chamber Pressure (mm Hg)	1×10^{-7}	7×10^{-8}	7×10^{-8}	3×10^{-8}	1×10^{-7}
Cesium Temperature (°C)	354	358	372	361	348
Radiator Temperature (°C)	534	576	548	576	560
Collector Temperature (°C)	623	629	595		
Seal Temperature (°C)	631	649	642	633	637
Observed Emitter Temperature (°C)	1660	1650	1640	1655	1635

TABLE 6-36

REPORT OF LIFE TEST RESULTS AS OF MONDAY, 28 OCTOBER 1963

PARAMETER	VI-S -18	VII-S -4	VII-S -5	VI-S -14	VI-Tep. -1
Time of Observation (hours)	13:35	13:30	13:25	13:40	13:33
Total Running Time (hours)	2384.6	2220.0	2157.0	2010.0	2021.0
Output Voltage (volts)	1.0	0.8	0.8	1.0	1.0
Output Current (amps)	11.6	19.2	16.7	10.6	5.3
Output Power Density (w/cm^2)	5.8	7.68	6.68	5.3	2.65
Power Input (watts)	376	430	351	378	300
Chamber Pressure (mm Hg)	1×10^{-7}	7×10^{-8}	7×10^{-8}	3×10^{-8}	3×10^{-7}
Cesium Temperature (°C)	354	359	379	364	348
Radiator Temperature (°C)	534	576	551	578	560
Collector Temperature (°C)	537	632	597		
Seal Temperature (°C)	635	652	633	652	637
Observed Emitter Temperature (°C)	1660	1650	1640	1655	1635

TABLE 6-37

REPORT OF LIFE TEST RESULTS AS OF MONDAY, 4 NOVEMBER 1963

PARAMETER	VI-S -18	VII-S -4	VII-S -5	VI-S -14	VI-Tep. -1
Time of Observation (hours)	13:50	14:03	14:15	14:00	14:10
Total Running Time (hours)	2492	2353	2325	2178	2152
Output Voltage (volts)	1.0	0.8	0.8	1.0	1.0
Output Current (amps)	12.0	20.0	16.7	10.6	4.4
Output Power Density (w/cm^2)	6.0	8.0	6.68	5.3	2.2
Power Input (watts)	376	430	351	378	300
Chamber Pressure (mm Hg)	3×10^{-7}	7×10^{-8}	7×10^{-8}	3×10^{-8}	2×10^{-7}
Cesium Temperature (°C)	345	353	379	364	348
Radiator Temperature (°C)	537	576	551	587	560
Collector Temperature (°C)	607	630	597		
Seal Temperature (°C)	630	650	635	652	637
Observed Emitter Temperature (°C)	1660	1650	1640	1655	1635

TABLE 6-38

REPORT OF LIFE TEST RESULTS AS OF MONDAY, 11 NOVEMBER 1963

PARAMETER	VI-S -18	VII-S -4	VII-S -5	VI-S -14	VI-Tep. -1
Time of Observation (hours)	13:35	13:50	13:50	13:40	13:45
Total Running Time (hours)	2660	2521	2493	2345	2324
Output Voltage (volts)	1.0	0.8	0.8	1.0	1.0
Output Current (amps)	12.0	20.2	16.7	10.6	4.4
Output Power Density (w/cm^2)	6.0	8.08	6.68	5.3	2.2
Power Input (watts)	376	430	351	378	300
Chamber Pressure (mm Hg)	1.2×10^{-7}	5×10^{-8}	7×10^{-8}	3×10^{-8}	2×10^{-7}
Cesium Temperature (°C)	348	360	379	364	348
Radiator Temperature (°C)	543	576	551	581	560
Collector Temperature (°C)	616	647	597		
Seal Temperature (°C)	652	652	635	642	637
Observed Emitter Temperature (°C)	1660	1650	1640	1655	1635

TABLE 6-39

REPORT OF LIFE TEST RESULTS AS OF MONDAY, 18 NOVEMBER 1963

PARAMETER	VI-S -18	VII-S -4	VII-S -5	VI-S -14	VI-Tep. -1
Time of Observation (hours)	09:10	09:28	09:34	09:16	09:24
Total Running Time (hours)	2823.9	2684.9	2657.0	2509.0	2483.9
Output Voltage (volts)	1.0	0.8	0.8	1.0	1.0
Output Current (amps)	12.0	20.0	16.0	10.6	4.4
Output Power Density (w/cm^2)	6.0	8.0	6.3	5.3	2.2
Power Input (watts)	376	430	351	378	300
Chamber Pressure (mmHg)	1×10^{-7}	5×10^{-8}	7×10^{-8}	3×10^{-8}	2×10^{-7}
Cesium Temperature (°C)	348	360	381	361	348
Radiator Temperature (°C)	541	576	546	579	560
Collector Temperature (°C)	612	628	597		
Seal Temperature (°C)	648	642	626	637	637
Observed Emitter Temperature (°C)	1660	1645	1640	1655	1635

TABLE 6-40

REPORT OF LIFE TEST RESULTS AS OF MONDAY, 25 NOVEMBER 1963

PARAMETER	VI-S -18	VII-S -4	VII-S -5	VI-S -14	VI-Tep. -1
Time of Observation (hours)	10:03	09:45	09:55	09:56	10:00
Total Running Time (hours)	2992.0	2853.1	2825.4	2677.8	2652.5
Output Voltage (volts)	1.0	0.8	0.8	1.0	1.0
Output Current (amps)	12.0	20.2	16.3	10.4	4.4
Output Power Density (w/cm^2)	6.0	8.08	6.52	5.2	2.2
Power Input (watts)	376	430	351	378	300
Chamber Pressure (mm Hg)	1×10^{-7}	5×10^{-8}	7×10^{-8}	3×10^{-8}	1.8×10^{-7}
Cesium Temperature (°C)	350	362	382	365	348
Radiator Temperature (°C)	547	576	552	583	560
Collector Temperature (°C)	617	631	597		
Seal Temperature (°C)	654	648	633	641	637
Observed Emitter Temperature (°C)	1660	1645	1635	1655	1635

TABLE 6-41

REPORT OF LIFE TEST RESULTS AS OF MONDAY, 2 DECEMBER 1963

PARAMETER	VI-S -18	VII-S -4	VII-S -5	VI-S -14	VI-Tep. -1
Time of Observation (hours)	14:35	14:48	14:50	14:45	14:45
Total Running Time (hours)	3165.0	3026.0	2998.4	2832.0	2825.0
Output Voltage (volts)	1.0	0.8	0.8	1.0	1.0
Output Current (amps)	12.0	20.2	16.1	10.3	4.5
Output Power Density (w/cm^2)	6.0	8.08	6.44	5.15	2.25
Power Input (watts)	376	430	351	378	300
Chamber Pressure (mm Hg)	1×10^{-7}	5×10^{-8}	7.5×10^{-8}	3×10^{-8}	1.8×10^{-7}
Cesium Temperature (°C)	350	363	383	372	348
Radiator Temperature (°C)	548	576	553	583	560
Collector Temperature (°C)	618	630	597		
Seal Temperature (°C)	654	650	633	644	637
Observed Emitter Temperature (°C)	1660	1645	1635	1655	1635

TABLE 6-42

REPORT OF LIFE TEST RESULTS AS OF TUESDAY, 10 DECEMBER 1963

PARAMETER	VI-S -18	VII-S -4	VII-S -5	VI-S -14	VI-Tep. -1
Time of Observation (hours)	09:30	09:20	09:05	10:00	09:30
Total Running Time (hours)	3352.3	3212.2	3184.6	3013.0	3010.4
Output Voltage (volts)	1.0	0.8	0.8	1.0	1.0
Output Current (amps)	12.2	20.5	16.0	10.5	5.0
Output Power Density (w/cm^2)	6.1	8.2	6.4	5.25	2.5
Power Input (watts)	376	430	351	378	300
Chamber Pressure (mm Hg)	1.2×10^{-7}	7×10^{-8}	7×10^{-8}	2.5×10^{-8}	1.2×10^{-7}
Cesium Temperature (°C)	341	361	379	364	348
Radiator Temperature (°C)	542	576	551	584	560
Collector Temperature (°C)	615	628	597		
Seal Temperature (°C)	649	642	628	649	637
Observed Emitter Temperature (°C)	1660	1645	1635	1655	1635

TABLE 6-43

	VI-S -18	VII-S -4	VII-S -5	VI-S -14	VI-Tep. -1
Starting Conditions					
a. Output Power Density (w/cm^2)	6.65	7.8	7.2	7.0	4.4
b. Power Input (watts)	370	430	350	344	300
c. Cesium Temperature (°C)	360	357	345	355	348
d. Seal Temperature (°C)	670	642	659	614	634
e. Observed Emitter Temperature (°C)	1665	1655	1660	1655	1655
At 1000 Hours (hours)	1049	1043	997.6	1046.6	1016.8
a. Output Power Density (w/cm^2)	6.2	7.6	7.0	5.7	3.65
b. Power Input (watts)	376	430	351	378	284
c. Cesium Temperature (°C)	316	362	374	360	348
d. Seal Temperature (°C)	653	661	642	644	637
e. Observed Emitter Temperature (°C)	1670	1650	1650	1655	1655
At 2000 Hours (hours)	2047	2051.2	1988.7	2010	2021
a. Output Power Density (w/cm^2)	5.8	7.68	6.68	5.3	2.65
b. Power Input (watts)	376	430	351	378	300
c. Cesium Temperature (°C)	354	358	372	364	348
d. Seal Temperature (°C)	633	649	642	652	637
e. Observed Emitter Temperature (°C)	1660	1650	1640	1655	1635
At 3000 Hours (hours)	2992	3026	2998.4	3013	3010.4
a. Output Power Density (w/cm^2)	6.0	8.08	6.44	5.25	2.5
b. Power Input (watts)	376	430	351	378	300
c. Cesium Temperature (°C)	350	363	383	364	348
d. Seal Temperature (°C)	654	650	633	649	637
e. Observed Emitter Temperature (°C)	1660	1645	1635	1655	1635